New insights into S100A4-induced colon cancer metastasis: The role of exo- and endogenous inhibitors

D i s s e r t a t i o n
zur Erlangung des akademischen Grades
d o c t o r r e r u m n a t u r a l i u m
(Dr. rer. nat.)
im Promotionsfach Biologie
eingereicht an der

Mathematisch-Naturwissenschaftlichen Fakultät I
der Humboldt-Universität zu Berlin
von

MSc in Mol-Biol. Ulrike Sack

Präsident der Humboldt-Universität zu Berlin
Prof. Dr. Jan-Hendrik Olbertz

Dekan der Mathematisch-Naturwissenschaftlichen Fakultät I
Prof. Dr. Andreas Herrmann

Gutachter: 1. Prof. Dr. Achim Leutz
2. Prof. Dr. Matthias Selbach
3. Prof. Dr. Ulrike Stein

Tag der mündlichen Prüfung: 30.03.2011

This study was conducted at the Max Delbrück Centrum for Molecular Medicine Berlin-Buch supervised by Prof. Dr. Ulrike Stein in the research group of Prof. Dr. Dr. h.c. Peter M. Schlag.

Für meine Familie

INDEX OF CONTENTS

ABBREVIATIONS

AP-1	activating protein-1
BCA	bicinchoninic acid
BSA	bovine serum albumin
CBF	core-binding-factor
CCN3	cystein-rich 61-connective tissue growth factor-nephroblastoma overexpressed-family member 3
CDC4	cell division control protein 4
CIN	chromosomal instability
CK-1α	casein kinase-1α
DKK	dickkopf
DMSO	dimethylsulfoxide
DTT	dithiothreitol
dvl	disheveled
EGFR	epidermal growth factor receptor
ELISA	enzyme-linked immunosorbent assay
EMT	epithelial mesenchymal transition
EMT-TF	EMT-specific transcription factor
ErbB2	erythroblastosis oncogene B B2
F-actin	filamentous actin
FAP	familial adenomatous polyposis
FDA	Food and Drug Administration
GSK-3β	glycogen synthase kinase -3β
HNPCC	hereditary nonpolyposis colorectal cancer
HTS	high throughput screening
IFN-γ	interferon-γ
LEF-1	lymphocyte enhancer factor-1
LRP-5/-6	low density lipoprotein receptor-related protein-5 or -6
MAP	microfibrill-associated glycoprotein
MAPK	mitogen-activated protein kinase
MetAP2	methionine aminopeptidase 2
MMP	matrix metalloproteinase
NF-κB	nuclear factor κB
PBS	phosphate buffered saline
PI3K	phosphatidylinositol-3 kinase

PP2A	protein phosphatase 2A
PTEN	phosphatase tensine homolog
RAGE	receptor for advanced glycation end products
RT	reverse transcription
S100A4	soluble in 100% ammonium sulphate solution-family member A4
SDS-PAGE	sodiumdodecylsulphate polyacrylamide gel electrophoresis
sFRP	secreted frizzled-related protein
shRNA	short-hairpin RNA
TCF	T-cell factor
TGFRII	TGF-β receptor 2
TGF-β	tumor growth factor-β
TNF-α	tumor necrosis factor α
UTR	untranslated region
WIF-1	Wnt inhibitor factor-1
Wnt	Int1 and wingless (drosophila homolog)

ABSTRACT

Metastasis is the major burden for colon cancer patients as it reduces their five-year survival chances to less than 10%. Efforts made to identify the molecular players in metastasis formation revealed the calcium binding protein S100A4. S100A4 is a Wnt/β-catenin target gene which promotes migration, invasion and angiogenesis. Its overexpression leads to aggressive tumor growth and metastasis formation in colon cancer. Consequently, inhibition of S100A4 expression is a promising strategy for anti-metastatic treatment of colon cancer patients. Moreover, knowledge on the gene regulations that occur upon S100A4 overexpression helps to further understand its metastasis promoting function.

In this vein, the present study characterizes the small molecules niclosamide and calcimycin as transcriptional inhibitors of S100A4 which reduced S100A4 expression concentration- and time-dependently. Niclosamide and calcimycin treatment restricted cell migration, invasion and wound healing capabilities in a S100A4-specific manner, and inhibited cell proliferation and colony formation of colon cancer cells.

Both small molecule inhibitors interfere with the constitutively active Wnt pathway. Targeting β-catenin expression by calcimycin or interfering with the β-catenin/TCF transcription activating complex by niclosamide resulted in reduced Wnt target gene transcription, among them S100A4.

The study further presents a human colon cancer xenograft mouse model for monitoring S100A4-induced metastasis formation via non-invasive bioluminescence imaging. Treatment of xenograft mice with niclosamide resulted in a significant reduction of the S100A4 mRNA level in the tumor accompanied by inhibition of metastasis formation.

Moreover, this study presents evidence that S100A4 is an inhibitor of DKK-1 expression. In colon cancer cells DKK-1 and S100A4 expression was negatively correlated. Ectopic S100A4 overexpression inhibited DKK-1 expression. Targeting S100A4 via shRNA recovered the repressed DKK-1 expression and vice versa.

In summary, the study describes a novel positive feedback loop in the Wnt pathway regulation formed by S100A4 repressing its antagonist DKK-1. This novel mechanism further strengthens the need for S100A4 inhibitors such as niclosamide or calcimycin. Consequently, such small molecules provide immense potential for the treatment of colon cancer patients who are at high risk for S100A4-induced colon cancer metastasis.

ZUSAMMENFASSUNG

Dickdarmkrebs wird zu einer lebensbedrohlichen Krankheit wenn sich Metastasen bilden. Daher ist die Erforschung der molekularen Mechanismen, die der Metastasierung zu Grunde liegen für die Entwicklung neuer Therapien für das Kolonkarzinom wichtig. Ein zentraler molekularer Beschleuniger für die Metastasierung ist das Protein S100A4. Die S100A4 Expression in Kolonzellen wird durch den Wnt Pathway reguliert, der in 90% der Kolontumore konstitutiv aktiv ist. Eine Überexpression von S100A4 erhört die Zellmotilität und fördert damit die Metastasierung von Kolonkarzinomen. Um dies therapeutisch unterbinden zu können, ist die Hemmung der S100A4 Expression ein vielversprechender Ansatz. Des Weiteren ist bekannt, dass S100A4 im Zellkern vorkommt. Jedoch ist wenig darüber bekannt, welche transkriptionellen Konsequenzen aus der S100A4 Überexpression folgen.

Die vorliegende Arbeit präsentiert die beiden Small Molecules Niklosamid und Calcimycin als neue Inhibitoren der S100A4 Transkription. In Kolonkarzinomzellen, die mit einem der beiden Inhibitoren behandelt wurden, wurde die S100A4 Expression konzentrations- und zeitabhängig unterdrückt. Des Weiteren war die Zellmigration und -invasion in Abhängigkeit von S100A4 in behandelten Zellen vermindert. Niklosamid und Calcimycin Behandlung verhinderten die Zellproliferation und die Koloniebildung von Kolonkarzinomzellen.

Beide Inhibitoren hemmten den konstitutiv aktiven Wnt Pathway von Kolonkarzinomzellen. Calcimycin Behandlung verminderte die Expression von β-catenin. Niklosamid hemmte die Bildung des β-catenin/TCF Komplexes und unterband damit die Expression von Wnt Pathway Genen, wie z.B. S100A4.

Im Rahmen dieser Arbeit wurde ein in vivo Tiermodell entwickelt mit dem die S100A4-induzierte Metastasierung mit Hilfe von nicht-invasivem Biolumineszenz Imaging visualisiert werden konnte. In diesem Model konnte gezeigt werden, dass Niklosamid signifikant die S100A4 Expression im Tumor vermindert und damit die Metastasierung hemmt.

Des Weiteren zeigt diese Arbeit, dass eine S100A4 Überexpression die Expressionshemmung des Wnt Pathway Antagonisten DKK-1 in Kolonkarzinomzellen induziert. Die Expression von S100A4 und DKK-1 in Kolonkarzinomzelllinien korrelierte signifikant negativ. S100A4 Überexpression verminderte die DKK-1 Expression und die Hemmung der S100A4 Expression mit shRNA führte zur vermehrten DKK-1 Expression. Umgekehrt erfolgte durch die Hemmung der DKK-1 Expression mit shRNA

ein Anstieg in der S100A4 Expression. Letztere konnte durch die Behandlung mit rekombinantem DKK-1 vermindert werden.

Zusammenfassend beschreibt die vorliegende Arbeit einen neuen regulativen Mechanismus im Wnt Pathway, der die S100A4 Expression im Kolonkarzinom fördert. Diese Beobachtung verdeutlicht die Notwendigkeit für wirksame S100A4 Inhibitoren, wie Niklosamid und Calcimycin. Solche Inhibitoren haben das Potenzial in einer klinischen Anwendung die Metastasierung von Kolonkarzinompatienten mit einer erhöhten S100A4 Expression zu hemmen und damit deren Überlebenschance wesentlich zu erhöhen.

1. INTRODUCTION

1.1. Colon cancer

1.1.1. Colon cancer epidemiology

According to the World Health Organization, colon cancer is the third most common cancer worldwide and even the second most frequent type of cancer concerning men and women in developed countries. In the Western world colon cancer occurs with a lifetime incidence of 5% (1). Thus, colon cancer is a leading cause of cancer death worldwide.

Intensive health programs comprising novel screening methods for early diagnosis of colon cancer induced a declining trend of colon cancer cases and deaths in the developed countries. The decline further correlated with the access to specialists and the availability of modern drug therapy (1, 2). Nonetheless, colon cancer still represents 13% of all diagnosed neoplasms in Europe (2). In Germany, 16% of all cancers are situated in the colon, rectum or anus. The latest German cancer report states that there are yearly about 70,000 new colon cancer cases diagnosed and each year 28,000 colon cancer patients die (3).

The overall five year survival rate for colon cancer lies between 53 and 63%. However, survival is highly dependent on the tumor stage at the time of diagnosis. For instance, the five year survival rate for patients with a local tumor in its early stages is 90%. However, less than 40% of early stage tumors are detected. The majority of colon tumors are diagnosed at a more progressed stage, when regional lymph node or even distant metastases have already been formed. Diagnosis of colon cancer with regional lymph node metastases decreases the five year survival rate to about 65%. Drastically, only 10% of colon cancer patients will survive the five years post diagnosis when their tumor has spread to distant organs. Thus, metastatic dissemination of primary colon tumors accounts for 90% of all colon cancer deaths rendering metastasis formation one central process to be inhibited in colon cancer therapy (4).

1.1.2. Risk factors and causes for colon cancer

The major cause for the development of colon cancer lies in the personal genetic predisposition. 20 to 30% of colon cancer patients present a personal familial history of colon tumors implicating that a certain genetic background increases the risk for colon cancer (5). Only 5 to 10% of those patients present well-characterized hereditary cancer syndromes, such as familial adenomatous polyposis (FAP), hereditary non-

polyposis colon cancer (HNPCC) and MUTYH-associated polyposis (MAP). These autosomal-dominant (FAP, HNPCC) or autosomal-recessive (MAP) inherited diseases are caused by a highly penetrant mutation leading to the development of colon cancer early in lifetime (6). For instance, FAP is caused by a germline mutation of the adenopolyposis coli (APC) protein which is the gatekeeper protein of the canonical Wnt/β-catenin pathway. The resulting constitutively active Wnt pathway causes the formation of hundreds to thousands polyps during childhood which further develop into carcinoma at the age of about 45 (7). HNPCC, also referred to as the Lynch syndrome, is caused by a mutation in the MLH1 gene coding for a mismatch repair protein. Loss of MLH1 leads to increased accumulation of mutations in the DNA and a characteristic microsatellite instability (8).

In contrast, 90 to 95% of all colon cancers are sporadic and the genetic causes for cancer development are manifold and multivariable. Moreover, risk factors such as age, sex and dietary aspects can promote the development of sporadic colon cancer (5). For instance, with each decade of age the colon cancer incidences in women and men increase rapidly. In Germany, less than 10 out of 100,000 women and men at the age of 40 are diagnosed with colon cancer. However, at the age of 70 this incidence increases to 400 men and 200 women, respectively (3). Furthermore, a diet which is poor in red meat and fat and rich in fiber, folate and calcium can decrease the risk to develop colon cancer. Increased uptake of fiber stimulates butyrate production, which in turn was found to inhibit histone deacetylation and thereby restricts carcinogenesis (9). Besides age and dietary aspects, co-morbidities such as ulcerative colitis or Crohn's colitis often increase the risk of developing colon cancer.

1.2. The development of metastatic colon cancer

The development of colon cancer and its metastases is thought to be a progressive process which is mediated by a sequence of certain mutations. The following sections deal with the histology of the normal colon crypt, the tumor initiation and the progression towards metastasis formation as well as the molecular processes underlying colon cancer.

1.2.1. The normal colon crypt

Together with the rectum and the anus, the colon constitutes the final part of the gastrointestinal tract. It is composed by the endoderm-derived layer of colon epithelium and the two mesoderm-derived layers containing smooth muscle cells needed for

peristalsis and stroma cells as connective tissue (10). The epithelial layer presents the characteristic crypts of Lieberkühn (Fig 1.1), which are separated into two functional compartments: the proliferative compartment at the lower part of the crypt and the differentiated compartment at the luminal side of the crypt.

The proliferative compartment contains slowly dividing multipotent stem cells which give rise to transit amplifying cells. These progenitor cells divide twice as fast as the stem cells and migrate to the apex of the crypt in coherent bands. During migration these cells differentiate into one of the four major epithelial cell types: the absorptive enterocyte and the secretory Goblet, as well as the enteroendocrine and Paneth cells (11).

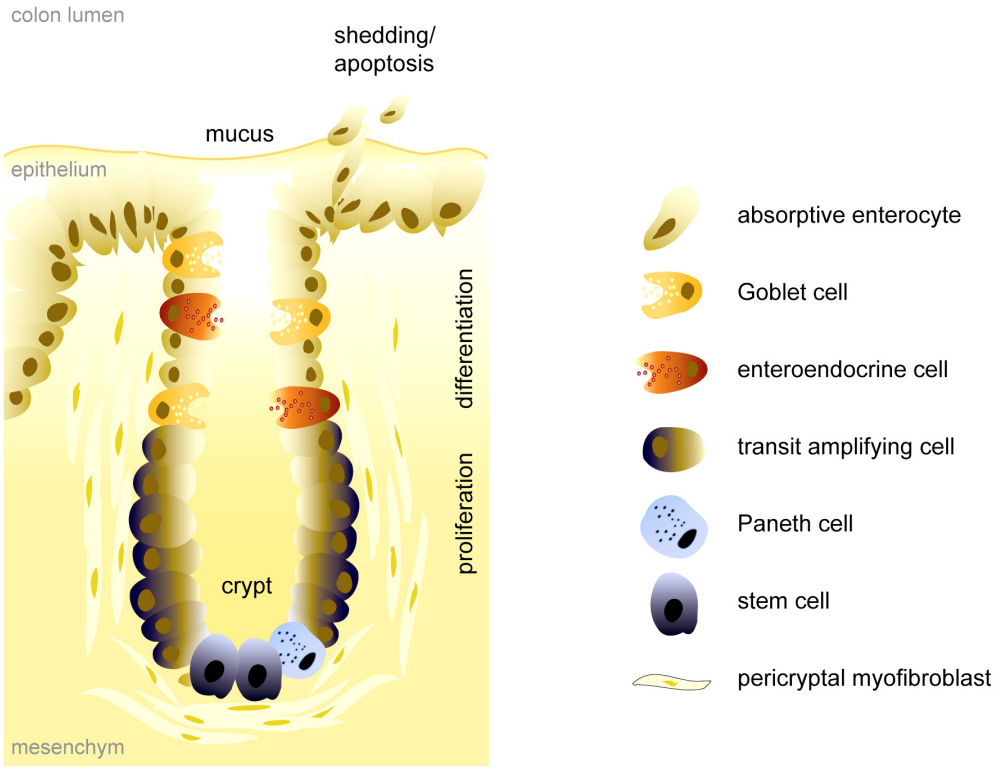

Fig. 1.1 Histology of the colon crypt. The scheme represents one crypt of Lieberkühn which is divided into the compartments of proliferation and differentiation. At the bottom of the crypt, multipotent stem cells give rise to transit amplifying cells. Those rapid dividing cells migrate in coherent bands towards the luminal side of the crypt. Along their way to the crypt apex these progenitor cells differentiate into absorptive enterocytes, Goblet cells, enteroendocrine and Paneth cells. Differentiated cells at the apex of the colon crypt are mechanically shedded or undergo apoptosis. Their loss is permanently compensated by new stem-cell derived cells from the crypt bottom. Modified after Radtke and Clevers (12).

In the differentiated compartment of colon crypts, enterocytes and Goblet cells are the most prominent cell types. Absorptive enterocytes reabsorb water and electrolytes from the chime. Goblet cells produce mucus to protect the colon epithelium against chear

stress and chemical damage. Enteroendocrine cells secrete hormones such as secretin, serotonin, substance P and somatostatin. Paneth cells are sometimes present in the ascending colon and in inflammatory states. These cells reside at the bottom of the crypt where they secrete anti-microbial peptides such as cryptins, defectins, lysozyme and phospholipase A2 (13). Differentiated cells migrate towards the crypt apex were they are either mechanically shedded or enter apoptosis. Lost cells are permanently replaced by new stem-cell derived upcoming cells from the bottom of the crypt. The lifespan of differentiated epithelial cells ranges over 3 to 5 days, except for Paneth cells, which have a lifespan of 20 days (10, 11, 14).

1.2.2. The adenoma-carcinoma cascade

Colon cancer mostly arises from precancerous lesions in the epithelium which can be caused by chronic inflammation and the accumulation of genetic mutations. Two models for the nascence of colon tumors were recently discussed which differ in the origin of the cancer initiating cell: the “top-down” and the “bottom-up”-model.

The “top-down”-model is based on one study in histological tissue sections of sporadic colon tumors where dysplastic cells were located at the crypt apex while the cells at the bottom of the crypts were morphologically normal. Therefore, it was hypothesized that transformed precursor cells migrated up the crypt, resided at the surface and initiated tumor formation. Then the tumor expands as transformed clones migrate laterally and downwards into adjacent crypts to displace the normal epithelium (15).

This “bottom-up”-model summarized in Fig. 1.2 is nowadays the most widely accepted model for the development of colon cancer (13). It is based on the hypothesis that tumors arise from transformed stem cells located at the bottom of the crypt. The mutated stem cell divides and colonizes a single crypt forming a monocryptal microadenoma. This is consistent with the observation that the macroscopical count of adenomas in FAP patients is linear to the number of microscopically counted aberrant crypts suggesting an unicryptal evolution of adenoma (16). The development of microadenoma into small adenoma in the colon occurs by crypt fission and budding (17). Aberrant crypt foci are a frequent phenomenon in early adenomas isolated from FAP and sporadic APC mutated colon cancer patients (18-20). Crypt fission allows the progression from small adenoma to large adenoma rising into the colonic lumen. As the adenoma expands, nutrient supply via diffusion becomes insufficient (21). This leads to secretion of angiogenic factors that allow extensive vascularisation of the now early carcinoma to assure sufficient nutrient supply within the tumor mass. The early carcinoma laterally expands into adjacent crypts and further

infiltrates the mesenchymal layers thereby turning into a late carcinoma (22). Recent evaluations show that the timeframe for the adenoma-carcinoma take about two decades. In contrast, the transition from malignant carcinoma to the formation of distant metastases is believed to take less than two years (23).

1.2.3. Metastasis formation

A profound step for metastasis formation is the epithelial-mesenchymal transition (EMT) of colon cancer cells which is initiated by the tumor stroma cells. During tumor outgrowth, regional mesenchymal stroma cells are incorporated into the tumor mass. Besides regional stroma cells, further mesenchymal bone-marrow stem cells, which entered the blood circulation, can invade and migrate to the tumor tissue where they differentiate into myofibroblasts and endothelial cells. Stroma cells release paracrine and endocrine growth factors which are needed to initiate neovascularization of blood and lymph vessels and support tumor growth (24). The stroma cells are believed to take on attributes of cells that are chronically inflamed or exposed to wound healing processes during tumor progression thereby activating EMT (25). EMT is a highly conserved cellular program needed to allow epithelial cells to convert to mesenchymal cells. Epithelial cells are polarized, immotile cells that form a monolayer by tight intercellular connections. They can only migrate laterally along the epithelial cell-band, but are unable to invade the basal layer tissue. In contrast, mesenchymal cells form rarely contacts to neighboring cells, are highly motile and able to invade the tissue. During embryogenesis, mesenchymal cells arise from epithelial cells that performed EMT. EMT also occurs in the adult organism in the process of wound healing, for instance, during chronic inflammation.

In the initiating process of metastasis formation (Fig. 1.2), EMT allows the transformed epithelial cell to acquire a mesenchymal phenotype characterized by the loss of cell-adhesion, destruction of the extracellular matrix, invasion of the neighboring tissue and directed migration towards blood or lymph vessels (26). Invading tumor cells enter the circulation mostly by intravasation of thin-walled lymphatic channels or blood vessels.

The majority of tumor cells entering the circulation will fail to form metastasis due to several hurdles (27). Once the tumor cell left the tumor tissue, the growth activating signals from the stroma cells are lost. Furthermore, cells can be damaged mechanically during circulation. Cells that survived the circulation are trapped in the lymph nodes or in the narrow capillaries. The cells need to express specific adhesion molecules to adhere to the vessel endothelium and extravasate into the foreign tissue. In the distant organ tissue, the invaded cell is exposed to foreign signaling factors and different

extracellular matrix proteins to which it needs to attach in order to establish a microenvironment needed for the formation of micrometastases (28). These micrometastases are thought to perform the reverse mesenchymal-epithelial transition to establish the primary metastasis which can give rise to further secondary metastases (25).

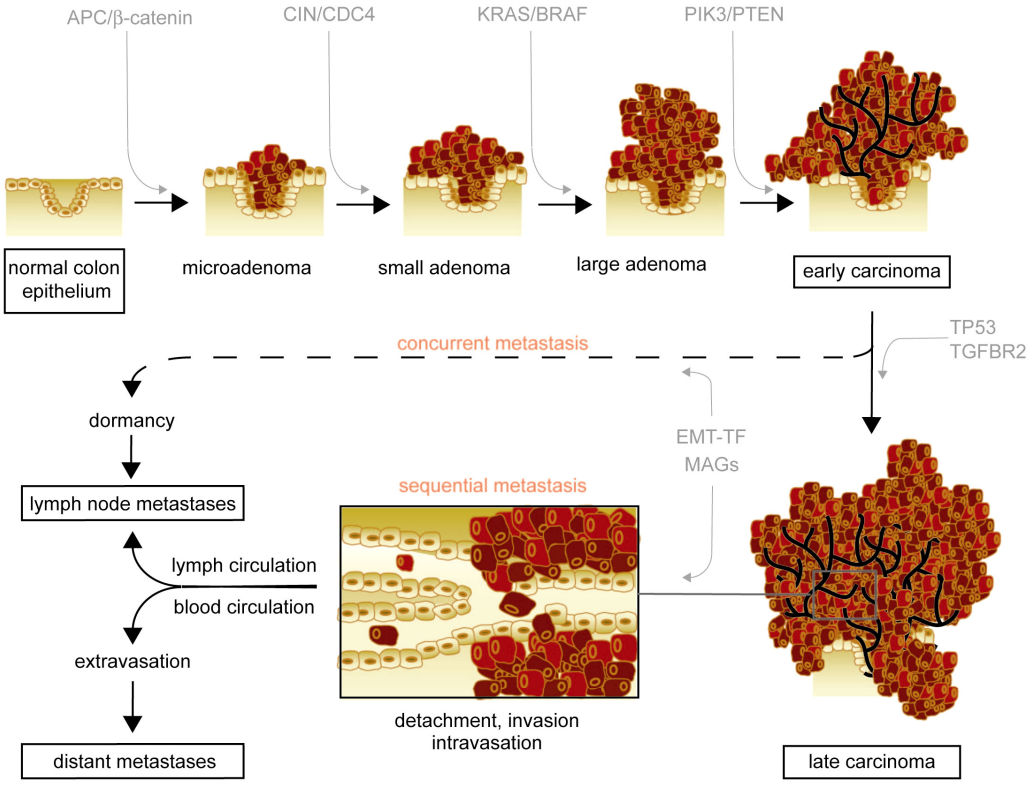

Fig. 1.2 Colon cancer development and metastasis formation. Colon cancer is initiated by a mutated colon stem cell which colonizes a crypt, thereby forming a microadenoma. Further accumulation of certain mutations and incorporation of regional stroma cells drives the transition to a large adenoma rising into the colon lumen. Neovascularization assures the nutrient supply within the tumor mass of the early carcinoma which further infiltrates into the basal layers and into neighboring crypts. Expression of EMT-TFs enables invasion of the neighboring tissue, followed by intravasation into the lymph and blood circulation, extravasation into foreign tissue and metastasis formation in lymph nodes and distant organs. Sequentially occurring mutations that regulate the development of colon cancer metastasis are indicated in grey. APC, adenomatous polyposis coli; CDC4, cell division control protein 4; CIN, chromosomal instability; EMT-TF, epidermial-mesenchymal transition-transcription factors; MAGs, metastasis-associated genes; PI3K, phosphatidylinositol-3 kinase; PTEN, phosphatase tensine homolog; p53, tumor suppressor protein 53; TGFRII, TGF-β receptor 2. Modified after Jones, Pantel et al. (23, 29).

The above described model is often referred to as the classical metastatic model which describes a sequential development of metastasis. Recently, a second model has been described which indicates that tumor dissemination could occur early, concurrent to tumor development (30). This hypothesis is based on the observation that especially in breast cancer patients tumor cells are present in the circulation and in the bone marrow even after the resection of the early primary tumor (29). It was hypothesized that circulating tumor cells extravasate into bone marrow or lymph nodes and perform cell cycle arrest due to different growth signals and foreign extracellular-matrix-proteins. Those “metastatic seeds” can persist in a dormant state rendering them resistant to most chemotherapeutics which attack the active proliferating cell (31). It is yet unclear what reactivates dormant disseminated tumor cells. Recently, it was shown that overexpression of integrins in the extracellular matrix lead to proliferation of prior dormant cancer cells (32). These cells could again enter the circulation, extravasate into distant organ tissue and give rise to primary and secondary metastases (29, 33).

1.2.4. Molecular pathways involved in colon cancer metastasis

Comparative lesion sequencing recently revealed that most of the mutations enabling metastasis formation are not acquired late in the adenoma-carcinoma development, but are rather present in the correspondent premalignant lesion (23). Consistently, many prognostic markers for metastasis formation are already expressed early in the development of colon cancer (25, 34, 35).

Accumulation of activating mutations in oncogenes and inactivating mutations in tumor suppressor genes is a profound step in cancer development (36). Sequential accumulation of certain mutations (Fig. 1.2) drives the development of colon cancer (37). The initial mutation thereby occurs in the canonical Wnt/β-catenin pathway, which is mutated in 90% of colon tumors (38). Additionally, the majority of colon cancers present chromosomal instability (CIN). Activating mutations of CIN-causing genes is a key step in the development of microadenoma. For instance, as mentioned above, inactivating mutations in the mismatch-repair gene MHL1 lead to accumulation of single nucleotide mutations and thus to genetic instability often found in HNPCC patients (8). Furthermore, mutation in the ubiquitin ligase subunit named cell division control protein 4 (CDC4) causes CIN in most colorectal cancers (39, 40). CIN further leads to mutations in KRAS and BRAF, which activate the MAPK pathway resulting in increased cell proliferation and motility. Mutated BRAF is found even in small adenoma. Active MAPK signaling is thought to drive the transformation from small to large adenoma (37).

Mutations promoting proliferation can further occur in the phosphatidylinositol-3 kinase (PI3K) pathway, either activating mutations on PI3K in 30% of colorectal cancers or, less often, loss of the PI3K inhibitor phosphatase tensine homolog (PTEN) (41). Inactivation of the tumor suppressor protein p53 is a second crucial step in the transition towards malignant carcinoma. Upon DNA-damage non-mutated p53 induces either DNA-repair or cell-cycle arrest and apoptosis. Loss of p53 results in the inability to undergo apoptosis which is a hallmark of cancer cells (36). Finally, inactivating mutations of the tumor growth factor-β (TGF-β) signaling pathway, usually occurring in the TGF-β receptor 2 (TGFRII), coincide with the transition of early carcinoma to highly invasive carcinoma (22).

A key step in the dissemination of metastatic cells from the primary colon tumor is the upregulation of EMT-specific transcription factors (EMT-TFs). These transcription factors are highly conserved during evolution and under normal conditions regulate the EMT during embryogenesis. In cancer cells EMT-TFs enhance the invasive phenotype of metastatic cells, thereby initiating dissemination from the primary colon tumor (25). Finally, metastasis-specific mutations are needed to enhance the transition from the invasive carcinoma to a metastatic seeding cell (23).

1.3. The canonical Wnt/β-catenin pathway

The canonical Wnt/β-catenin pathway is one of the most crucial pathways in colon stem cell homeostasis regulating cell differentiation along the crypt-villus axis (42). Mutation of the Wnt pathway is an initiating event in colon cancer development and constitutively active Wnt signaling constitutes the basis for metastasis formation (31).

1.3.1. Components of the Wnt pathway

The initial identification of Wnt signaling components came from the field of developmental biology two decades ago. Not until one decade later the oncogenic and tumor suppressor abilities of many of those components were recognized. The first component identified in 1973 was *int1* which was overexpressed in mammary gland tumors. Int1 later on was identified as the vertebrate homologue of *wingless* in Drosophila from which the wnts – as a combination of wingless and int1 - finally gained their name (43).

In the absence of Wnt signaling, β-catenin levels are tightly controlled by the destruction complex (Fig. 1.3). In this complex β-catenin is anchored by APC and Axin.

This offers a platform for the kinases casein kinase-1α (CK1α) and glycogen synthase kinase-3β (GSK3-β) to enter the complex and sequentially phosphorylate β-catenin (44). The initial phosphorylation occurs at the conserved serine 45 of β-catenin by CK-1α which is followed by further phosphorylation of serine 33, 37 and threonine 41 by GSK3-β (45, 46). Phosphorylation on β-catenin generates a binding site for E3 ubiquitin ligase and leads to rapid proteasomal degradation. Suppressed levels of β-catenin assure that groucho proteins in the nucleus bind to transcription factors of the T-cell factor (TCF) family to inhibit transcription of β-catenin target genes (47, 48).

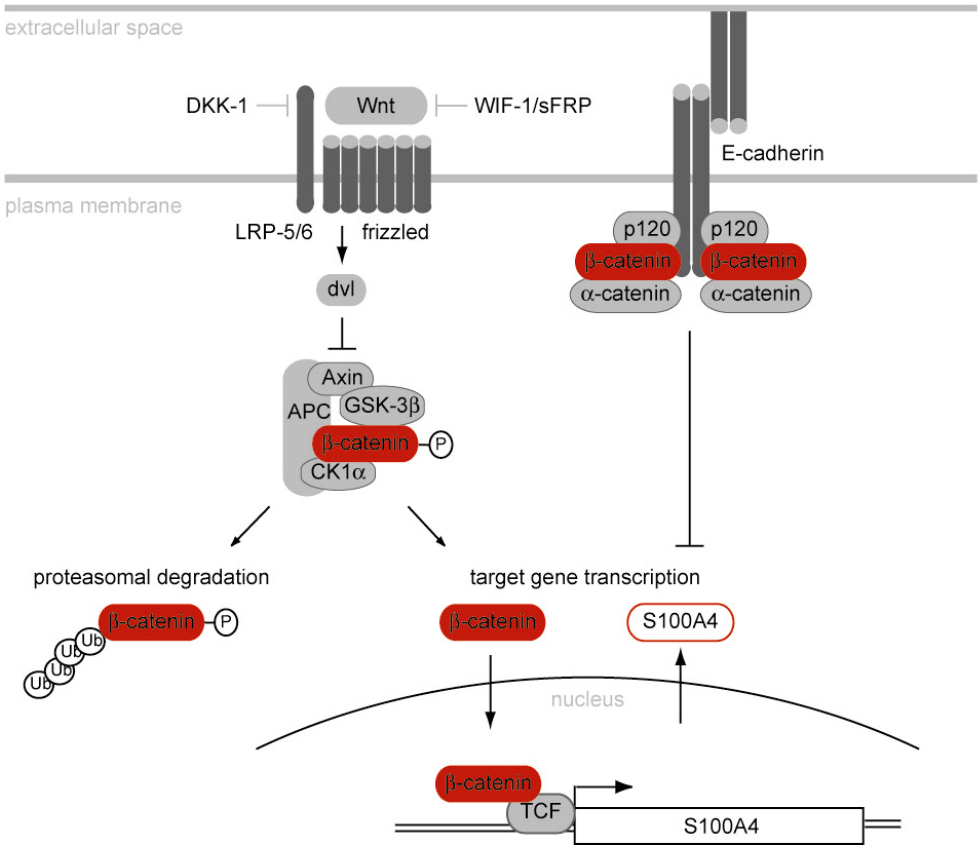

Fig 1.3 The canonical Wnt/β-catenin pathway. In the absence of extracellular Wnts, β-catenin levels are tightly controlled by the destruction complex which enables β-catenin phosphorylation and subsequent proteasomal degradation or by E-cadherin which binds to β-catenin thus hindering it from entering the nucleus. Upon extracellular complexation of Wnt and frizzled/LRP-5/6 receptor, dishevelled sequesters Axin 2 from the destruction complex, β-catenin accumulates in the cytoplasm and translocates into the nucleus, binds TCF transcription factors and activates target gene transcription. APC, adenomatous polyposis coli; CK1α casein kinase 1α; DKK-1, dickkopf-1, Dvl, disheveled; GSK-3β, glycogen synthase kinase -3β; LRP-5/6, low density lipoprotein receptor-related protein-5/6; sFRP, secreted frizzled-related protein; TCF, T-cell factor; WIF-1, Wnt inhibitor factor-1. Modified after following Barker. Jeanes et al. (47, 49).

Activation of the Wnt/β-catenin signaling pathway is initiated by binding of secreted Wnts to their receptor from the frizzled family and their co-receptor named low density lipoprotein receptor-related protein-5 or -6 (LRP-5/-6). Association of dishevelled (dvl) with the cytoplasmic tail of frizzled receptor is thereby triggered. That activates phosphorylation of LRP-5/-6 by CK1γ which further sequesters Axin from the destruction complex to the membrane. Disruption of the destruction complex leads to the accumulation of cytoplasmic β-catenin which thus translocates into the nucleus. Nuclear β-catenin displaces groucho proteins and activates transcription factors from the TCF family. This family consists of four members: TCF-1, TCF-3, TCF-4 and lymphocyte enhancer factor- 1 (LEF-1) which share the same high mobility box needed for definition of TCF-family transcription sites. Target gene expression is further enhanced by recruitment of transcriptional enhancers such as legless, mediator, Hyrax or mastermind-like 1 (47, 50).

1.3.2. Wnt signaling antagonists

In non-malignant cells Wnt signaling is tightly controlled by its antagonists that can be divided into two functional classes: the secreted frizzled-related protein (sFRP) class and the dickkopf (DKK) class. Proteins of the sFRP class such as sFRP family members, Wnt inhibitor factor-1 (WIF-1) and Cerberus bind directly to secreted Wnts and thereby sequester the Wnts from their receptor (51). In contrast, proteins of the DKK class specifically inhibit canonical Wnt signaling by interacting with LRP-5/6 and thus disrupting the Wnt receptor signaling complex.

The DKK class comprises the secreted glycoproteins Wise and the proteins of the dickkopf family DKK-1 to -4. DKK-1 and DKK-4 act as inhibitors for Wnt signaling, whereas DKK-2 and DKK-3 were shown to have activating and inactivating actions on Wnt signaling which is dependent on the cellular context (52). DKK-1 is the most well studied member of its family. It was firstly identified as Wnt inhibitor in Xenopus where it controls head formation during embryogenesis (53). In the adult organism DKK-1 plays a crucial role in bone formation and bone mass regulation and initiates the restitution of colon epithelium during inflammation and wound healing (52, 54). Overexpression of DKK-1 in transgenic mice inhibits intestinal epithelial cell proliferation and leads to complete loss of colon crypts (55).

DKK-1 inhibits Wnt signaling by two distinct mechanisms. Firstly, DKK-1 binds to LRP-5/6 and thus inhibits the formation of the Wnt receptor signaling complex (56-58). Secondly, DKK-1 forms a ternary complex with LRP-6 and the transmembrane receptor Kremen 2 which initiates rapid complex internalization and thus removal of the Wnt

signaling receptor LRP-6 (59). In colon cells DKK-1 itself is a Wnt/β-catenin target gene (60). Moreover, DKK-1 expression can be increased by the active vitamin D metabolite 1α25-dihydroxyvitamin D_3, or pro-inflammatory cytokines such as tumor necrosis factor-α (TNF-α) or interferon-γ (IFN-γ) (61). During tumorigenesis the DKK-1 gene expression is frequently aborted due to promoter hypermethylation which contributes to uncontrolled Wnt signaling in colon cancer (14).

1.3.3. Wnt pathway in metastasis formation

Aberrant Wnt pathway activity is an initial event during colon tumorigenesis and substantially contributes to metastasis formation. The majority of colon cancers bear mutated components of the Wnt/β-catenin pathway. In about 90% of colon carcinomas the Wnt/β-catenin pathway is constitutively active due to a loss-of-function mutation in the APC gene (62). Mutated non-functional APC leads to disruption of the β-catenin destruction complex and thus to unhindered β-catenin/TCF target gene transcription. Non-APC mutated colon cancer cells often express either mutated Axin 2 which disrupts the destruction complex as well, or mutant β-catenin which is resistant to degradation-activating phosphorylation (63, 64). Besides initial mutations targeting at β-catenin degradation, the loss of Wnt antagonist expression can further amplify the aberrant β-catenin/TCF target gene transcription. Moreover, the loss of E-cadherin adhesion receptors which usually sequester cytoplasmic β-catenin from entering the nucleus potentiates constitutively active β-catenin/TCF target gene transcription (49, 60).

One target gene that increases the metastatic potential of the colon cancer cells is S100A4 (65). Stein et al. firstly identified S100A4 as Wnt/β-catenin target gene by comparing gene expression profiles of colon cancer cells that were heterozygous for a gain-of-function mutated β-catenin with derivative cells which only expressed wildtype β-catenin. As a result they found S100A4 to be massively upregulated due to increased levels of nuclear β-catenin. Promoter analysis of S100A4 demonstrated that β-catenin/TCF directly regulates the expression of S100A4. Moreover, β-catenin–induced effects on cell migration and invasion were mediated by S100A4. Those results provided the link between two previously unconnected molecular pathways which play important roles in tumor progression and metastasis in colorectal cancer: the Wnt/β-catenin pathway and S100A4.

1.4. S100A4

S100A4 was independently discovered by several groups under various names such as metastasin 1 (mts1), fibroblast-specific protein (FSP1), calcium placental protein (CAPL), murine placental homolog, 18A2, pEL98, p9Ka, 42A, and calvasculin (66). This ubiquitous 11 kDa Ca^{2+}-binding protein is one of the today 24 members of the S100 protein family which were named after their ability to be soluble in 100% ammonium sulphate (67). The expression of S100A4 is associated with many physiological processes such as wound healing, neurit outgrowth, fibrosis and neovascularisation, but also with pathological conditions such as cardiovascular diseases, tumor outgrowth, EMT, and metastasis formation (68, 69).

1.4.1. S100A4 gene structure and transcription

The S100A4 gene clusters together with most of the S100 gene family members in the epidermal differentiation complex located on human chromosome 1 (1q21). This region is frequently rearranged in human cancers (70). Consistently, S100A4 is overexpressed in many different types of cancer such as gallbladder, bladder, breast, oesophageal, gastric, pancreatic, hepatocellular, non-small cell lung, and colorectal cancer (71).

The S100A4 promoter region contains an erythroblastosis oncogene B (Erb) B2 signal response element which activates S100A4 expression in medulloblastoma via the MAPK pathway (72). In breast cancer cells the S100A4 promoter was sensitive to α6β4 integrin signaling which activated S100A4 transcription via the nuclear factor of activated T-cells-5 (NFAT5) transcription factor (73). In colon cancer cells S100A4 expression is activated via the TCF-4 binding site in the S100A4 promoter (65).

The S100A4 gene consists of four exons and three introns. The first intron of the S100A4 gene contains a positive regulatory enhancer region comprising at least six different *cis*-elements forming binding site for transcription factors such as SP-1, κB-motif binding protein, activating protein-1 (AP-1) and core-binding-factor (CBF) family members (74-76). Moreover, the first intron of S100A4 bears a hypoxia responsive element motif. In gastric cancer cells hypoxia inducible factor (HIF) binds within the first intron of the S100A4 gene to activate S100A4 expression upon hypoxia induced cellular stress (77).

The first two exons are located in the 5' UTR and are thus non-coding (78). Exon 2 is only present in the longer variant of the two S100A4 mRNA splice variants which are 512 and 564 bp in size, respectively. Both splice variants are differentially expressed in

different tissues; for instance the long variant is predominantly present in normal colon tissue, whereas the short variant is predominantly expressed in liver and blood cells. However, no functional differences between those splice variants were defined up to now, since both S100A4 mRNA variants encode the same amino acid sequence and are equally efficiently translated (79).

1.4.2. S100A4 protein structure

The S100 protein family of Ca^{2+}-binding proteins presents high sequential and structural homology. Like most of the S100 proteins, S100A4 is a symmetrical homodimer which is stabilized by non-covalent binding of the first and the last helix of each subunit.

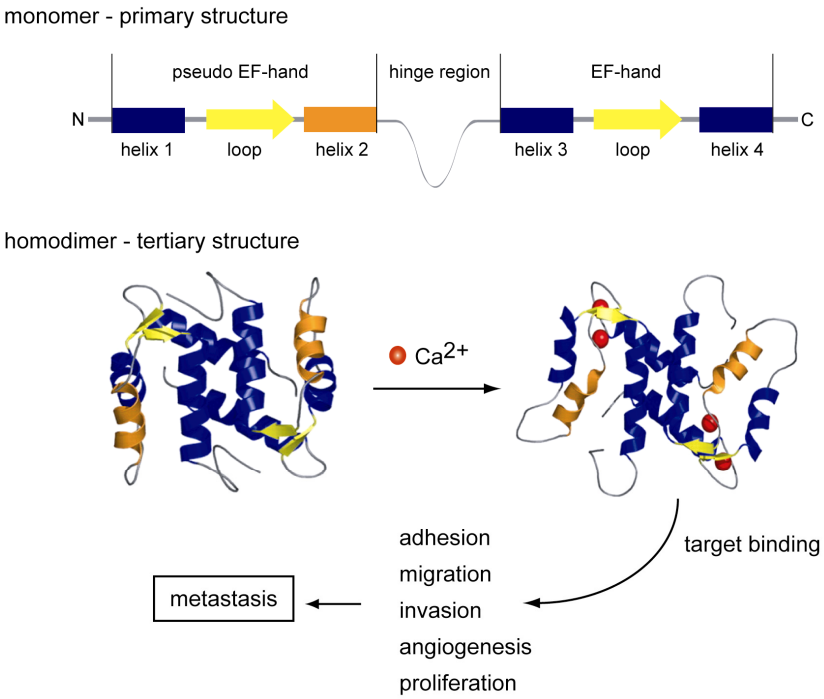

Fig. 1.3 The S100A4 protein. The primary structure of S100A4 consists of two EF-hands which are connected by a hinge region. Each EF-hand consists of a helix-loop-helix-motif, whereas each loop can bind one Ca2+ ion. Upon Ca2+-binding the S100A4 protein undergoes a conformation shift, thus opens up the hinge region which is needed for interaction with S100A4 binding partners. Via its interaction with a list of different target proteins, S100A4 regulates many cellular processes needed for metastasis formation. Modified after Garrett (66).

Each subunit of S100A4 consists of two EF hands connected by a less sequentially conserved hinge region (80). EF hands are defined by a helix-loop-helix motif of which the 12 amino acid long loop region constitutes a binding pocket for one Ca2+ ion. Additionally to the canonical EF hand at the C-terminus, S100 proteins are characteristic for their N-terminal pseudo EF hand. The loop of the N-terminal EF hand

consists of 14 amino acids. This elongation by two amino acids results in a lower affinity to Ca2+. Consequently, Ca2+-binding occurs sequentially, first at the C-terminal and subsequently at the N-terminal EF-hand (81). Upon Ca2+-binding a conformational shift is triggered which opens up two major hydrophobic binding sites partly formed by the hinge region (82). Residues of the hinge region as well as the long C-terminal tail of S100A4 share almost no sequence homology within the S100 protein family (83). Hence those regions confer specificity towards potential protein targets which are the basis for the manifold interactions of S100A4 that drive metastasis formation.

1.4.3. S100A4 loosens cell adhesion

Reduction of cell adhesions enables the dissociation of a cell from its tight tissue assembly which is an initial step in the process of cancer cell invasion. S100A4 was found to modulate cell-cell adhesion via downregulation of E-cadherin. E-cadherin is a transmembrane cell surface glycoprotein which mediates Ca^{2+}-dependent cell-cell adhesion and therefore acts as invasion suppressor. Ectopic overexpression of E-cadherin results in a decrease in S100A4-expression (84). *Vice versa*, S100A4 overexpression suppresses E-cadherin expression, thereby reducing cell adhesion and inducing a more invasive cell phenotype (85). Consistently, S100A4 and E-cadherin are inversely expressed in many tumor types, whereby high levels of S100A4 and low level of E-cadherin promoted a highly metastatic phenotype (84-88).

S100A4 was further found to influence cell-matrix adhesions by interacting with liprin β1 (89). S100A4 binds to liprin β1 thereby masking the PKC-mediated phosphorylation sites (89). Phosphorylation of liprin β1 is needed for crosslinking of leukocyte common antigen-related (LAR) protein on the cell surface to stably form focal adhesions (90). Inhibition of the liprin β1-LAR complex by S100A4 loosens cell adhesion and allows cell invasion.

1.4.4. S100A4 increases cell migration

The process of migration comprises the formation of flexible protrusions, lamellipod extensions, formation of focal contacts at the leading edge, and finally the retraction of the opposed cell tail towards the leading lamella. This process is dependent on the rearrangement of cytoskeleton proteins such as actin, myosin or tropomyosin.

The presence of intracellular S100A4 is known to increase cell migration. Consistently, S100A4 was found to co-localize with actin filaments in transformed rat embryonic fibroblasts leading to disorder of stress fibers (91). Moreover, co-sedimentation assays revealed that S100A4 aggregated with F-actin in the presence of Ca^{2+}. S100A4 further

binds to tropomyosin and non-muscle myosin II-A (92-95). Non-muscle myosin II-A is a chemo-mechanical cytoskeleton protein that participates in cell division, cell motility, and secretion. S100A4 binds to myosin II-A in a Ca^{2+}-dependent manner and inhibits the actin-regulated ATPase activity of myosin II-A (93, 96). Thereby it promotes the disassembly of myosin filaments and inhibits their reassembly (95, 96).

S100A4 is located at the leading edge of migrating cells (97), where it induces the formation of flexible protrusions. Moreover, in the presence of a chemo-attractant, S100A4 enhances directed migration (98). Directed migration is dependent on the interaction of S100A4 with myosin II-A, since an antibody which binds at the S100A4 binding sites of myosin II-A also mimicked the formation of directed protrusions. In conclusion, the S100A4-myosin II-A interaction does not only increase cell motility, but also enhance cell polarization and directed migration.

In contrast, the S100A4-myosin II-A interaction is inhibited in the presence of S100A1. Yeast two hybrid screening identified the S100 family protein S100A1 as a binding partner for S100A4 (99, 100). Titration of S100A1 to S100A4 and myosin II-A inhibited the S100A4-mediated depolimerization of myosin filaments. Furthermore, in a rat breast cancer model, the co-expression of S100A4 and S100A1 inhibited S100A4-driven metastasis formation (101). Consistently, in colon cancer tumors S100A1 overexpression occurs in non-malignant epithelial cells, but S100A1 is absent in metastatic cells with overexpressed S100A4 (102).

S100A4 was found to bind to the septines 2, 6 and 7 (103). Septines play a central role in cytokinesis, cell polarity determination, cytoskeletal reorganization, and membrane dynamics (104). Therefore, the S100A4-septine interaction might contribute to the process of migration. However, no direct function of this protein-protein interaction has been determined so far.

More recently, a yeast two hybrid screening identified CCN3 (cystein-rich 61-connective tissue growth factor-nephroblastoma overexpressed-family member 3), as a binding partner of S100A4 (105). Furthermore, it was shown that CCN3 overexpression in glioma and neuroblastoma cells increases intracellular Ca^{2+} concentration in cell protrusions. This would be in line with S100A4 being dependent on increased Ca^{2+} concentrations to increase cell motility.

Table 1.1 Interaction partners of S100A4 and their functional impact on metastasis formation.

Target	Cellular function	Model	Ref.
intracellular			
CCN3	unknown	yeast two hybrid assay	(105)
F-actin	disorder of stress fibers	rat embryonic fibroblasts; cell-free assays	(91, 95)
liprin-β1	decrease of cell adhesion	mouse mammary adenocarcinoma cells	(89)
MetAP2	potential enhancement of angiogenesis	human embryonic kidney cells; mouse endothelial cells; yeast two hybrid assay; cell-free assays	(106)
myosin II-A	depolymerization of myosin filaments, formation of flexible protrusion	human acute myeloid leukemia and breast cancer cells; mouse mammary adenocarcinoma cells; cell-free assays	(93-98, 107)
p37	increased Ca^{2+} affinity	cell-free assay	(108)
p53	oligomerization/ nuclear localization of p53	human breast cancer, osteosarcoma, colon cancer, rabdomyosarcoma, prostate cancer and pancreas carcinoma cells; mouse mammary adenocarcinoma cells and fibroblasts; cell-free assay	(70, 109-113)
p63, p73	unknown	cell-free assay	
S100A1	inhibition of S100A4-induced metastasis	human breast cancer cells; rat mammary cells; mouse mammary adenocarcinoma cells; yeast two hybrid assay; cell-free assays	(99-101)
septin 2, 6, 7	unknown	cell-free assay	(103)
tropomyosin	interference with tropomyosin-F-actin interaction	mouse embryonic fibroblasts	(92)
extracellular			
amphiregulin	stimulation of EGFR signaling	mouse embryonic fibroblasts	(114)
annexin II	conversion of plasminogen to plasmin, induction of angiogenesis	primary human cerebromicrovascular endothelial cells	(115)
MAP	rearrangement of extracellular matrix	bovine aortic smooth muscle cells	(116)
RAGE	stimulation of MMP expression for invasion	chondrocytes, cell-free assay	(117-119)
S100A4 oligomer	increase of intracellular Ca^{2+}, angiogenesis	mouse mammary adenocarcinoma cells; cell-free assays	(117, 120, 121)

The table summarizes all the proteins which are known to interact with S100A4 both in the intracellular or extracellular compartments. CCN3, cystein-rich 61-connective tissue growth factor-nephroblastoma overexpressed-family member 3; MetAP2, methionine aminopeptidase 2; MAP, microfibrill-associated glycoprotein; RAGE, receptor for advanced glycation endproducts.

1.4.5. S100A4 increases cell invasion

Cell invasion is dependent on the rearrangement of extracellular matrix proteins. S100A4 was firstly discovered to bind microfibrill-associated glycoprotein (MAP) in the extracellular compartment of bovine aortic smooth muscle cells (116). This binding was Ca^{2+}-dependent. It was suggested that S100A4 binding affects the network of extracellular matrix proteins thereby enabling cell invasion.

Cell invasion is further facilitated by matrix metalloproteinases (MMPs) which catalyze the proteolytical cleavage of extracellular matrix proteins. Extracellular S100A4 was shown to induce the expression of several MMPs. In mouse endothelial cells extracellular S100A4 stimulates the expression and secretion of MMP-13 which leads to increased cell invasion (122). In osteosarcoma and neuroblastoma cells downregulation of S100A4 was concomitant with a decrease of MMP-2 expression and activity, accompanied with impaired cell invasion (123, 124). S100A4 overexpression lead to induction of MMP-9 expression and increased MMP-9 proteolytic activity in human prostate cancer (125). Extracellular oligomeric S100A4 induced the expression of MMP-1, MMP-3, MMP-9 and MMP-13 in human synovial fibroblasts which were isolated from rheumatoid arthritis or osteoarthritis patients (126).

Stimulation of MMP expression by extracellular S100A4 is likely to depend on a membrane associated receptor. One receptor that mediates S100A4 signaling is the receptor for advanced glycation endproducts (RAGE). In chondrocytes S100A4 stimulated MMP-13 overexpression via binding to RAGE (119). Furthermore, extracellular S100A4 mediated effects can be abolished by extracellular addition of soluble RAGE, which has no signaling activity but captures S100A4 from binding to membrane-associated RAGE (127). In human salivary gland cells extracellular S100A4 induced RAGE expression via activation of the NFκB pathway (128). Thereby, S100A4 induces a positive feedback loop in RAGE signaling. However, extracellular S100A4 is able to induce cell invasion and capillary-like growth in RAGE-negative cells through a yet undefined cell surface receptor (122, 129).

1.4.6. S100A4 enhances angiogenesis

Angiogenesis describes the development of new blood vessels from pre-existing ones to optimize the oxygen and nutrient supply within the tumor tissue and the removal of waste products. Ambartsumian et al. firstly described that the blood vessel network in S100A4 positive tumors was more pronounced than that of S100A4-negative tumors *in vivo* (120). Furthermore, increase of extracellular S100A4 oligomers enhanced endothelial cell motility *in vitro* and stimulated the corneal neovascularization *in vivo*.

S100A4 was further found to bind annexin II (115). S100A4-annexin II interaction induced capillary-like tube formation of primary human cerebromicrovascular endothelial cells. Annexin II was exposed on the surface of endothelial cells. In the presence of S100A4 the conversion of plasminogen to plasmin was stimulated. Active plasmin further activates MMPs. Active MMPs and plasmin together induce extracellular matrix remodeling and thereby facilitate angiogenesis (130).
Intracellular S100A4 also enhances angiogenesis by interacting with methionine aminopeptidase 2 (MetAP2). MetAP2 is known to catalyze the removal of translation initiating methionine from nascent peptides in endothelial cells (106). Moreover, MetAP2 is a common target for pharmaceutical inhibition of angiogenesis. Ca^{2+}-dependent binding of S100A4 to MetAP2 modulated the MetAP2 activity which could promote endothelial growth and angiogenesis. However, the exact mechanism still needs to be elucidated.

1.4.7. S100A4 and cell growth

In certain entities S100A4 was found to control cell proliferation. Targeting S100A4 by shRNA led to decreased cell proliferation in pancreatic and breast cancer cells and reduced tumor growth in gastric cancer xenograft mice (14, 73, 131). Cell proliferation of S100A4-null mouse embryonic fibroblasts was stimulated by extracellular interaction of S100A4 with amphiregulin which subsequently activated epidermal growth factor receptor (EGFR) signaling (114).
Several studies have demonstrated the binding of S100A4 to p53 (70, 109, 110, 112, 113). Upon recognition of a variety of cellular stresses and DNA damages, p53 controls cell cycle arrest, DNA repair and/or apoptosis. Mutation of this tumor suppressor gene is a frequent event in all types of human cancers (132). S100A4 controls the localization of p53 within the cell. Nuclear co-localization of p53 and S100A4 was observed in colon cancer cells (133). Nuclear transition of p53 occurs preferably in its monomeric state (134). Consistently, S100A4 binds at the tetramerization domain of p53 and therefore shifts the equilibrium from p53 oligomers to the monomeric state (70). Moreover, nuclear translocation of p53 is inhibited by C-terminal PKC phosphorylation. Phosphorylation stabilizes p53 tetramerization and aborts its nuclear translocation. S100A4 was found to mask those C-terminal PKC phosphorylation sites on p53 (109). By controlling p53 nuclear translocation S100A4 could abolish the tumor suppressor function of p53, thus enhancing tumor growth. However, no direct impact of the p53-S100A4 interaction on cancer growth or metastasis was yet shown and therefore requires further investigation (132).

1.4.8. S100A4 drives metastasis formation *in vivo*

S100A4 was firstly shown to promote metastasis formation of mouse mammary adenocarcinoma cells by Ebralidze et al. (135). Since then several studies have confirmed the metastatic potential of S100A4 in xenograft models for a great many of different cell types (69). For instance, overexpression of S100A4 in usually non-metastatic mouse or human breast cancer cells led to increased tumor invasiveness, and the formation of lymph node and distant lung metastases (136, 137). Comparison of the metastatic potential of human pancreatic cancer cells in xenograft mice revealed that only S100A4 overexpressing cell lines were able to form liver metastases (138). In colon cancer cells, the exogenous overexpression of S100A4 increased the number and size of liver metastasis after intracardial and intrasplenic transplation of xenograft mice (65).

Surprisingly, S100A4 knock-in mice present no abnormal phenotypic features and especially do not develop tumors per se, suggesting that S100A4 itself is not tumorigenic (139). However, when crossed into a tumorigenic background, the offspring presented highly aggressive primary tumors and increased formation of metastasis (140). Further, tumors in those mice were massively infiltrated by leukocytes generating an inflammatory milieu which facilitated tumor spreading (141).

S100A4 knock-out mice are fertile, grow normally and show no severe abnormalities, but present impaired chemotactic recruitment of macrophages to inflammatory sites (142). Orthotopic injection of highly metastatic mouse mammary carcinoma cells into these mice lacked the formation of lung metastases. However, the metastatic potential of these mammary carcinoma cells was reactivated, when cells were co-injected with S100A4 positive fibroblasts (143). Co-injection of oestrogen-dependent breast cancer cells with S100A4 overexpressing fibroblasts in xenograft mice also increased tumor growth even in the absence of oestrogen (144). These studies further constitute S100A4 as a mediator for metastasis formation *in vivo.*

1.4.9. S100A4 expression correlates with metastasis in colon cancer patients

S100A4 overexpression is associated with poor survival and increased occurrence of metastasis in many cancer entities such as breast, gallbladder, pancreatic, lung squamous cell, renal cell, prostate, and esophageal squamous cell cancer (145-151).

In colon cancer the level of S100A4 expression increases with the developmental stage of the colon tumor. In normal colon tissue S100A4 mRNA and protein is not or only very weak expressed (65, 152). Similarly, in adenomas S100A4 expression is very rare. In contrast, in early carcinomas the expression of S100A4 is more frequent and

the frequency even increases in late carcinomas. However, S100A4 expression is most abundant in liver metastasis (153, 154).

Several independent studies analysed the correlation of S100A4 expression levels in colon tumor tissue with clinical data in order to investigate the prognostic value of S100A4. For instance, high levels of S100A4 protein expression were associated with lymph node metastasis (152). Increased levels of S100A4 mRNA significantly correlate with reduced metastasis-free and overall-survival of colon cancer patients (65). In resected colon tumor tissue S100A4-positive immunohistological staining correlated with a 2-fold reduction of patient's five year survival rate (34, 155). S100A4 was prognostic for metastasis and adverse disease outcome independent on the progression stage of the disease (155). Moreover, the subcellular localization of S100A4 was found to be differentially prognostic for metastasis and overall survival. Immunohistochemical staining for nuclear S100A4 highly correlated with metastasis formation and reduced overall survival of colon cancer patients. In contrast, cytoplasmatic S100A4 was not statistically prognostic for the disease outcome (156, 157). More recently, quantification of S100A4 mRNA in blood of colon cancer patients was shown by Stein and colleagues to be specifically and sensitively diagnostic for the colon cancer stage and prognostic for the patient's risk to develop metastases (158).

In summary, these studies establish a prognostic value of S100A4 and thus further emphasize the central role for S100A4 in the progression of colon cancer metastasis.

1.5. Inhibition of S100A4 expression for therapeutic intervention

Since the discovery of S100A4, many studies have proven its central role in metastasis formation (69). Hence targeting S100A4 expression provides a promising strategy for rational anti-metastatic therapies (159). In cooperation with the National Cancer Institute in Frederick, Maryland, USA, PD. Dr. W. Walther, Prof. Dr. U. Stein (both Experimental and Clinical Research Center, Charité University Medicine, Berlin at the Max Delbrück Centrum Berlin-Buch) and colleagues performed a high throughput screening (HTS) to identify potential S100A4 expression inhibitors.

The HTS was based on the S100A4 promoter comprising the sequence from -1487 bp to +33 bp surrounding the S100A4 transcription start site which was cloned upstream of the firefly luciferase reporter gene (Fig. 1.4). This construct was stably introduced into the human colon cancer cell line HCT116, which bears a constitutively active Wnt pathway and therefore presents high activity of the S100A4-promoter. In the HTS these generated HCT116/S100A4pLUC cells were exposed to compounds of the Library of

Pharmacologically Active Compounds (LOPAC). The LOPAC library represents a collection of well characterized small molecules which were shown to interfere with different biological functions. HCT116/S100A4pLUC cells were treated with 0.1 µM, 1 µM, 10 µM and 100 µM dilutions of each compound for 24 h, respectively, and luciferase activity as read-out for S100A4 promoter-driven reporter gene expression as well as cell viability were analyzed. From a total number of 1,280 compounds, 34 compounds were found to inhibit luciferase activity to less than 50% of control cells. In parallel, cell viability was determined to separate cytotoxicity-related reporter reduction from real expression inhibitory effects. From the 34 effective compounds, 11 compounds efficiently inhibited luciferase activity at concentrations which were non-toxic or only slightly affected cell viability. These 11 compounds were titrated using twenty 2-fold dilutions with a high test concentration of 100 µM. The titration confirmation identified niclosamide and calcimycin as the strongest candidates to inhibit luciferase activity at maximum with minimal cytotoxicity. The effective concentration 50 (EC_{50}) in the high throughput screening was measured to be 1.7 µM and 2.7 µM for niclosamide and calcimycin, respectively.

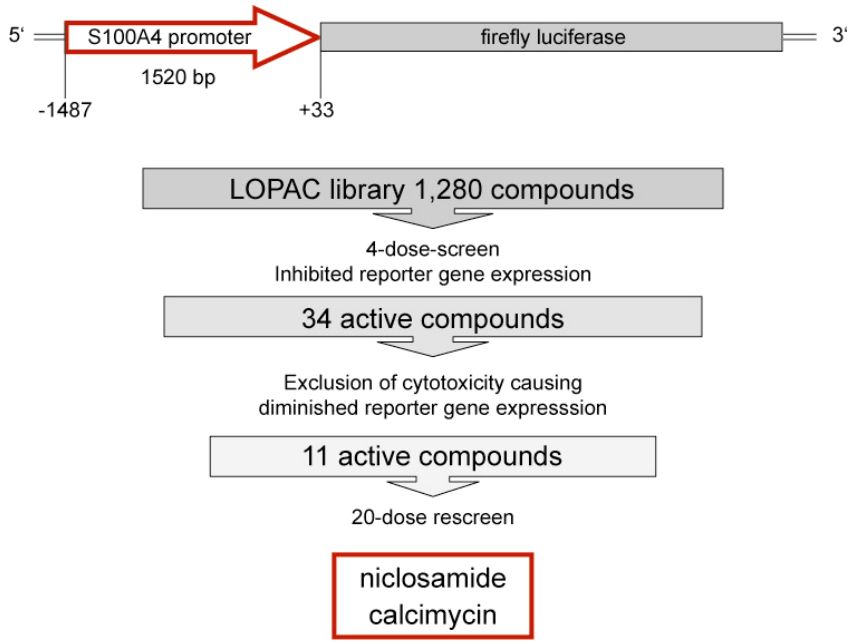

Fig. 1.4 High throughput screening for S100A4 expression inhibitor. The S100A4 promoter was cloned upstream of a reporter gene. The cloned construct was stably introduced into human colon cancer cells which were exposed to 1,280 compounds of the library of pharmaceutically active compounds (LOPAC). In a 4 dose-screen 34 compounds presented reduced luciferase activity. Of those, 11 compounds reduced luciferase activity without affecting cell viability to less than 50%. A 20-dose re-screen identified niclosamide and calcimycin to be the strongest candidates with respect to reduce reporter activity at non-toxic concentrations.

1.6. Identification of the molecular mechanism underlying S100A4-driven metastasis

Many interaction partners of S100A4 that explain the action of S100A4 in the cell to drive metastasis formation have been identified (160). However, less is known about the transcriptional changes which occur upon S100A4 upregulation and which are needed for the metastatic phenotype. To identify the transcriptional mechanism underlying S100A4-driven metastasis, Stein and colleagues performed a gene expression profiling using a Human OncoChip array (35K probe cDNA arrays from the NCI/CCR microarray center) at the National Cancer Institute, Frederick. They applied the HCT116 derivative cell line HAB92^{wt} which is monoallelic for wildtype β-catenin and thus presents reduced Wnt pathway activity and very low levels of S100A4 expression. HAB92^{wt} cells were further stably transfected with S100A4 cDNA or the empty vector as control.

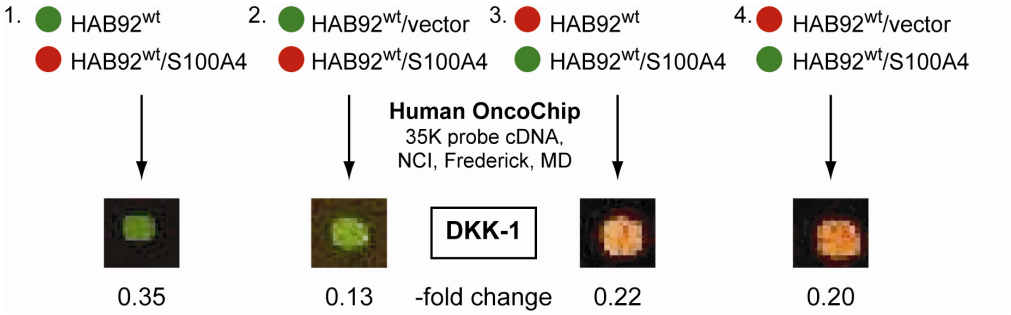

Fig 1.5 Gene expression profiling of S100A4 overexpressing cells. HAB92^{wt} cells are HCT116 derivate cells in which the mutated β-catenin allele was depleted. Thus these cells present reduced Wnt pathway activity and very low expression of S100A4. HAB92^{wt} cells were either transfected with the S100A4 cDNA (HAB92/S100A4) or the empty vector as control (HAB92/vector). The reverse-transcribed mRNA was labeled with Cy5 (red) and Cy3 (green) as indicated and applied on a Human OncoChip 35K probe cDNA array. 256 genes were regulated more than 3-fold, with DKK-1 being 4-fold down regulated due to overexpression of S100A4.

To set up the microarray, isolated mRNA from HAB92^{wt}, HAB92^{wt}/vector and HAB92^{wt}/S100A4 cells was reversely transcribed and labeled with Cy5 (red) and Cy3 (green) as indicated in Fig 1.5. Labeled cDNA was hybridized to the arrays and fluorescence was read in GenePix 4100A microarray scanner. The data was analyzed through GenePix Pro 4.1 software and the microarray intensity was normalized by setting the Ratio of Medians to 1. Data was analyzed with available tools on mAdB including Significance Analysis of Microarrays (SAM) (161), prediction analysis of Microarrays (PAM) (162), and DAVID/EASE functional analysis (163). Among the 256 genes which were more than 3-fold regulated, the Wnt antagonist DKK-1 was identified.

2. AIM

Taken together, the intensive research of the last two decades that is summarized in the preceeding pages provides profound evidence that S100A4 is a central mediator for metastasis formation which is still the major burden for colon cancer patients. Many interaction partners of S100A4 were described explaining its metastasis promoting ability. However, fewer investigations were concentrated on the inhibition of S100A4 to impair its metastasis-driving functions. Moreover, little is known about the transcriptional consequences of S100A4 overexpression, which might play a decisive role in S100A4-induced metastasis formation.

Against this background, the aim of this study is to evaluate the potential of the small molecules niclosamide and calcimycin to function as inhibitors targeting S100A4 expression and to investigate their efficiency to repress S100A4-induced cell motility. Moreover, the mechanism by which the small molecules could interfere with S100A4 expression was to be elucidated. Thus, with respect to future anti-metastatic treatments, the applicability and efficiency of the small molecules to inhibit S100A4-induced metastasis formation was to be investigated. Within the scope of the project, a human colon cancer xenograft mouse model needed to be installed to monitor S100A4-induced metastasis formation *in vivo* by non-invasive bioluminescence imaging. Moreover, the relation of S100A4 to the Wnt/β-catenin pathway inhibitor DKK-1 was investigated to further understand the molecular mechanism of S100A4 action in metastasis formation.

3. MATERIALS AND METHODS

3.1. Cloning

DNA was digested with FastDigest® Restriction Enzymes in 1x FastDigest® Buffer (both Fermentas) at 37 °C for 1 h. Digested DNA was separated by agarose gel electrophoresis at 100 V for 30 min in gels containing 0.8% w/v agarose (Invitrogen) in TAE-buffer (40 mM Tris, 1 mM Na_2EDTA and 20 mM acetic acid, pH 8).
DNA was purified from the agarose gel using Invisorb® Spin DNA extraction Kit (Invitek) according to the manufacturer's instructions. DNA was ligated in a 1:10 ratio of vector backbone and inserted using 0.25 U/µl T4 Ligase in 1x Ligase Buffer (both Fermentas) at 14°C, overnight. Bacterial transformation was performed in Subcloning Efficiency™ DH5α™ Chemically Competent Cells (Invitrogen) according to the manufacturer's instructions. Transformed bacteria were spread on selective agar plates and allowed to grow overnight at 37°C. DNA plasmid preparation from positive colonies was performed with Invisorb ® Spin Plasmid Mini Two (Invitek). Control digest of plasmids followed by agarose gel electrophoresis identified positive clones. For transfection, plasmids were isolated with endotoxin-free plasmid DNA Maxi Prep using the JETSTAR 2.0 Maxi (Genomed). Cloned constructs were sequenced for correct in frame orientation (sequencing service, Invitek).

3.1.1. S100A4 cDNA expression vector

The S100A4 cDNA was cloned into a vector with a puromycin resistance cassette to allow selection of successful transfected HAB92wt cells which already beard a neomycin resistance.
The S100A4 cDNA was cut with HindIII and XbaI from the pcDNA3-neomycin-S100A4cDNA vector, which was a kind gift from Claus Heizmann (University of Zurich, Zurich, Switzerland) and ligated into the pcDNA3-puromycin vector, which was a kind gift from Dr. Jörn Lausen (AG Leutz, MDC, Berlin, Germany). Control digest of plasmids with NcoI or SmaI identified positive clones. Plasmid was purified and sequenced as described in section 3.1.

3.2. Cell culture

3.2.1. Colon cancer cell lines

Cell culture media, PBS and Trypsin/EDTA solution were obtained from PAA Laboratories. Cell culture plastic ware was obtained from TPP, BD Biosciences or Greiner BioOne. All human colon cancer cell lines used in this study are summarized in Table 3.1. If not stated otherwise, the colon cancer cell lines were kindly provided by Prof. Dr. W. Birchmeier and Prof. Dr. Ulrike Stein. Cells were maintained in DMEM or RPMI 1640 medium supplemented with 10 % FBS in a humidified incubator at 37°C and 5 % CO_2. Cells were trypsinized and split in a 1:4 ratio every 3-4 days.

Table 3.1 Summary of all colon cancer cell lines used in this study

Cell line	Medium	ATCC number
Caco2	DMEM, 10 % FBS	HTB-37
Colo205	RPMI 1640, 10 % FBS	CCL-222
DLD1	DMEM, 10 % FBS	CCL-221
HCT15	RPMI 1640, 10 % FBS	CCL-225
HCT116	RPMI 1640, 10 % FBS	CCL-247
HT29	DMEM, 10 % FBS	HTB-38
KM12	RPMI 1640, 10 % FBS	CRL-12496
Lovo	RPMI 1640, 10 % FBS	CCL-229
LS174T	DMEM, 10 % FBS	CCL-188
SW48	RPMI 1640, 10 % FBS	CCL-231
SW480	RPMI 1640, 10 % FBS	CCL-227
SW620	RPMI 1640, 10 % FBS	CCL-228
WiDr	RPMI 1640, 10 % FBS	CCL-218

The central column depicts the cell culture medium used for each cell line. All cell lines are registered in the American type culture collection (ATCC).

3.2.2. Transfections

The constructs used in transfection experiments are summarized in Tables 3.2 and 3.3. $1x10^6$ cells were plated in a 10 cm Ø dish 24 h before transfection occurred. For each transfection reaction 15 µl Fugene HD (Roche), 10 µg plasmid and 500 µl serum-free DMEM were incubated for 15 min at room temperature, and then added to the cells of 70% confluence in a total volume of 5 ml RMPI 1640 medium. After 48 h, selection of positive transfected cells occurred with 1 mg/ml neomycin and/or 1 µg/ml puromycin. Antibiotics were continuously present and only removed 24 h before cells were used in experiments to avoid their interference.

3.2.3. HCT116 derivative cells

The HCT116 derivative cells HAB92^{wt} and HAB68^{mut} were a kind gift from Todd Waldman (Georgetown University, Washington). HAB92^{wt} and HAB68^{mut} cells were generated from HCT116 cells, which are heterozygous for a gain-of-function mutated Δ45-β-catenin. To obtain HAB92^{wt} and HAB68^{mut} cells the respective mutated or wild-type allele of β-catenin was replaced by a neomycin resistance cassette via homologous recombination (164). Cell lines were tested regularly for the correct β-catenin genotype by restriction fragment length polymorphism (section 3.4.4).

HCT116/S100A4 and HCT116/vector cells as well as HAB92^{wt}/S100A4 and HAB92^{wt}/vector cells were obtained by transfection of HCT116 or HAB92^{wt} cells, respectively, with pcDNA3.1-cmv-S100A4cDNA or the empty vector as control. Stable expression of transgene was regularly tested with quantitative real-time PCR (section 3.4.3).

HCT116/LUC cells applied in *in vivo* imaging experiments were obtained by transfection of HCT116 with pcDNA3.1-puro-LUC. Stable expression of transgene was controlled regularly by Steady Glow^{TM} Luciferase Assay System (Promega) according to the manufacturer's instructions.

Table 3.2 Plasmids used for colon cancer cell transfection

Plasmid	Features
gene overexpression	
pcDNA3.1-puro-S100A4	CMV promoter-driven S100A4 cDNA (long variant); puromycin resistance
pcDNA3.1-puro	CMV promoter; puromycin resistance
pcDNA3.1-puro-LUC	CMV promoter-driven firefly luciferase cDNA; puromycin resistance
shRNA interference	
pGeneClip-puro-shDKK-1	U1 promoter driven shRNA sequence targeting DKK-1; 5'-GGA CAA GAA GGT TCT GTT TGT-3'; puromycin resistance
pGeneClip-puro-shS100A4	U1 promoter driven shRNA sequence targeting S100A4; 5'-CCA GAA GCT GAT GAG CAA CTT-3'; puromycin resistance
pGeneClip-puro-shcon	U1 promoter driven control shRNA sequence; 5'-GGA ATC TCA TTC GAT GCA TAC-3'; puromycin resistance

The table depicts the plasmids and their features used for gene overexpression of RNA interference. The DKK-1 or S100A4 gene-specific shRNA sequences and the sequence of the non-targeting shRNA are given.

3.3. Drugs and treatments

3.3.1. RNA interference

RNA interference using short hairpin RNA (shRNA) which target the S100A4 or DKK-1 mRNA was performed with SureSilencing^{TM}shRNA plasmids (SA Biosciences). For each gene four different shRNA sequences were designed and tested by transient transfection of cells. The expression of the shRNA targeted mRNA was analyzed by quantitative real-time PCR (section 3.4.3) after 24 h and 48 h of transfection. The most efficient shRNA sequence, decreasing target gene expression to less than 50 %, is shown in Table 3.2 and was used for stable transfection of HCT116 or HAB92^{wt} cells. As a control a non-functional shRNA sequence, tested by SA Biosciences to have no mRNA target, was used. Selection of stable transfectants was performed with neomycin (1 mg/ml) and/or puromycin (1 µg/ml).

3.3.2. Small molecules

The small compound inhibitors niclosamide (2',5-dichloro-4'-nitrosalicylanilide) and calcimycin were obtained from Sigma. Niclosamide derivatives were obtained from the Drug Synthesis and Chemistry Branch, Developmental Therapeutics Program, NCI, Bethesda, MD. Analysis of the 2D and 3D structure of niclosamide and its derivatives was performed with MarvinSketch and MarvinSpace version 5.2.3_1. All drugs were solubilized in dimethylsulfoxide (DMSO) for *in vitro* application. To exclude adverse effects caused by DMSO, control cells were always treated with the equal amount of solvent. *In vivo* niclosamide was administered as suspension in 10 % cremophore EL (BASF) and 0.9 % NaCl solution.

3.3.3. Recombinant DKK-1 protein

Recombinant DKK-1 protein (rDKK-1) was obtained lyophilized from R&D Systems and was dissolved in sterile filtered 1 % w/v BSA/PBS solution. Dissolved rDKK-1 was stored at 4 °C for two weeks at maximum. Control cells were treated with the respective amount of 1 % w/v BSA/PBS solution.

3.3.4. Cytotoxicity assay

Analysis of cell cytotoxicity was performed with AlamarBlue™ *(*AbD Serotec) according to the manufacturer's instruction. Briefly, 1x10^5 cells were seeded into 96-well-plates and allowed to accommodate for 24 h. The cells were exposed to different concentrations of a compound or its solvent for 24 h. 10 % v/v AlamarBlue™ was

added and incubation for 3 h at 37°C in a humidified incubator allowed AlamarBlue reduction to occur. The absorbance of reduced and oxidated AlamarBlue was measured at 620 nm and 560 nm, respectively, in the absorbance reader SpectraFluor Plus (Tecan). Cell viability was determined by dividing the absorbance ratio of reduced and oxidated AlamarBlue of treated cells by the ratio obtained from untreated cells which was defined as 100 % cell viability.

3.4. Gene expression analysis

3.4.1. RNA isolation

Total RNA was isolated from $4x10^5$ cells plated in a 6-well-plate 24 h before cells were lyzed with Trizol Reagent (Invitrogen). RNA was isolated according to the Trizol/chloroform extraction protocol as described earlier (165). Precipitation of RNA from the watery phase occurred by addition of isopropanol at -20°C overnight and subsequent centrifugation at 14,000 rpm for 15 min. Precipitated RNA was resolved in ddH_2O and stored at -80°C. Quantification of the RNA concentration was performed with Nanodrop (Peqlab).

3.4.2. Reverse transcription

For each sample, 50 ng total RNA was reversely transcribed. Reverse transcription of 250 ng total RNA isolated from HCT116 cells was used for the standard curve. Reverse transcription was performed with random hexamers in 10 mM $MgCl_2$; 1x RT-buffer, 250 µM pooled dNTPs, 1 U/µl RNAse inhibitor and 2.5 U/µl MuLV reverse transcriptase (all Applied Biosystems). Reaction occurred at 42 °C for 15 min, 99 °C for 5 min and subsequent cooling at 5 °C for 5 min. Reverse transcripts were either stored at -20 °C or directly used for quantitative real-time PCR or restriction fragment length polymorphism analysis.

3.4.3. Quantitative real-time PCR

If not stated otherwise, all material used for quantitative real-time PCR (qPCR) was obtained from Roche. The primer and probe design was obtained from the Sigma OligoDesign Service. Probes were obtained from Sigma and primers were obtained from Biotez. Table 3.3 summarizes all primers and probes used for qRT-PCR in this study.

For quantification of β-catenin, DKK-1 and S100A4 cDNA hybrid probe based qRT-PCR was performed with the FastStart DNA Master HybProbe Kit according to the manufacturer's instructions. Quantification of Cyclin D1 and c-myc cDNA was performed with SYBR green based qRT-PCR using the FastStart DNA Master SYBR Green I Kit according to the manufacturer's instructions. Each qRT-PCR reaction was performed in duplicate and in parallel to the cDNA quantification of the housekeeping gene glucose-6-phosphate dehydrogenase (G6PDH) using primers and probes from the LightCycler® hG6PDH Housekeeping Gene Set.

Table 3.3 Primers and probes used in quantitative real-time PCR

Primer/probe	Sequence 5'- 3'
β-catenin-F	GTG CTA TCT GTC TGC TCT AGT A
β-catenin-R	CTT CCT GTT TAG TTG CAG CAT C
β-catenin-FITC	AGG ACT TCA CCT GAC AGA TCC AAG TCA-FITC
β-catenin-LCRed640	LCRed640-CGT CTT GTT CAG AAC TGT CTT TGG ACT CTC-phosphate
c-myc-F	ACC CTT GCC GCA TCC ACG AAA C
c-myc-R	CGT AGT CGA GGT CAT AGT TCC TGT TGG
Cyclin D1-F	CTG TTT GGC GTT TCC CAG AGT CAT C
Cyclin D1-R	AGC CTC CTC CTC ACA CCT CCT C
DKK-1-F	TAG CAC CTT GGA TGG GTA TTC
DKK-1-R	ATA TTT CTA GTC CAT GAG AGC C
DKK-1-FITC	GTC TCC GGT CAT CAG ACT GTG CC-Fluorescein
DKK-1-LCRed640	LCRed640-AGG ATT GTG TTG TGC TAG ACA CTT CTG G-phosphate
S100A4-F	CTC AGC GCT TCT TCT TTC
S100A4-R	GGG TCA GCA GCT CCT TTA
S100A4-FITC	TGT GAT GGT GTC CAC CTT CCA CAA GT-Fluorescein
S100A4-LCRed640	LCRed640-TCG GGC AAA GAG GGT GAC AAG T-phosphate

Primers and probes were applied to a final concentration of 250 and 150 nM, respectively.

Each PCR reaction was performed in a total volume of 10 µl in 96-well-plates in the LightCycler 480. The PCR protocol for hybrid probe based qRT-PCR comprised a pre-incubation step at 95 °C for 10 min followed by 45 cycles of (a) denaturation at 95 °C for 10 sec, (b) annealing at 61 °C for 30 sec and (c) elongation at 72 °C for 4 sec. The PCR protocol for SYBR green based qRT-PCR comprised a pre-incubation step at 95 °C for 10 min followed by 45 cycles of (a) denaturation at 95 °C for 7 sec, (b) annealing at 61 °C for 10 sec and (c) elongation at 72 °C for 5 sec. To control for primer dimers or unwanted PCR side products the melting curve was measured with a continuous temperature increase from 65°C to 95°C with a rate of 0.1 °C/sec.

Data analysis was performed with LightCycler® 480 Software release 1.5.0 SP3. For each qRT-PCR reaction a mean of the duplicate was calculated. Each mean value of the expressed gene was normalized to the respective mean amount of the G6PDH cDNA.

3.4.4. Restriction fragment length polymorphism analysis

Restriction fragment length polymorphism (RFLP) analysis was performed as described earlier to analyze the β-catenin genotype of HCT116 and its derivative cells (65). Total RNA was isolated from $4x10^5$ cells and reverse transcribed as described in section 3.4.2. The region comprising the deletion mutation of the S45 of β-catenin was PCR amplified using 1.25 U AmpliTaq Gold (5 U/µl), 1x GeneAmp PCR Gold buffer, 250 µM pooled dNTPs, 2.5 mM $MgCl_2$ (all Applied Biosystems) and 750 µM forward and reverse primers (Biotez) shown in Table 3.4.

Table 3.4 Sequences of primers used in RFLP assay

Primer	Sequence 5'- 3'
RFLP-cat-fwd	CCT GTT CCC CTG AGG GTA TTT
RFLP-cat-rev	CAG CTA CTT GTT CTT GAG TGA AG

PCR was performed in the T3000 Thermocycler (Biometra) with a pre-incubation at 95 °C for 10 min, followed by 40 cycles of (a) denaturation at 95 °C for 30 sec, (b) annealing at 61 °C for 30 sec and (c) elongation at 72 °C for 1 min. Final elongation at 72 °C was performed for 7 min. PCR product was precipitated with 161 mM NaCl and 62 % v/v ethanol at -20 °C overnight, followed by centrifugation at 14,000 rpm for 15 min. Precipitated DNA was washed once with 75 % v/v ethanol, digested with Bsl I FastDigest® Restriction Enzyme (Fermentas) and separated with agarose gel electrophoresis as described in section 3.1. Appearance of 2 bands at 100 and 200 bp represented the Δ45-mutated allele of the β-catenin gene, a 300 bp band represented the wildtype allele of the β-catenin gene.

3.4.5. Protein extraction

Cultured cells were trypsinized, scraped into 1.5 ml tubes and pelleted at 6,000 rpm for 5 min. The pellet was either frozen at -20 °C or immediately subjected to protein extraction.

For total protein extraction cells were lysed with RIPA buffer (50 mM Tris-HCl, 150 mM NaCl, 1 % Nonidet P-40, supplemented with complete protease inhibitor tablets; Roche) for 30 min on ice. Cell debris was pelleted at 14,000 rpm for 10 min at 4 °C.

The supernatant was transferred to a new tube, stored at -20°C or directly subjected to Western blot analysis.

For isolation of the nuclear protein fraction, the NE-PER Nuclear and Cytoplasmic Extraction Kit (Pierce) was used according to the manufacturer's instructions. Briefly, cell membranes were broken in a hypotonic buffer and nuclei were isolated by centrifugation. Nuclei were washed once with PBS to remove residual cytoplasmic protein and resuspended in nuclear extraction buffer. Sonication for 1 pulse at 40 % output was performed to break the nuclear membrane. Membrane debris was removed by centrifugation at 14,000 rpm for 10 min and supernatant was transferred to a new tube. Protein extracts were stored at -20 °C or directly subjected to Western blot analysis.

3.4.6. Protein quantification

Protein concentration was quantified before samples were applied in Western Blot analysis. Quantification was performed with Bicinchoninic Acid (BCA) Protein Assay Reagent (Pierce) according to manufacturer's instructions using 2 mg/ml BSA solution for the standard curve (166). BCA reaction was incubated at 37 °C for 15 min and absorption was measured at 560 nm in the absorbance reader SpectraFluor Plus (Tecan).

3.4.7. Western blot analysis

Sodiumdodecylsulphate polyacrylamide gel electrophoresis (SDS-PAGE) and immunoblotting was used to analyze protein expression levels. All the materials were obtained from Invitrogen, unless stated otherwise.

Protein extracts were diluted with PBS to obtain 50 µg total protein in 1x NuPAGE® loading buffer and 10 % DTT. Protein samples were loaded onto pre-cast NuPAGE® Novex 10 % Bis-Tris Gels or NuPAGE® Novex 4-12 % Bis-Tris Gels. Protein electrophoresis occurred in running buffer 1x NuPAGE® MES or 1x NuPAGE® MOPS at 200 V for 60 min within the XCell SureLock™ Mini Cell System. The pre-stained Spectra™ Multicolor Broad Range Protein Ladder (Fermentas) was used to determine band size.

Semi-dry electrotransfer blotting of proteins onto the Hybond C Extra nitrocellulose membrane (Amersham Biosciences) occurred in blotting buffer (25 mM Tris-HCl, 200 mM glycin, 0,1 % SDS, 20 % methanol, pH7.5) at 20 V for 30-60 min in the Trans-Blot® SD Cell (Bio-Rad). Quality of the protein transfer was analyzed by protein staining with Ponceau S solution (Sigma).

The membrane was washed with TBS-T (50 mM Tris-HCl, 150 mM NaCl, 0.05 % Tween 20, pH 7.5) and blocked for 1 h at room temperature with blocking buffer (TBS-T, 5 % milk powder, 1 % BSA). Primary antibodies were diluted in blocking buffer and incubated at 4 °C overnight. Secondary antibodies were diluted in TBS-T and incubated for 1 h at room temperature. Table 3.5 summarizes the antibodies used and their dilution. Proteins bands were visualized by incubation of the membrane in electrochemical-luminescence reagent (100 mM Tris-HCl, 0.025 % w/v luminol, 0.011 % w/v para-hydroxycoumaric acid, 10 % v/v dimethylsulfoxide, 0.004 % v/v H_2O_2, pH 8.6) for 1 min and its exposure to CL-XPosure™ Films (Pierce) for 1 sec to 20 min.

Table 3.5 Antibodies used for Western blot analysis, their dilutions and their origins

Target	Dilution	Antibody
primary antibodies		
anti-β-catenin	1:1000	mouse monoclonal IgG, BD Biosciences
anti-GAPDH	1:1000	goat polyclonal IgG, Santa Cruz
anti-PCNA	1:1000	mouse monoclonal IgG, CellSignaling
anti-S100A4	1:1500	rabbit polyclonal IgG, Dako
anti-tubulin	1:1000	mouse monoclonal IgM, BD Pharmingen
secondary antibodies		
anti-goat-HRP	1:10000	HRP conjugated antibody, Santa Cruz
anti-rabbit-HRP	1:10000	HRP conjugated antibody, Promega
anti-mouse-IgG-HRP	1:10000	HRP conjugated antibody, Pierce

3.4.8. Enzyme-linked immunosorbent assay

For quantification of secreted DKK-1, the DuoSet® human DKK-1 ELISA System (R&D Systems) was used according to manufacturer's instructions. 96-well stripes (NUNC) were coated with 4 µg/ml DKK-1 capture antibody in PBS overnight. In parallel, $4x10^5$ cells were plated into 6-well plates and after 24 h the supernatant was collected and centrifuged at 6000 rpm for 10 min to remove residual cells. Wells were blocked with blocking reagent (PBS with 1 % BSA) for 1 h. Supernatant was diluted 1:4 and 1:8 with blocking reagent before entering the blocked wells. A standard recombinant human DKK-1, dissolved in blocking reagent, was used at a maximum concentration of 18 ng/ml. DKK-1 protein was incubated with 50 ng/ml detection antibody and HRP-conjugated streptavidin (R&D Systems). For colorimetric quantification, 3,3',5,5'-tetramethylbenzidine liquid substrate system (Sigma) solution was added and the reaction was stopped with STOP solution (Biosource) containing 2 N H_2SO_4. Each

experiment was performed in duplicates with at least two different dilutions to assure that ELISA reaction occurred in the linear range of sensitivity. The mean values of secreted DKK-1 from each supernatant were normalized to the amount of total protein extracted from the respective cells.

3.5. Functional *in vitro* Assays

3.5.1. Migration assay

Cell migration was quantified applying the Boyden chamber assay (167). Transwells were incubated in RPMI 1640 medium 24 h before $2.5x10^5$ cells were seeded onto the filter membrane of the transwell. The filter membrane comprised pores of 12 µm in diameter through which the cells needed to migrate to reach the lower chamber (Millipore). Cells were allowed to accommodate for 15 h before drugs were added, and then incubated for additional 24 h. To quantify cells which migrated to the lower chamber, transwells were removed and cells were trypsinized and counted in a Neubauer chamber. Each well was counted ten times and each migration experiment was performed in duplicates.

3.5.2. Invasion assay

Analysis of cell invasion was based on the Boyden chamber assay and was performed in analogy to quantification of cell migration (167). To measure cell invasion, transwells were covered with Matrigel (BD Biosciences) simulating the extracellular matrix. Matrigel was diluted 1:3 in cell culture media and 50 µl were applied to coat the filter membrane in transwells. Incubation in a humidified incubator at 37 °C and 5 % CO_2 for 30 min allowed polymerization of the Matrigel. $5x10^5$ cells were seeded onto the Matrigel layer 15 h before treatment occurred. Cells which invaded the Matrigel and migrated to the bottom of the well were trypsinized and counted in a Neubauer chamber. Each well was counted ten times and each cell invasion experiment was performed at least in triplicates.

3.5.3. Wound healing assay

The wound healing assay was used to analyze directed cell migration. On day 0, $2.5x10^5$ cells were seeded into a 6-well plate and were allowed to accommodate for 24 h to reach about 60 % confluence. A wound of about 300 µm width was inflicted into this monolayer of cells with a pipette tip and the medium was exchanged to remove cell

debris. The progress of wound closure was monitored daily and microphotographs of 10x and 40x magnification were taken with the Leica DM IL light microscope (Leica Microsystems) on day 0 and day 4. Each wound healing assay was performed in triplicates.

3.5.4. Proliferation assay

For determination of anchorage-dependent cell proliferation, $8x10^3$ cells were plated into 96-well-plates and were allowed to accommodate for 15 h, before treatment was started. Cells were treated daily for 4 days with inhibitor or solvent. For determination of viable cells 3-(4,5-dimethyl-2-thiazol)-2,5-diphenyl-2H-tetrazolium bromide (MTT; Sigma) was added to a final concentration of 0.5 mg/ml, incubated for 3 h, and dissolved by 10 % SDS in 10 mM HCl overnight. The optical density (OD) was measured at 560 nm. Each cell proliferation experiment was performed in triplicates.

3.5.5. Colony formation assay

Analysis of anchorage-independent cell proliferation was achieved by soft agar colony formation assay. A bottom layer containing 0.5 % w/v agarose, RPMI 1640 medium, 10 % FBS and inhibitor or solvent was added to a 6 cm Ø dish. Onto the solidified bottom layer a top layer was added containing $8x10^3$ cells, 0.33 % w/v agarose, RPMI 1640 medium, 10 % FBS and inhibitor or solvent. Cells were seeded as single cells into the soft agar and incubated in a humidified incubator at 37 °C and 5 % CO_2 for 7 days. Colony formation was visualized by 10x magnification for an overview and 40x magnification for single colonies in the Leica DM IL light microscope (Leica Microsystems). Colony quantification was achieved by counting cell colonies of more than 4 cells in 10 squares of 1 μm^2.

3.6. Wnt/β-catenin pathway analysis

3.6.1. TOP/FOPflash reporter assay

The TOP/FOPflash assay (Promega) was used to determine Wnt/β-catenin pathway activity. The TOPflash contained a hexameric repetition of the T-cell factor (TCF)-binding element upstream of a thymidine kinase (TK) promoter and firefly luciferase as reporter gene. The FOPflash plasmid comprised the exact sequence of the TOPflash plasmid, but with point mutated TCF-binding sites. In the assay, $8x10^5$ cells were plated in 24-well-plates and let accommodate for 15 h. Cells were transfected with

TOPflash or FOPflash plasmids 24 h before being treated with inhibitor or solvent. Luciferase activity was measured by the Steady Glow™ Luciferase Assay System (Promega) according to the manufacturer's instructions in the luminescence reader SpectraFluor Plus (Tecan) with 1,500 ms exposure time and a gain of 150. TOPflash reporter gene expression, representing the Wnt pathway activity, was normalized to FOPflash reporter gene expression, representing basal reporter gene expression and transfection efficiency. Each assay was performed in triplicates.

3.6.2. Electrophoretic mobility shift assay

Electrophoretic mobility shift assay (EMSA) for analysis of the β-catenin/TCF-S100A4-promoter-complex was described earlier (65). If not stated otherwise, the materials were obtained from Pierce. In a total volume of 20 µl, 5 µg of nuclear extracted protein was incubated for 30 min at room temperature along with 0.05 % w/v poly dI·dC, 0.5 mM Tris, 0.05 mM EDTA, 2.5 % v/v glycerol, 0.2 % v/v NP-40, 5 mM $MgCl_2$ and double-stranded biotinylated oligonucleotides encompassing the TCF-binding site of the S100A4-promoter (Biotez; for sequence see Table 3.6). For supershift 1.25 µg monoclonal β-catenin antibody (BD Biosciences) was added. Electrophoretic separation of the protein-oligonucleotide-complexes was performed in pre-cast Novex 6 % TBE gels (Invitrogen) and in TBE buffer (45 mM Tris, 45 mM boric acid, 1 mM EDTA, pH 8.3) for 60 min at 100 V. Capillary transfer of the protein-oligonucleotide-complexes to the Hybond™-N nylon membrane (Amersham Biosciences) occurred in 20x SSC buffer (3 M NaCl, 300 mM Na3C6H5O7, pH 7) overnight. Cross-linkage of transferred DNA to the membrane occurred at 250 mJ/cm^2 for 1 min in the FL-20-M FluoLink Crosslinker (Bachofer). Visualization of biotin-labeled DNA was performed with LightShift Chemiluminescent EMSA Kit (Pierce) according to manufacturer's instructions.

Table 3.6 Oligonucleotide sequences used for EMSA

Primer	Sequence 5'- 3'
TCF-site-antisense	Biotin-TGT CTC TTA AAA AAA TAA AGA TTC AGA AAC AAA AAC TGG GGT GGG GAT CCC CAT GCC CGG
TCF-site-sense	Biotin-CAC CGG GCA TGG GGA TCC CCA CCC CAG TTT TTG TTT CTG AAT CTT TAT TTT TTT AAG AGA CA

The sequence of the oligonucleotides comprised the TCF-binding site of the S100A4-promoter and was described by Stein et al. (65).

3.6.3. Chromatin immunoprecipitation assay

Chromatin immunoprecipitation (ChIP) was described earlier to measure the binding of β-catenin to the S100A4-promoter (65, 168). For the preparation of cell lysates 1x106 cells were plated in 10 cm Ø dish 15 h before being treated with inhibitor or solvent. Cells were incubated with 1 % formaldehyde for 10 min at room temperature to assure reversible cross-linking of proteins and DNA. Cells were washed twice with ice-cold PBS and lyzed with Lysis Buffer A (1 % SDS, 10 mM EDTA, 50 mM Tris-HCl, pH 8) for 10 min on ice. Cell lysates were sonicated for 20 pulses at 40 % output and centrifuged at 10,000 rpm for 10 min. Supernatant was transferred to a new tube and diluted with Lysis buffer A to reach an absorption at 260 nm of 2 units/ml. One third of the diluted supernatant was stored at -20 °C and served in the end as input control.

For immunoprecipitation the diluted supernatant was incubated with 5 µg monoclonal β-catenin antibody or 5 µg control IgG (both BD Biosciences) overnight at 4 °C. Protein G beads (Invitrogen) were added and incubated for 2 h at 4 °C. Non-bound protein was washed away twice with Wash Buffer A (10 mM Tris, 0.1 % SDS, 0.1 % Na-deoxycholate, 1 % Triton X-100, 1 mM EDTA, 0.5 mM EGTA, 140 mM NaCl, pH 8), once with Wash Buffer B (Wash Buffer A, 6 % w/v NaCl) and twice with TE buffer (20 mM Tris, 1 mM EDTA, pH 8). Elution of the protein-DNA-complex from the beads occurred by incubation with 1.5 % w/v SDS solution for 15 min at room temperature followed by centrifugation at 3,000 rpm for 1 min. To assure complete elution a second elution step was performed by incubation of the beads in 0.5 % SDS solution for 15 min at room temperature followed by centrifugation at 3,000 rpm for 1 min.

Cross linking of protein and DNA was reversed at 68 °C for 4 h and residual protein was digested by proteinase K (Fermentas) at 55 °C for 2 h. DNA was purified by precipitation as described in section 3.4.4. PCR amplification of the S100A4-promoter TCF-binding site was performed with the Taq-PCR protocol as described in section 3.4.4 with primers summarized in Table 3.7. PCR amplification of the non-β-catenin regulated fos-promoter sequence served as a control. The expected amplicons were 167- or 149 bp in size, respectively.

Table 3.7 Primer sequences applied in the ChIP assay

Primer	Sequence 5'- 3'
fos-promoter-F	CCT TAA TAT TCC CAC ACA TGG C
fos-promoter-R	CTG CGT TTG GAA GCA GAA AGT
S100A4 promoter-F	TGT TCC CCT CCA GAT CCC
S100A4 promoter-R	GGC TAT GCT CAA GCC ACT G

Primers were designed by Stein et al. (65) and used to a final concentration of 750 nM.

3.7. *In vivo* metastasis formation and bioluminescence imaging

All animal experiments were performed in accordance with the UKCCCR guidelines and in cooperation with Dr. Iduna Fichtner (MDC Berlin, Germany). Further, all animal experiments were approved by the State Office of Health and Social Affairs, Berlin, Germany in the G0413 permit.

3.7.1. Intrasplenal tumor transplantation

For intrasplenical transplantation 6-week-old female non-obese diabetic/ severe combined immunodeficiency (NOD/SCID) mice (EPO GmbH) and SCID beige mice (Charles Rives Laboratories) were used. Disinfectant, suture and surgical instruments were obtained from Heiland, syringes and needles were obtained from Braun. For intrasplenal tumor application, mice were anesthetized with 35 mg/kg Hypnomidate® (Jassen-Cilag) and the skin and peritoneum were laterally incised to exteriorize the spleen. HCT116/LUC cells were resuspended in PBS and kept on ice during the surgery. 3×10^6 of these cells were intrasplenically injected with a 27-gauge needle. The spleen was carefully placed back, the peritoneum was closed with Surgicryl ® absorbable suture and the skin was clamped twice.

3.7.2. *In vivo* dose-finding for niclosamide

For dose finding experiments intrasplenical transplanted NOD/SCID mice were randomly assigned to four groups with 2 animals per group. Treatment started 24 h after transplantation and was performed daily by intraperitoneal injection of 6, 12 or 24 mg/kg niclosamide or the respective amount of solvent. Body weight was analyzed daily to observe toxic effects of the drug. Mice were sacrificed at day 24 for ethical reasons. The size and number of metastases was determined as described in section 3.7.3.

3.7.3. Analysis of metastasis formation *in vivo*

Intrasplenical transplanted NOD/SCID mice were randomly assigned to 3 groups of 9 animals. Treatment of animals started 24 h after cell transplantation. Mice were daily treated intraperitoneally with either one dose of 20 mg/kg or two doses of 15 mg/kg niclosamide. Control animals received the corresponding amount of solvent. Mice were sacrificed at day 24 for ethical reasons. Spleen (as the transplantation site) and liver (as a metastasis target organ) were removed. The level of metastasis was evaluated

by scoring considering both the number and the size of metastatic nodules (1 mm = score 1; 2 mm = score 8; 3 mm = score 27; 4 mm = score 64; 5 mm = score 125).

3.7.4. *In vivo* bioluminescence imaging

Intrasplenically transplanted SCID mice were randomly assigned to 2 groups of 4 animals each. Mice were treated intraperitoneally with daily doses of 20 mg/kg niclosamide or solvent. For non-invasive bioluminescence imaging mice were anesthetized every 3 days with 35 mg/kg Hypnomidate® (Jassen-Cilag) and received intraperitoneally 150 mg/kg D-luciferin (Biosynth) dissolved in PBS. Imaging was performed with the NightOWL LB 981 system (Berthold Technologies) with exposure times of 1 sec to 20 sec. ImageJ version 2.3 was used for color coding of the signal intensity (presenting a 256 grayscale) and for overlay pictures.

3.7.5. Human S100A4 expression in murine xenograft tissue

Spleen tumor tissue was shock frozen with liquid nitrogen after resection and stored at -80°C. For isolation of mRNA, the tumor tissue was fixed with Tissue-Tek Medium (satura Tek) in a Cryomicrotom (CM1900, Leica) and dissected into 6 slices each of 10 µm in size. Trizol reagent was added to tissue slices and samples were sonicated for 10 pulses at 40 % output to assure complete cell lysis. RNA isolation and reverse transcription was performed as described in sections 3.4.1 and 3.4.2, respectively. Primers for quantification of S100A4 cDNA were designed to be specific to the human sequence of S100A4 excluding murine S100A4 cDNA to interfere with the measurements.

3.8. Statistical analysis

All calculations and statistics were performed with GraphPad Prism version 4.01. Comparison of two groups was done by Student's t-test. Comparison of a control versus several treated groups was performed by one-way analysis of variance (ANOVA) and Bonferroni post hoc multiple comparison. The inhibiting concentration 50 (IC_{50}) and the effective concentration 50 (EC_{50}) were calculated by sigmoidal dose-response curve fit of x=log(x) transformed data. For correlation analysis data was tested for Gaussian distribution with Shapiro-Wilk normality test. Since no Gaussian distribution was detected, correlation analysis was performed with non-parametric Spearman correlation test. All significance tests were two-sided, and P values smaller than .05 were defined as statistically significant.

4. RESULTS

Walther, Stein and colleagues identified niclosamide and calcimycin in a high throughput screening for S100A4 transcription inhibitors. The two compounds were most efficient to reduce firefly luciferase activity without affecting cell viability. Expression of the reporter firefly luciferase was regulated by the S100A4-promoter. From the reduced firefly luciferase activity it was hypothesized that S100A4-promoter activity was repressed. Based on those results, the small molecules bore a great potential to inhibit S100A4 expression in colon cancer cells. In the present study, this potential and the applicability of the two small molecules was investigated. As a cellular model, the colon cancer cell line HCT116 was used due to its endogenous high level of S100A4 expression, which was earlier described by Stein et al. (65).

4.1. Small molecules interfere with cell viability

To analyze the inhibitory potential of niclosamide and calcimycin on S100A4 expression, a concentration range needed to be defined in which the inhibitors were applicable to HCT116 cells. In the high throughput screening both small molecules showed an inhibitory effect at concentrations between 1-100 µM. To cover a wider concentration range, HCT116 cells were exposed to 12 2-fold dilutions of niclosamide and calcimycin starting at 300 µM. Cell viability was evaluated 24 h post treatment.

Niclosamide treatment affected the viability of HCT116 cells in a concentration-dependent manner (Fig. 4.1A). The inhibiting concentration 50 (IC_{50}), representing the concentration at which cell viability was decreased to 50 %, was calculated to be 2.2 µM (95 % CI, 1.9-2.9 µM). In analogy, calcimycin treatment of HCT116 cells also reduced cell viability in a concentration-dependent manner (Fig. 4.1B) with a calculated IC_{50} of 2.1 µM (95 % CI, 1.5-2.2 µM). In contrast, DMSO as the solvent control affected the cell viability of HCT116 cells only slightly at the highest concentration added and otherwise did not interfere.

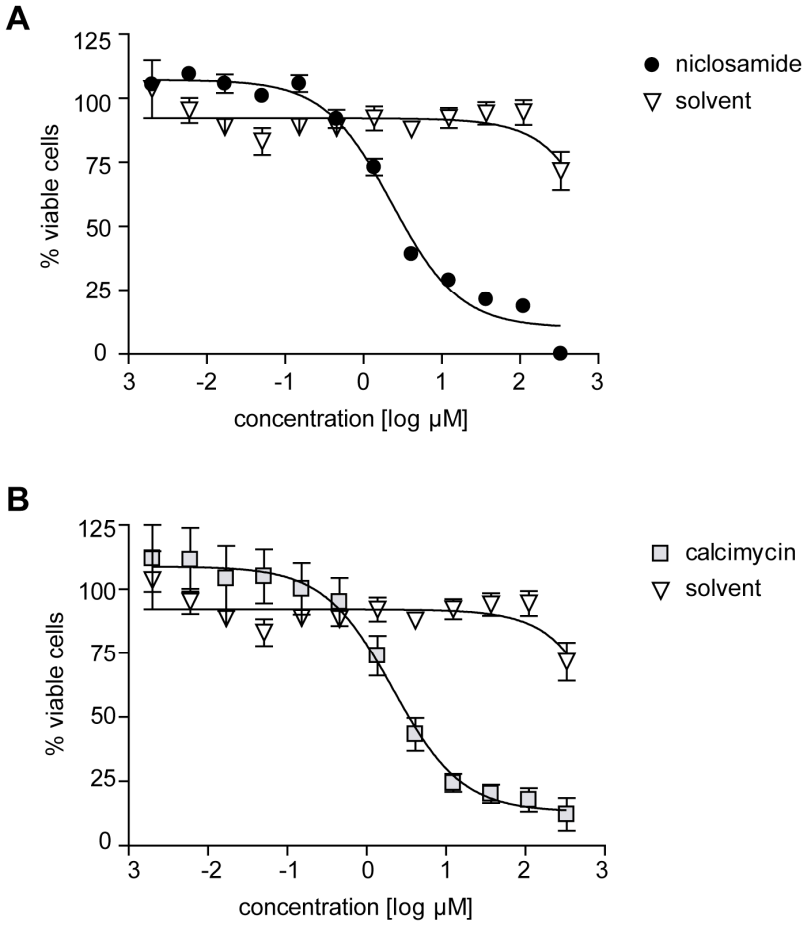

Fig. 4.1 Niclosamide and calcimycin inhibit cell viability in a concentration-dependent manner. HCT116 cells were exposed to increasing concentrations of niclosamide (A), calcimycin (B) or the respective amount of solvent. Cell viability was determined after 24 h. The IC_{50} for niclosamide and calcimycin were calculated to be 2.2 µM (95 % CI, 1.9-2.9 µM) and 2.1 µM (95 % CI, 1.5-2.2 µM), respectively. Data represent mean ± SE (n>3).

4.2. Small molecules restrict S100A4 expression

4.2.1. Inhibition of S100A4 expression is concentration-dependent

The ability of the small molecules to reduce endogenous S100A4 expression was analyzed in HCT116 cells treated with increasing concentrations of niclosamide or calcimycin for 24 h. Niclosamide treatment reduced the S100A4 mRNA level in a concentration-dependent manner (Fig. 4.2A). Concentrations of more than 0.5 µM niclosamide significantly reduced the endogenous S100A4 mRNA amount to less than 50 % of the solvent-treated control. In parallel, the S100A4 protein was clearly reduced in HCT116 cells treated with 1 µM and higher concentrations of niclosamide. No

change in S100A4 expression could be detected when cells were treated with concentrations lower than 1 µM niclosamide.

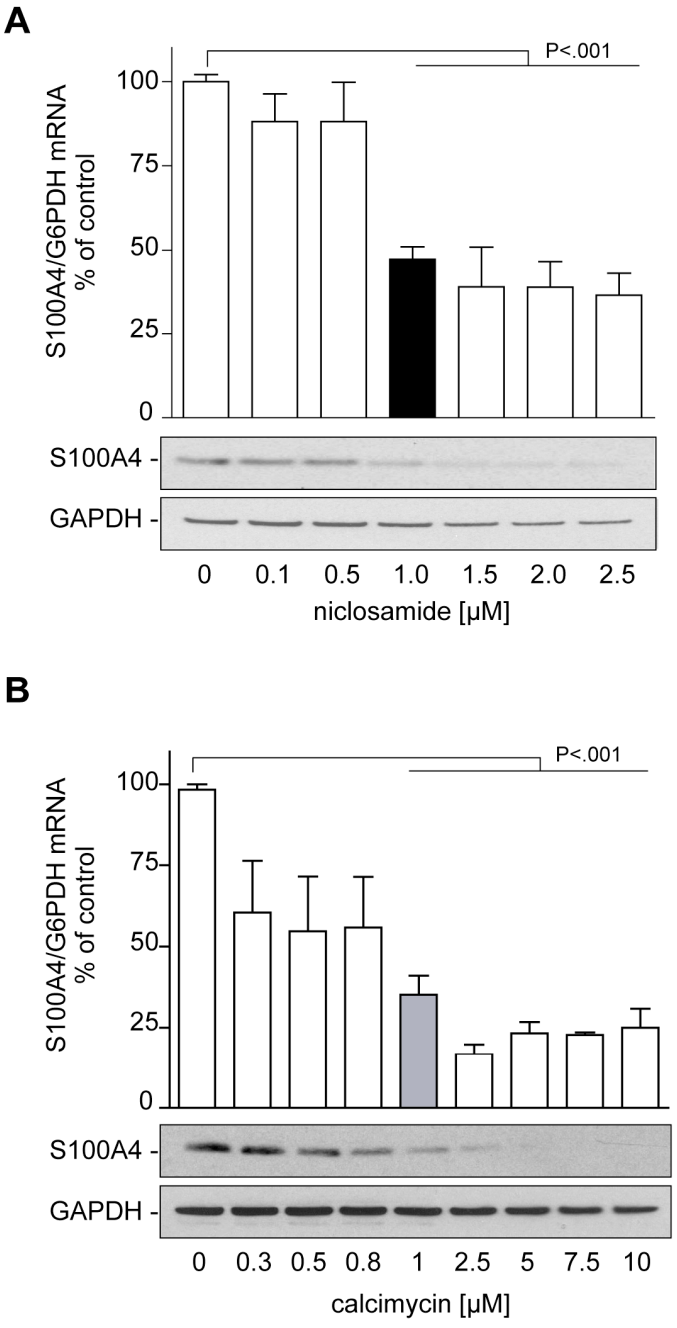

Fig. 4.2 Niclosamide and calcimycin inhibit S100A4 expression in a concentration-dependent manner. HCT116 cells were treated with increasing concentrations of niclosamide (A) or calcimycin (B) for 24 h and S100A4 mRNA and protein expression was determined by qRT-PCR and Western blot analysis, respectively. 1 µM niclosamide (black bar) or calcimycin (grey bar) were sufficient to inhibit S100A4 expression to less than 50 % of solvent-treated cells. Data represent mean ± SE (n>3). Statistical significance was analyzed by two-sided ANOVA and Bonferroni post hoc multiple comparison test.

Similar to the effects seen for niclosamide, increasing concentrations of calcimycin also inhibited S100A4 mRNA expression in a concentration-dependent manner (Fig. 4.2B). A slight reduction of the S100A4 mRNA level to about 60 % of the solvent-treated control was already seen when HCT116 cells were treated with 0.3 µM to 0.8 µM calcimycin. However, concentrations of 1 µM calcimycin or higher significantly restricted the S100A4 mRNA level to less than 30 % of the solvent-treated control. Additionally, treatment with 1 µM or higher concentrations of calcimycin led to a clearly reduced S100A4 protein expression.

For further experiments a drug concentration with a minimal effect on cell viability and a maximized inhibitory effect on S100A4 expression had to be selected. A concentration of 1 µM niclosamide or calcimycin was sufficient to restrict S100A4 expression to less than 50 % of the solvent-treated control. Moreover, at that concentration niclosamide and calcimycin treatment assured cell viability to be less affected. Therefore, the small molecules were used at a concentration of 1 µM for all further experiments.

4.2.2. Inhibition of S100A4 expression is time-dependent

With the applicable concentration evaluated for niclosamide and calcimycin the time dependency of the inhibitory effect on the S100A4 expression caused by the small molecules was analyzed. After 18 h exposure of HCT116 cells to a single dose of 1 µM of niclosamide, the S100A4 mRNA was significantly reduced to less than 50 % of the solvent-treated control (Fig. 4.3A). This reduction was maintained after 24 h before the S100A4 expression recovered and reached its starting level after 48 h. A single dose of 1 µM of niclosamide did also reduce the S100A4 protein expression after 24 h, an effect that was abolished after 30-48 h. To achieve a constant decrease of S100A4 expression, serial treatment of HCT116 cells with 1 µM niclosamide every 24 h was applied (Fig. 4.3B). Thereby, the S100A4 mRNA and protein levels were reduced to about 50 % of solvent-treated control cells for at least three consecutive days.

Analysis of the kinetics underlying calcimycin-mediated inhibition of the S100A4 expression revealed that a single dose of calcimycin reduced the S100A4 expression also in a time-dependent manner (Fig. 4.3C). After 6 h treatment of HCT116 cells with 1 µM of calcimycin, the S100A4 mRNA level was significantly reduced to less than 70 % of the solvent-treated control. After 12 h, the lowest S100A4 mRNA level was reached at about 30 % of the solvent-treated control cells. After 18 h the S100A4 protein was clearly reduced. In contrast to niclosamide which presented a reversible inhibitory effect, calcimycin treatment was irreversible within the time period analyzed.

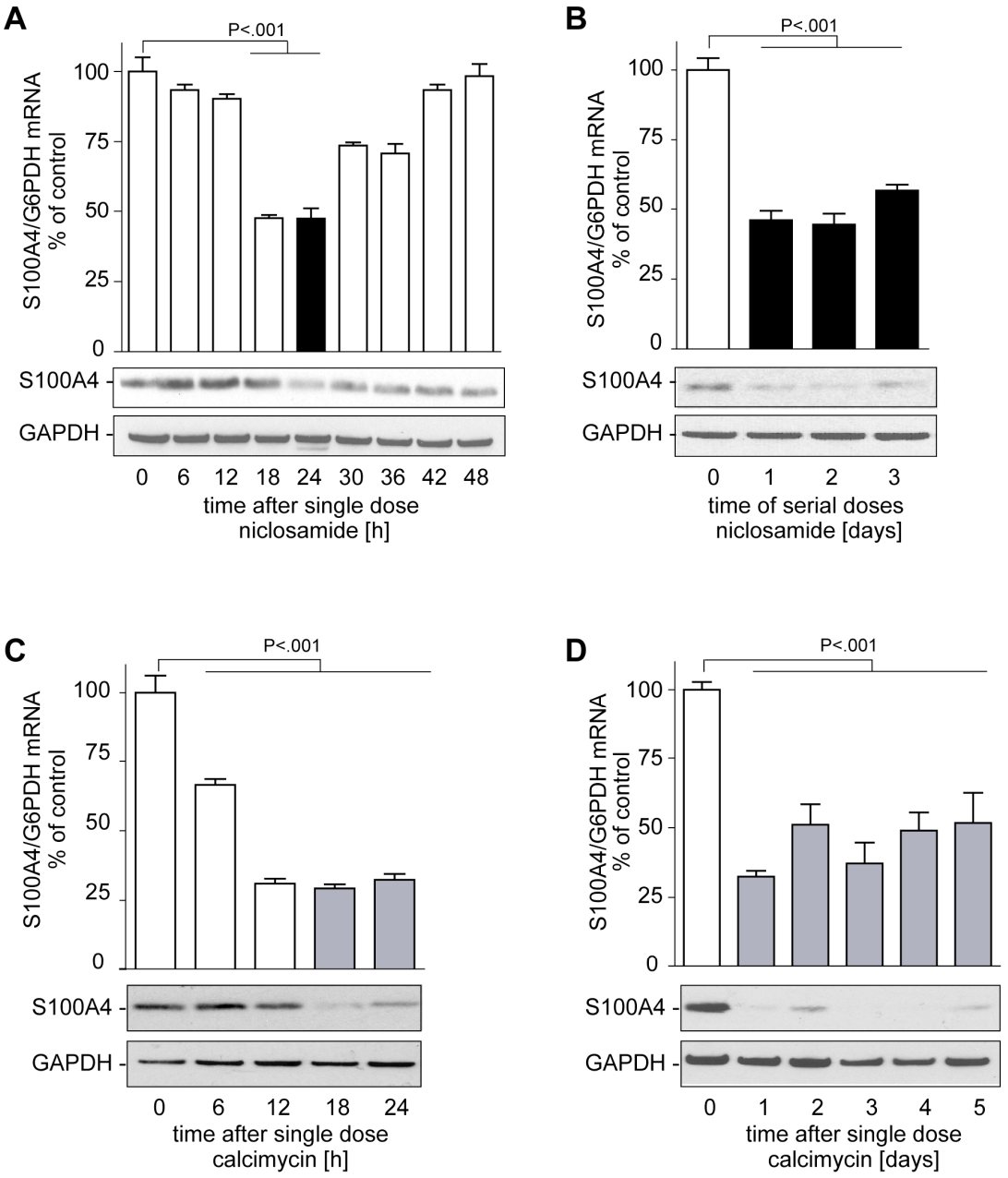

Fig. 4.3 Niclosamide and calcimycin inhibit S100A4 expression in a time-dependent manner. HCT116 cells were treated with 1 µM niclosamide (A,B) or calcimycin (C,D) for the time indicated. S100A4 mRNA and protein was analyzed by qRT-PCR and Western blot, respectively. (A) 24 h of niclosamide treatment (black bar) reduced S100A4 expression. (B) Treatment with 1 µM niclosamide every 24 h constantly reduced S100A4 expression. (C) 18 h to 24 h of calcimycin treatment (grey bar) reduced S100A4 expression. (D) A single dose of calcimycin constantly inhibited S100A4 expression. Data represent mean ± SE (n>3). Statistical significance was analyzed by two-sided ANOVA and Bonferroni post hoc multiple comparison test.

Treatment of HCT116 cells with a single dose of 1 µM of calcimycin was sufficient to reduce the S100A4 mRNA and protein level to less than 30 % of solvent-treated control

cells for at least five consecutive days. Interestingly, the decreased S100A4 protein expression induced by the treatment of HCT116 cells with either of the small molecules appeared with a 6 h delay relative to the decreased S100A4 mRNA level.

4.2.3. Exogenous expression of S100A4 is not affected by small molecules

To test if any effect of the small molecules was specific to their inhibition of S100A4 expression, a cellular model was needed which provided high levels of S100A4 despite the treatment with either of the small molecules. Considering that the small molecules were shown to inhibit the S100A4 expression by repressing the S100A4-promoter activity, it was hypothesized that CMV-promoter-driven S100A4 cDNA could be resistant to the inhibitory effect of niclosamide or calcimycin.

Therefore, HCT116 cells were stably transfected to express CMV-promoter-driven S100A4 cDNA or the empty vector as control. As result, HCT116/S100A4 cells had a 7-fold increased S100A4 mRNA level compared to HCT116/vector cells. Additionally, the S100A4 protein level was clearly increased in those cells compared to HCT116/vector cells.

Treatment of HCT116/vector cells with niclosamide reduced the S100A4 mRNA level to about 50 % of the solvent-treated control, which was similar to the effect observed in HCT116 cells (Fig. 4.4A). In contrast, the exposure of HCT116/S100A4 to niclosamide did not result in a significant reduction of the S100A4 mRNA. S100A4 protein expression in HCT116/vector cells was decreased when cells were treated with niclosamide, but stayed unchanged in niclosamide-treated HCT116/S100A4 cells.

Similar to niclosamide, the exposure of HCT116/vector cells to calcimycin reduced the S100A4 mRNA to less than 30 % of solvent-treated control cells, but had no significant effect on the S100A4 mRNA level of HCT116/S100A4 cells (Fig. 4.4B). Further, S100A4 protein expression was inhibited upon calcimycin treatment in HCT116/vector cells, but not in HCT116/S100A4 cells.

The vector backbone including an antibiotic resistance entered in HCT116/vector cells did not interfere with the inhibitory effect of the small molecules on the S100A4 expression, since the effects seen in HCT116/vector cells were similar to the effects observed in niclosamide- or calcimycin-treated HCT116 cells. In contrast, the exogenously overexpressed S100A4 cDNA under the control of a CMV-promoter was not targeted by niclosamide or calcimycin treatment since HCT116/S100A4 cells showed no significant reduction in S100A4 expression upon niclosamide or calcimycin treatment.

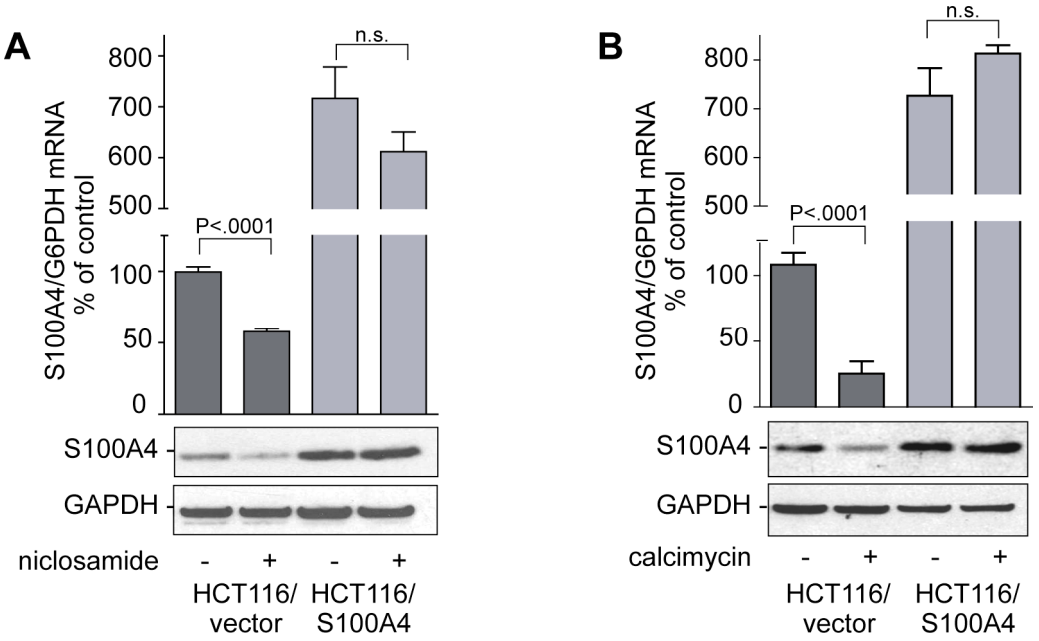

Fig. 4.4 Niclosamide and calcimycin do not affect exogenous S100A4 expression. HCT116 cells were either stably transfected to express CMV-promoter-driven S100A4 cDNA (HCT116/S100A4) or the empty vector (HCT116/vector) as control. Cells were treated with 1 µM niclosamide (A) or calcimycin (B) for 24 h and S100A4 mRNA and protein level was analyzed by qRT-PCR and Western blot, respectively. (A) Niclosamide reduced S100A4 expression in HCT116/vector cells, but not in HCT116/S100A4 cells. (B) Calcimycin decreased S100A4 expression in HCT116/vector cells, but had no effect on the S100A4 expression of HCT116/S100A4 cells. Data represent mean ± SE (n>3). Statistical significance was analyzed by Student's t-test.

4.3. Small molecules decrease cell migration, invasion and proliferation

S100A4 is an abundant protein in the cell, which interacts with a multitude of target proteins to drive cellular processes needed for metastasis formation (69). Stein et al. had previously shown that S100A4 increased cell migration and invasion of colon cancer cells (66). Since niclosamide and calcimycin were found to inhibit S100A4 expression, the functional consequences on cell migration, invasion and proliferation were analyzed.

4.3.1. Small molecules reduce cell migration of colon cancer cells

Intracellular S100A4 is a major regulator of cell migration which is one of the first cellular processes triggering metastasis formation (71, 97). Analysis of cell migration revealed that the number of migrated cells did not change in solvent-treated HCT116, HCT116/vector and HCT116/S100A4 cells (Fig. 4.5A). However, differences were

discovered, when cells were treated with either of the small molecules.

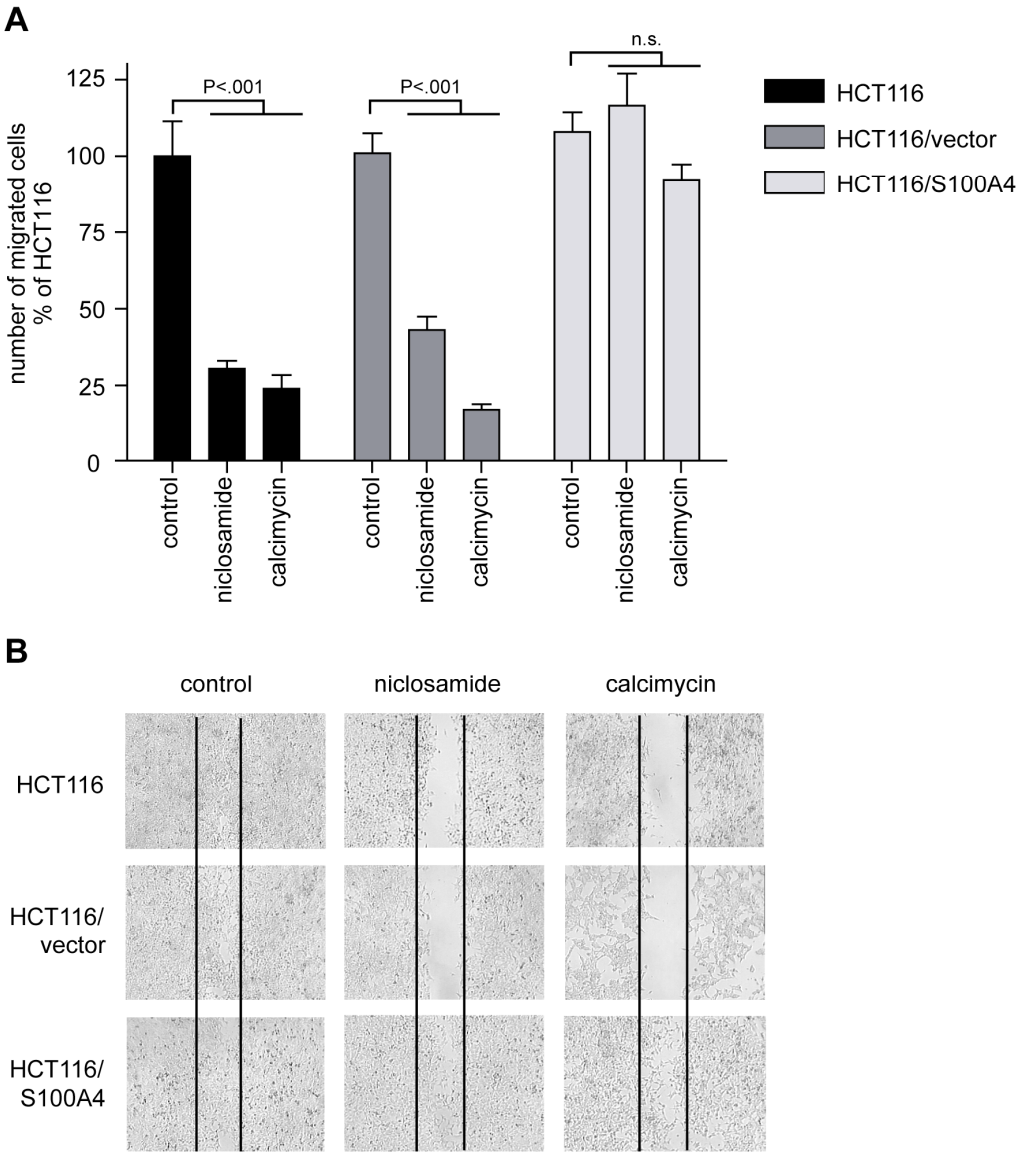

Fig. 4.5 Niclosamide and calcimycin inhibit cell migration in an S100A4-specific manner. (A) HCT116, HCT116/vector and HCT116/S100A4 cells were treated with 1 µM niclosamide or calcimycin for 24 h and cell migration was measured with the Boyden chamber assay. Both small molecules restricted cell migration in HCT116 and HCT116/vector cells, but not in HCT116/S100A4 cells. Data represent mean ± SE (n>3). Statistical significance was analyzed by two-sided ANOVA and Bonferroni post hoc multiple comparison test. (B) Directed migration of niclosamide-, calcimycin- or solvent-treated HCT116, HCT116/vector and HCT116/S100A4 cells was analyzed by wound healing assay. Both small molecules inhibited directed migration of HCT116 or HCT116/vector cells, but not of HCT116/S100A4 cells. Microphotographs were taken on day 4 with 10x magnification. Assay was performed three times; one representative picture for each condition is presented here.

In HCT116 cells treated with niclosamide or calcimycin the number of migrated cells was reduced to less than 35 % of the solvent-treated HCT116 cells. Cell migration of niclosamide- or calcimycin-treated HCT116/vector cells was also reduced to less than 50 % or even less than 25 % of HCT116 control cells, respectively. In contrast, the number of migrated HCT116/S100A4 cells was not significantly changed upon treatment with either of the small molecules. Since the S100A4 protein level in those cells was not affected by niclosamide or calcimycin, those cells were still able to migrate despite treatment with the small molecules.

Similar effects were seen for directed migration of HCT116, HCT116/vector and HCT116/S100A4 cells analyzed by wound healing assay as previously described (169). When cells were treated only with solvent, all three cell species were able to infiltrate the wound and close it until day 4 (Fig. 4.5B). Treatment of HCT116 and HCT116/vector cells with daily doses of 1 µM niclosamide inhibited wound closure until day 4. Moreover, a single dose of 1 µM calcimycin given on day 1 also impaired wound closure of HCT116 and HCT116/vector cells until day 4. In contrast, HCT116/S100A4 cells were able to infiltrate the wound and close the gap despite the treatment with niclosamide or calcimycin.

In summary, it can be concluded that the anti-migratory effect of the small molecules was due to the specific inhibition of the S100A4 expression, since this effect was absent in HCT116/S100A4 cells, which still expressed S100A4 protein despite treatment with niclosamide or calcimycin.

4.3.2. Small molecules impair cell invasion

S100A4 is a major activator of cell invasion which is crucial for tissue infiltration during metastasis formation (69, 122, 125). Comparing the cell invasion rate of solvent-treated HCT116, HCT116/vector and HCT116/S100A4 cells, no significant difference could be detected (Fig. 4.6). However, when HCT116 and HCT116/vector cells were treated with niclosamide the number of invaded cells was decreased to less than 50 % of HCT116 control cells. Cell invasion of calcimycin-treated HCT116 and HCT116/vector cells was inhibited to less than 30 % of the solvent-treated control cells. In contrast, cell invasion of HCT116/S100A4 cells was not significantly changed upon treatment of cells with either of the small molecules. Thus, the anti-invasive effect of niclosamide or calcimycin was dependent on a reduced S100A4 expression level.

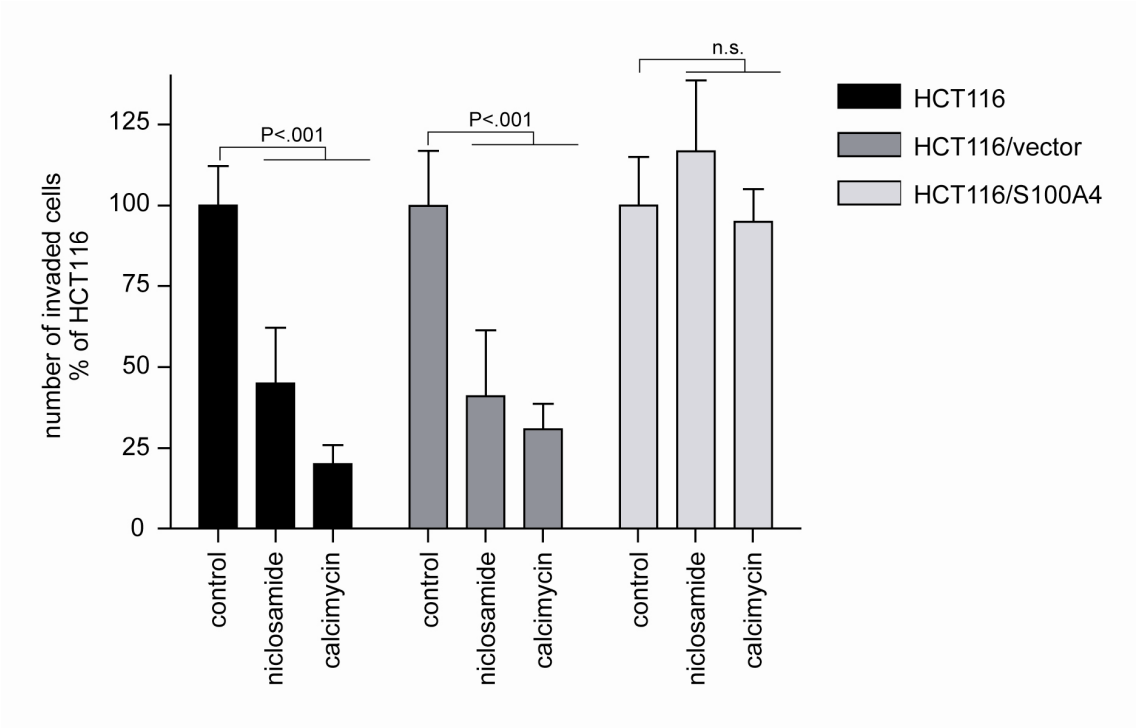

Fig. 4.6 Niclosamide and calcimycin inhibit S100A4-induced cell invasion. Cell invasion of HCT116, HCT116/vector and HCT116/S100A4 cells was analyzed in a Matrigel-coated Boyden chamber assay under the treatment of 1 µM niclosamide or calcimycin for 24 h. Both small molecules restricted cell invasion of HCT116 and HCT116/vector cells, but not of HCT116/S100A4 cells. Data represent mean ± SE (n>3). Statistical significance was analyzed by two-sided ANOVA and Bonferroni post hoc multiple comparison test.

4.3.3. Small molecules decrease cell proliferation

A major characteristic of cancer cells is their increased proliferation rate (36). Therefore, the effect of the small molecules on anchorage-dependent proliferation was analyzed. Despite their differences on the S100A4 expression level, the proliferation rate of solvent-treated HCT116, HCT116/vector and HCT116/S100A4 cells did not present significant differences (Fig. 4.7A). Treatment of HCT116 cells with either daily doses of niclosamide or a single dose of calcimycin on day 0 resulted in a significantly reduced cell proliferation on day 3 (Fig. 4.7B). Similarly, in HCT116/vector cells the same treatment inhibited anchorage-dependent cell proliferation (Fig.4.7C). Ectopic overexpression of S100A4 did not rescue cell proliferation. Exposure of HCT116/S100A4 cells to either of the small molecules restricted cell proliferation to a similar intent found in HCT116 and HCT116/vector cells. From those observations it could be concluded that the anti-proliferative effect of niclosamide and calcimycin was not influenced by the expression level of S100A4.

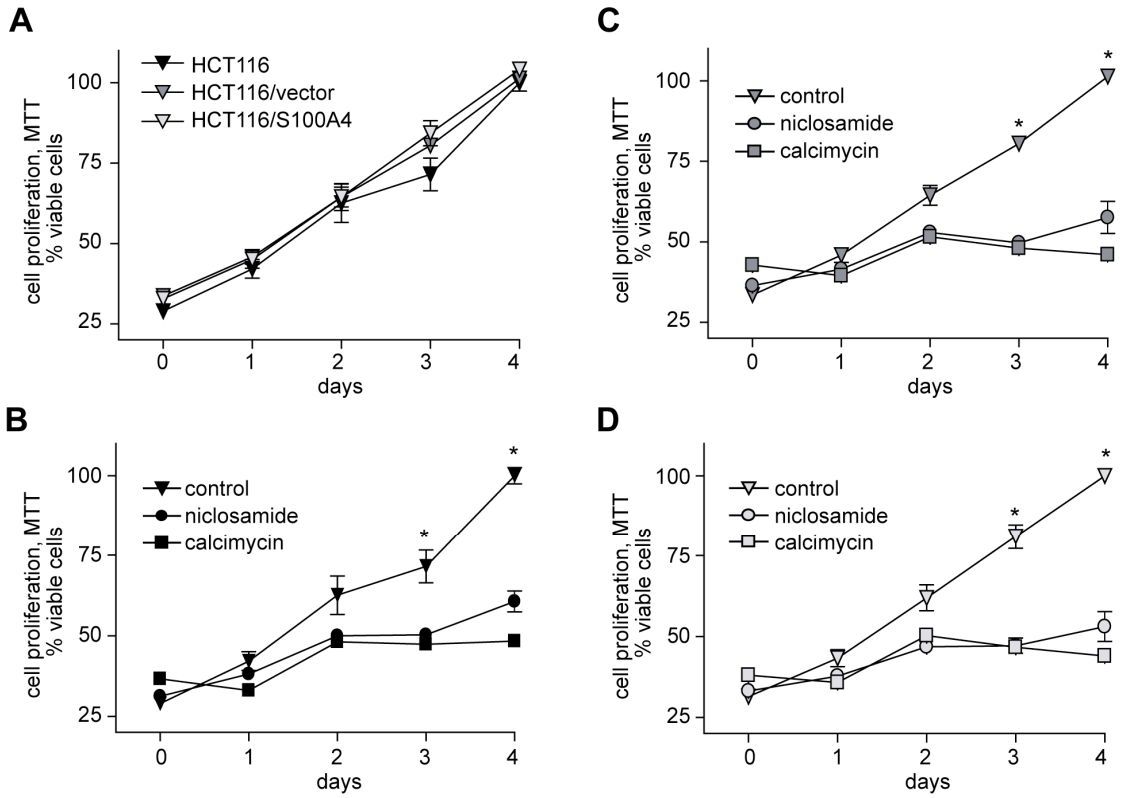

Fig. 4.7 Niclosamide and calcimycin inhibit anchorage-dependent cell proliferation. Cell proliferation rate of untreated (A) HCT116, HCT116/vector and HCT116/S100A4 cells or HCT116 (B), HCT116/vector (C) and HCT116/S100A4 (D) treated either with daily doses of 1 µM niclosamide or with a single dose of 1 µM calcimycin was analyzed daily with MTT assay. The proliferation rate of untreated HCT116, HCT116/vector and HCT116/S100A4 cells was not different. Both small molecules decreased cell proliferation of all three cell species. Data represent mean ± SD (n=3). Statistical significance (*, P<.05) of the difference between control and niclosamide- or calcimycin-treated cells was analyzed by two-sided ANOVA and Bonferroni post hoc multiple comparison test.

4.3.4. Small molecules arrest colony formation

The ability to grow in an anchorage-independent manner is a characteristic needed for metastatic cells to survive, for instance, in the blood stream during the progress of metastasis formation. Anchorage-independent growth was investigated with the colony formation assay. Solvent-treated HCT116, HCT116/vector and HCT116/S100A4 cells were able to form large, clearly visible colonies within 7 days (Fig. 4.8A). In contrast, the size of the colonies formed by these three cell species was severely reduced upon niclosamide or calcimycin treatment. Niclosamide treatment further reduced the number of colonies to less than 5 % of HCT116 control cells in all three cell species. Exposure of HCT116, HCT116/vector and HCT116/S100A4 cells to calcimycin reduced even more the number of colonies to less than 3 % of HCT116 control cells (Fig. 4.8B).

The inhibition of anchorage-independent cell proliferation was independent on the expression level of S100A4, since this effect was also seen in HCT116/S100A4 cells that express S100A4 despite the treatment with either of the small molecules.

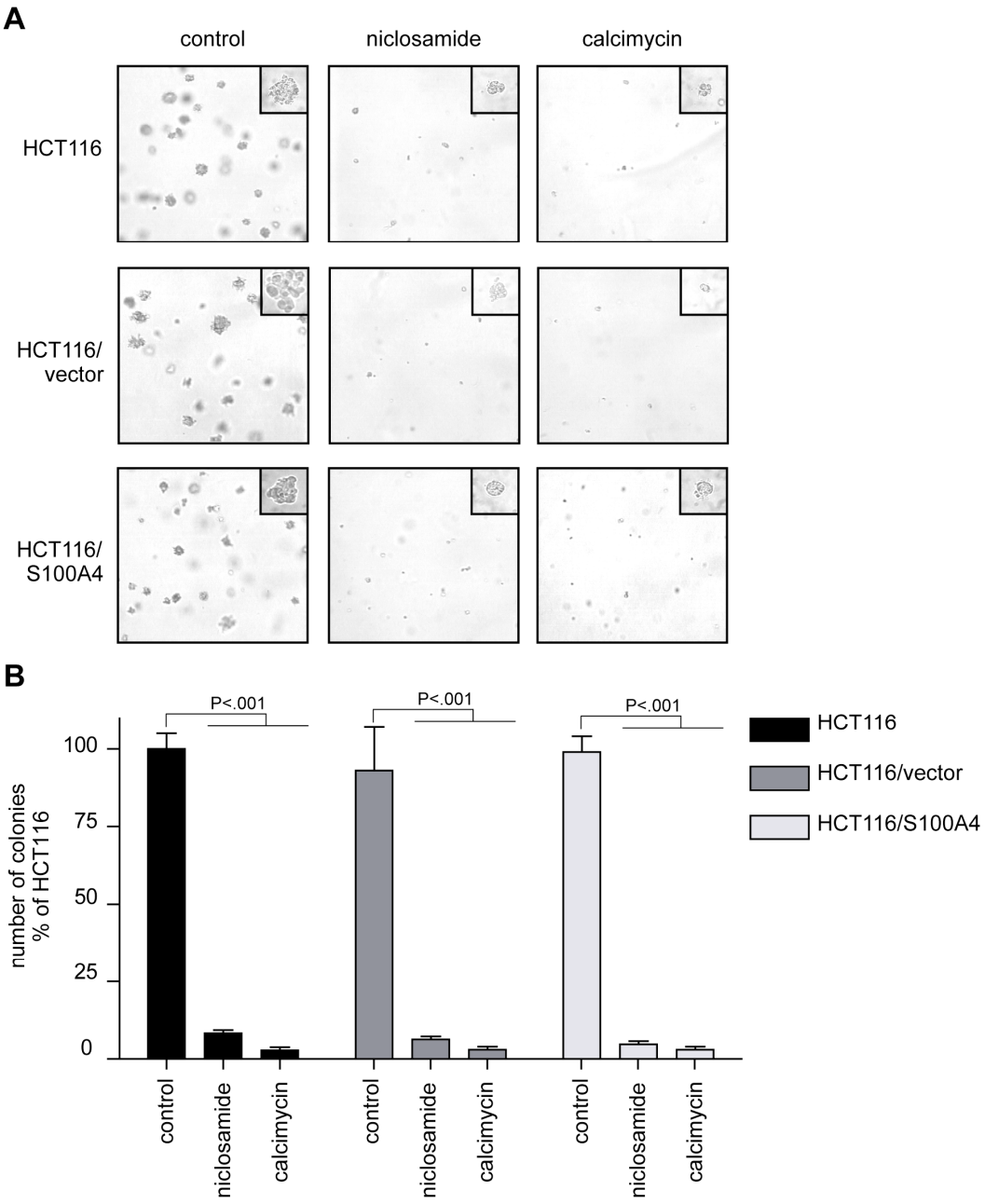

Fig. 4.8 Niclosamide and calcimycin inhibit anchorage-independent cell proliferation. Anchorage-independent growth of niclosamide or calcimycin-treated HCT116, HCT116/vector and HCT116/S100A4 cells was analyzed by colony formation assay. (A) Both small molecules reduced the size of HCT116, HCT116/vector and HCT116/S100A4 cell colonies. Microphotographs were taken on day 7 with 10x and 40x (insets) magnification. Assay was performed three times; one representative picture for each condition is presented here. (B) Both small molecules were able to reduce the number of HCT116, HCT116/vector and HCT116/S100A4 cell colonies. Data represent mean ± SE (n>3). Statistical significance was analyzed by two-sided ANOVA and Bonferroni post hoc multiple comparison test.

4.4. Structural changes on niclosamide reduce its inhibitory efficiency

The Drug Synthesis and Chemistry Branch, Developmental Therapeutics Program, NCI, Bethesda, MD, provided niclosamide derivatives which were synthesized by adding or removing chemical groups on or from the niclosamide structure as illustrated in Fig. 4.9.

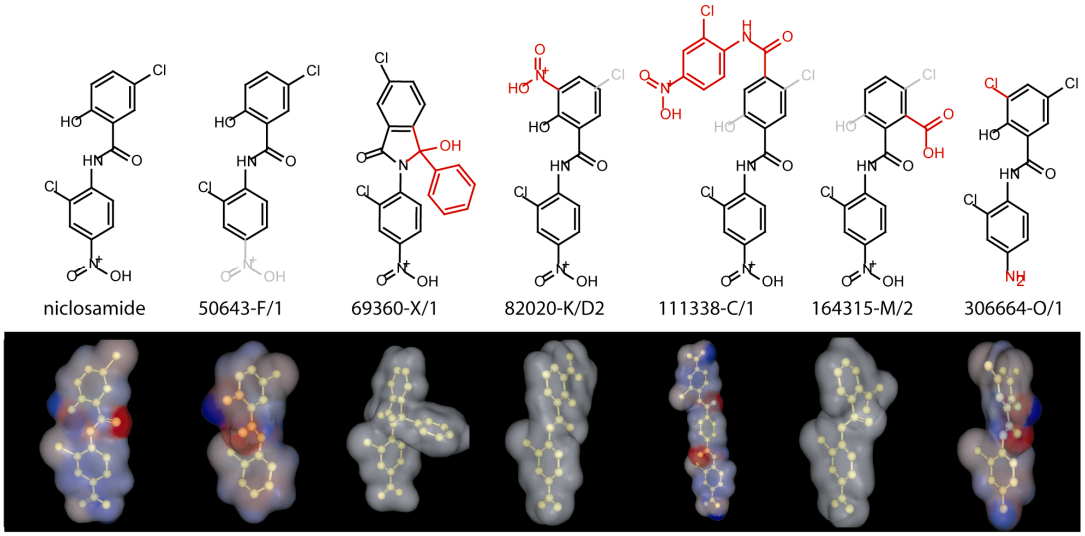

Fig. 4.9 Schematic drawing of niclosamide and its derivatives. Schema illustrates the comparison of the 2D and 3D structure of niclosamide to the structures of its derivatives; added and removed chemical groups were marked in red and grey, respectively. Grey clouds surrounding the 3D structure represent the van der Waals surface; red and blue indicate negative and positive charges, respectively.

The 3D structure prediction for the niclosamide derivatives was different to the 3D structure of niclosamide. Moreover, the van der Waals surface energy as predicted by MarvinSpace version 5.2.3_1 differed between niclosamide and its derivatives. Concluding from these observations, it was questioned how those structural differences between niclosamide and its derivatives would influence the inhibition of the S100A4 expression. To assess this efficiency of niclosamide and its derivates on S100A4 inhibition, HCT116 cells were treated with either of these compounds at the optimized treatment conditions defined for niclosamide. Exposure of HCT116 cells to any of the niclosamide derivatives had no significant effect on the S100A4 mRNA expression (Fig. 4.10A). In contrast, niclosamide inhibited the S100A4 mRNA level to less than 50 % of solvent-treated cells. Niclosamide treatment further reduced the S100A4 protein level, an effect that was not detected when cells were treated with any of the niclosamide derivatives. Consistently, cell migration was inhibited only upon niclosamide treatment, but not in the presence of any of the six derivatives (Fig. 4.10B). In summary, none of the niclosamide derivatives had a stronger inhibitory effect than niclosamide on S100A4 expression and S100A4-induced cell motility at the conditions

tested. Hence, changes in the structure of niclosamide result in a decrease of its efficiency towards S100A4 expression inhibition.

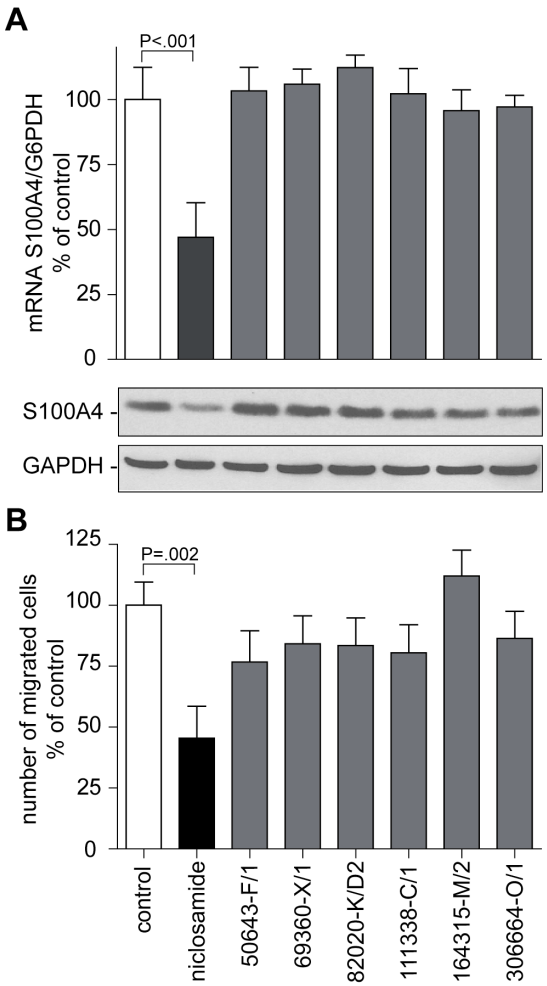

Fig. 4.10 Structural changes on niclosamide abolish its inhibiting function on S100A4 expression and S100A4-induced cell motility. HCT116 cells were treated with 1 µM niclosamide or with 1 µM of the niclosamide derivatives for 24 h and S100A4 expression was analyzed by qRT-PCR and Western blot, cell migration was analyzed with the Boyden chamber assay. (A) Niclosamide, but not its derivatives, inhibits S100A4 mRNA and protein expression. (B) Cell migration is most efficiently inhibited by niclosamide. Data represent mean ± SE (n>3). Statistical significance was analyzed by Student's t-test.

4.5. Small molecules interfere with the Wnt pathway

Both small molecules had a repressing function on the S100A4-promoter activity. However, the mechanism by which niclosamide or calcimycin performed this function was still to be elucidated. In 2006, Stein et al. described a TCF-binding site in the S100A4-promoter and provided evidence that S100A4 is a target gene of the canonical Wnt pathway (65). Therefore, it was analyzed if niclosamide or calcimycin might inhibit S100A4 expression by interfering with the Wnt pathway.

4.5.1. Small molecules inhibit the constitutively active Wnt pathway

The central player of the Wnt pathway is β-catenin, which is mutated in about 10% colon cancers (12, 64). Mutated β-catenin is resistant to proteasomal degradation resulting in a constitutively active β-catenin/TCF target gene transcription (38, 47).
HCT116 cells are heterozygous for a deletion mutation in the β-catenin allele. HAB68^{mut} cells are derivatives of HCT116 cells, in which the wildtype allele of β-catenin was deleted so that the cells had a constitutively active Wnt pathway (65). On the opposite, in HAB92^{wt} cells the mutated β-catenin allele was knocked-out so that the cells had wildtype β-catenin only which is not resistant to proteasomal degradation. Restriction fragment length polymorphism analysis as described in (65) allowed the verification of the β-catenin genotype of HCT116 and its derivative cells (Fig. 4.11)

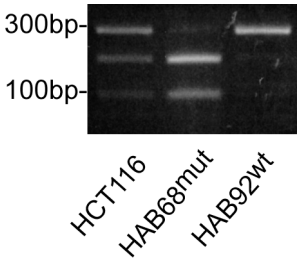

Fig. 4.11 β-catenin genotyping of HCT116 and its derivatives HAB68^{mut} and HAB92^{wt}. Restriction fragment length polymorphism analysis was used to identify the β-catenin genotype of HCT116, HAB68mut and HAB92wt cells. Deletion mutation of the serine 45 added a BsII restriction site, which was absent in the β-catenin wildtype allele. HCT116 are heterozygous bearing a wildtype and mutated β-catenin allele, HAB68mut cells were homozygous for the deletion mutation. HAB92wt cells were homozygous for the wildtype β-catenin allele.

Since S100A4 is a β-catenin/TCF target gene, its expression was analyzed in HCT116, HAB68^{mut} and HAB92^{wt} cells in the presence of either of the small molecules. Treatment of HCT116 and HAB68^{mut} cells with niclosamide reduced the S100A4 mRNA level to about 50-60% of solvent-treated HCT116 (Fig 4.12A). Further, niclosamide treatment reduced the S100A4 protein expression in these cells. HAB92^{wt} cells presented less than 10 % of the S100A4 expression level found in HCT116 cells. This weak expression of S100A4 in HAB92^{wt} cells was not significantly changed upon niclosamide treatment.
Consistently, with the S100A4 expression level, cell migration in niclosamide-treated HCT116 and HAB68^{mut} cells was significantly reduced to less than 50 % of solvent-treated HCT116 cells. Interestingly, niclosamide treatment reduced cell migration to the level of solvent- or niclosamide treated HAB92^{wt} cells (Fig. 4.12B).

Calcimycin reduced the S100A4 mRNA level of HCT116 and HAB68^{mut} cells to about 30 % of solvent-treated HCT116 cells (Fig 4.12C). S100A4 protein expression in those cells was clearly inhibited by calcimycin. Exposure of HCT116, HAB68^{mut} and HAB92^{wt} cells to calcimycin inhibited cell migration to less than 30 % of solvent-treated HCT116 cells (Fig. 4.12D). In summary, both small molecules were able to reduce the S100A4 expression and S100A4-induced cell migration independent on the β-catenin genotype. Thus, niclosamide and calcimycin inhibited β-catenin/TCF target gene transcription despite a constitutively active Wnt pathway.

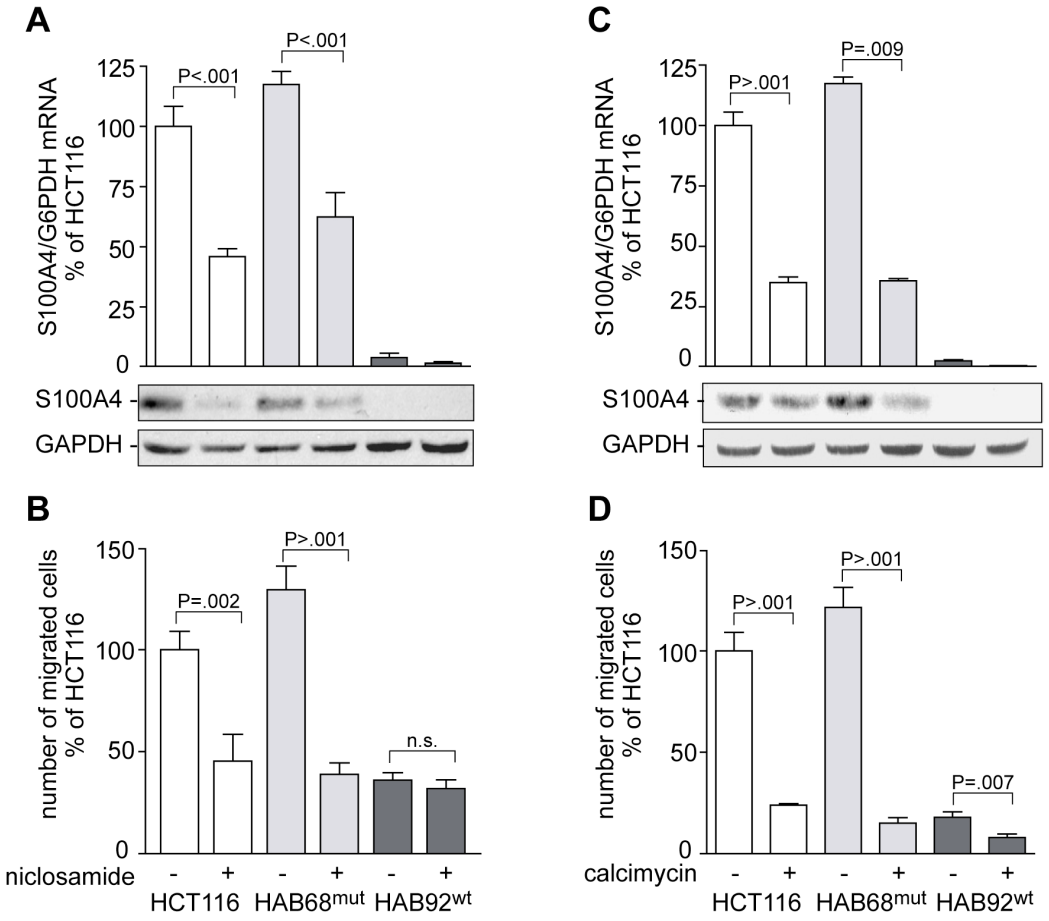

Fig. 4.12 Niclosamide and calcimycin inhibit S100A4 expression and S100A4-induced cell migration despite a constitutively active Wnt pathway. HCT116, HAB68^{mut} and HAB92^{wt} cells were treated with niclosamide or calcimycin and S100A4 expression was analyzed by qRT-PCR and Western blot. Cell migration was analyzed with the Boyden chamber assay. (A) Niclosamide inhibits the S100A4 expression despite mutated β-catenin. (B) Cell migration is inhibited in cells with constitutively active Wnt pathway upon niclosamide treatment. (C) Calcimycin inhibits S100A4 expression independent of the β-catenin genotype. (D) Calcimycin inhibits cell migration independent on the β-catenin genotype. Data represent mean ± SE (n=3). Statistical significance was analyzed by Student's t-test.

4.5.2. Calcimycin inhibits the β-catenin expression

To assess the mechanism underlying calcimycin inhibition of S100A4 expression, the Wnt pathway activity was analyzed by TOP/FOPflash reporter assay. According to their β-catenin genotype, the TOPflash reporter activity was increased in HAB68^{mut} cells and reduced in HAB92^{wt} cells to only 30 % of HCT116 cells (Fig. 4.13A). Exposure of HCT116 to calcimycin significantly reduced the TOPflash reporter activity to less than 30 % of solvent-treated HCT116 cells. In HAB68mut and HAB92wt cells calcimycin treatment reduced TOPflash reporter activity to less than 15 % of solvent-treated HCT116 cells.

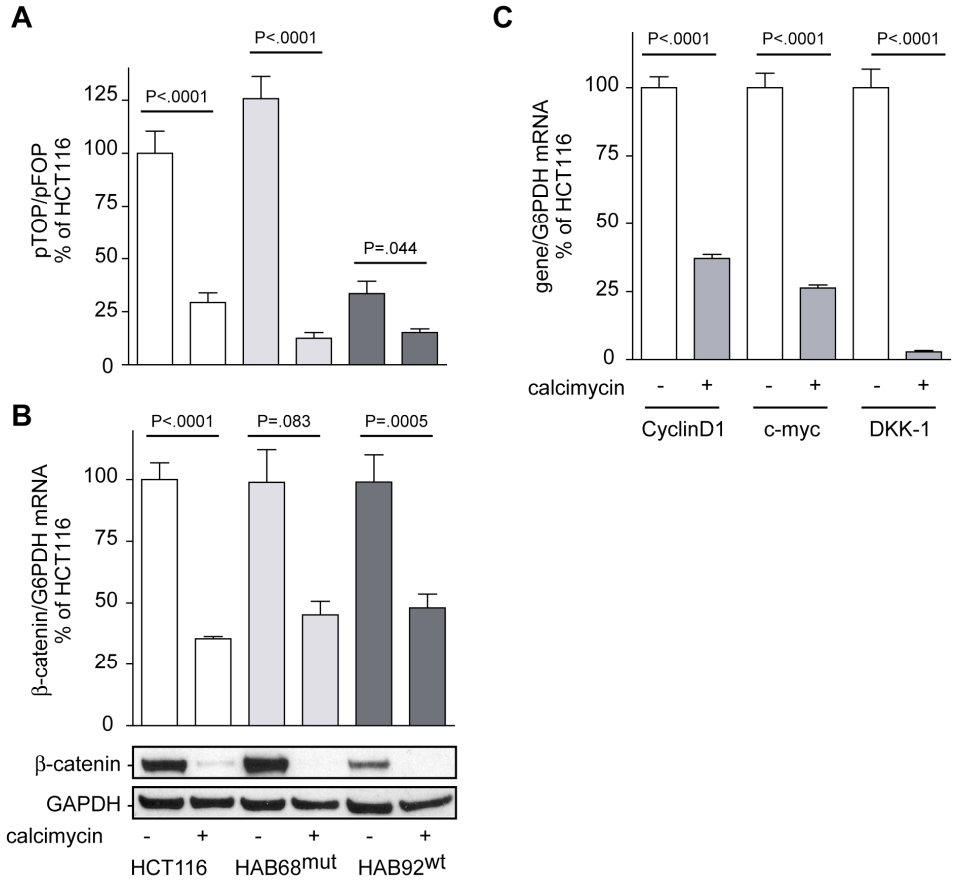

Fig 4.13 Calcimycin inhibits the Wnt pathway by interfering with β-catenin expression. HCT116, HAB68^{mut} and HAB92^{wt} cells were treated with 1 µM calcimycin for 18 h and Wnt pathway activity was determined with TOF/FOPflash assay while the expression of β-catenin or β-catenin/TCF target genes was analyzed with qRT-PCR and Western blot. (A) Calcimycin inhibited Wnt pathway activity in HCT116, HAB68^{mut} andHAB92^{wt} cells. (B) β-catenin mRNA and protein expression is reduced upon calcimycin treatment. (C) Calcimycin reduced β-catenin/TCF target gene mRNA levels in HCT116 cells. Data represent mean ± SE (n=3). Statistical significance was analyzed by Student's t-test.

The extent to which β-catenin/TCF target gene transcription is active is highly dependent on the expression level of β-catenin in the cells (47). In solvent-treated HCT116, HAB68^{mut} and HAB92^{wt} cells no significant differences in the β-catenin mRNA

level were detected (Fig 4.13B). Treatment of those three cell species with calcimycin reduced the β-catenin mRNA level to less than 50 % of solvent-treated HCT116 cells. Since HAB92^{wt} cells only expressed the wildtype β-catenin protein, which is not resistant to proteasomal degradation, the β-catenin protein level in those cells was reduced compared to solvent-treated HCT116 and HAB68^{mut} cells. Treatment with calcimycin further diminished β-catenin protein expression in all three cell species.
Reduced β-catenin levels might result in reduced target gene transcription. Thus the expression levels of prominent β-catenin/TCF target genes were analyzed such as Cyclin D1 (170), c-myc (171) and DKK-1 (60). Consistently, in calcimycin-treated HCT116 cells the expression of Cyclin D1, c-myc and DKK-1 was significantly inhibited to 35%, 25% and 2% of the solvent-treated control, respectively (Fig 4.13C).

4.5.3. Niclosamide interferes with the β-catenin/TCF-complex

TOP/FOPflash reporter assay was used to analyze whether niclosamide interfered with the Wnt pathway. As it was found for calcimycin, exposure of HCT116, HAB68^{mut} and HAB92^{wt} cells to niclosamide reduced the TOPflash reporter activity to less than 50 % of solvent-treated HCT116 cells (Fig. 4.14A). Thus, niclosamide inhibited the Wnt pathway activity. Consistently, transcription of β-catenin/TCF target genes such as Cyclin D1, c-myc and DKK-1 was significantly reduced in niclosamide treated HCT116 cells (Fig. 4.14B)
For β-catenin/TCF target gene transcription, β-catenin needs to translocate from the cytoplasm to the nucleus (47). Exposure of HCT116 cells to increasing concentrations of niclosamide for 18 h did not change the protein level of nuclear β-catenin (Fig. 4.14C). Nonetheless, despite the presence of nuclear β-catenin, the TOPflash reporter activity was reduced (Fig. 4.14A). To test if niclosamide inhibits the formation of the β-catenin/TCF transcription activating complex, electrophoretic mobility shift assay (EMSA) was performed. In the same nuclear extract used for determination of the β-catenin protein level, biotinylated oligonucleotides which encompassed the T-cell factor (TCF)-binding site of the S100A4-promoter were incubated and analyzed by EMSA. In solvent-treated HCT116 cells signal shifts were caused by binding of TCF and β-catenin/TCF to the oligonucleotides, which is consistent with previous findings (65). Exposure of HCT116 cells to increasing concentrations of niclosamide interrupted the β-catenin/TCF/oligo complex in a concentration-dependent manner (Fig 4.14C). The presence of β-catenin within the complex was verified by complexation with monoclonal anti-β-catenin leading to a supershift (Fig 4.14D). No supershift could be detected in nuclear extracts from 1 µM niclosamide-treated HCT116 cells.

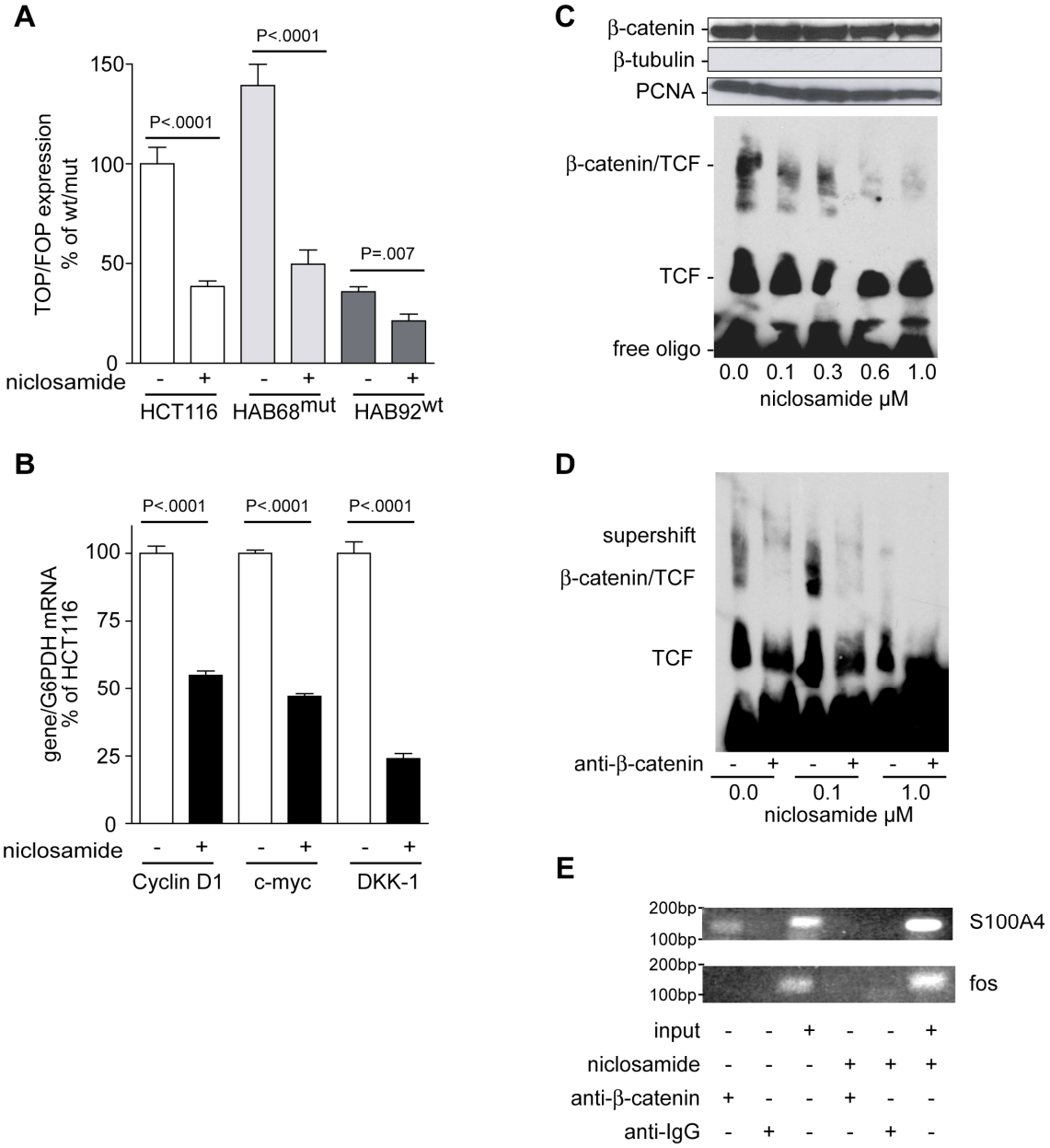

Fig. 4.14 Niclosamide inhibits the Wnt pathway by interfering with the β-catenin/TCF-complexation. HCT116, HAB68^{mut} and HAB92^{wt} cells were treated with 1 µM niclosamide for 18 h and Wnt pathway activity was analyzed by TOP/FOPflash reporter assay. (A) Niclosamide inhibited Wnt pathway activity in HCT116, HAB68^{mut} andHAB92^{wt} cells. (B) Niclosamide inhibited β-catenin/TCF target gene transcription. Data represent mean ± SE (n=3). Statistical significance was analyzed by Student's t-test. Nuclear extracts from HCT116 cells treated with indicated niclosamide concentrations for 24 h were analyzed with Western blot and EMSA. (C) Increasing concentrations of niclosamide had no effect on the nuclear β-catenin protein level, but inhibited the β-catenin/TCF complex on biotinylated oligonucleotides which comprised the TCF-binding site of the S100A4-promoter. (D) Supershift verified β-catenin protein in β-catenin/TCF/oligonucleotide complex. (E) No S100A4-promoter fragment could be PCR amplified after treatment of HCT116 cells with 1 µM niclosamide for 24 h. For Western blot, EMSA and ChIP data (n>2) one representative blot is shown here.

Similar results were found with chromatin immunoprecipitation (ChIP) assay (Fig. 4.14E). From solvent-treated cell extracts the S100A4-promoter sequence could be PCR amplified after β-catenin-immunoprecipitation, as described earlier (65). In contrast, no PCR-amplicon was obtained from niclosamide-treated HCT116 cells. Further, no PCR product could be detected when control immunoglobulin G was used for precipitation or when a fos-promoter sequence was PCR amplified. These results indicate that niclosamide treatment inhibited β-catenin/TCF complexation and thereby restricted Wnt target gene transcription.

4.6. Niclosamide inhibits metastasis formation in colon cancer xenograft mice

Since niclosamide inhibited the S100A4 expression and S100A4-induced cell migration and invasion of colon cancer cells *in vitro*, the anti-metastatic effects of this small molecule inhibitor were determined in xenograft mice. Stein et al. previously described that the intrasplenical application of HCT116 cells into xenograft mice was suitable to analyze their ability to form liver metastases (65).

4.6.1. Evaluation of an *in vivo* applicable niclosamide concentration

For dose-finding experiments in human colon cancer xenograft mice, NODSCID mice were intrasplenically injected with HCT116/LUC cells and were intraperitoneally treated with daily doses of 6 mg/kg, 12 mg/kg or 24 mg/kg niclosamide or the respective amount of solvent in cooperation with PD. Dr. Induna Fichtner (MDC, Berlin, Germany). Body weight was measured as a first indicator for toxic adverse effects (172). Body weight loss of mice treated with 12 mg/kg or 6 mg/kg niclosamide did not differ from the solvent-treated control (Fig. 4.15A).

In contrast, mice which received daily doses of 24mg/kg niclosamide presented increased weight loss until day 24. To evaluate a possible maximum concentration that could be applied to mice without toxic adverse effects, niclosamide was intraperitoneally applicated at concentrations of 20 mg/kg every 24 h or 15 mg/kg every 12 h. Analysis of body weight revealed no differences between niclosamide- and solvent-treated mice (Fig 4.15B). Thus these concentrations were further used to analyze metastasis formation.

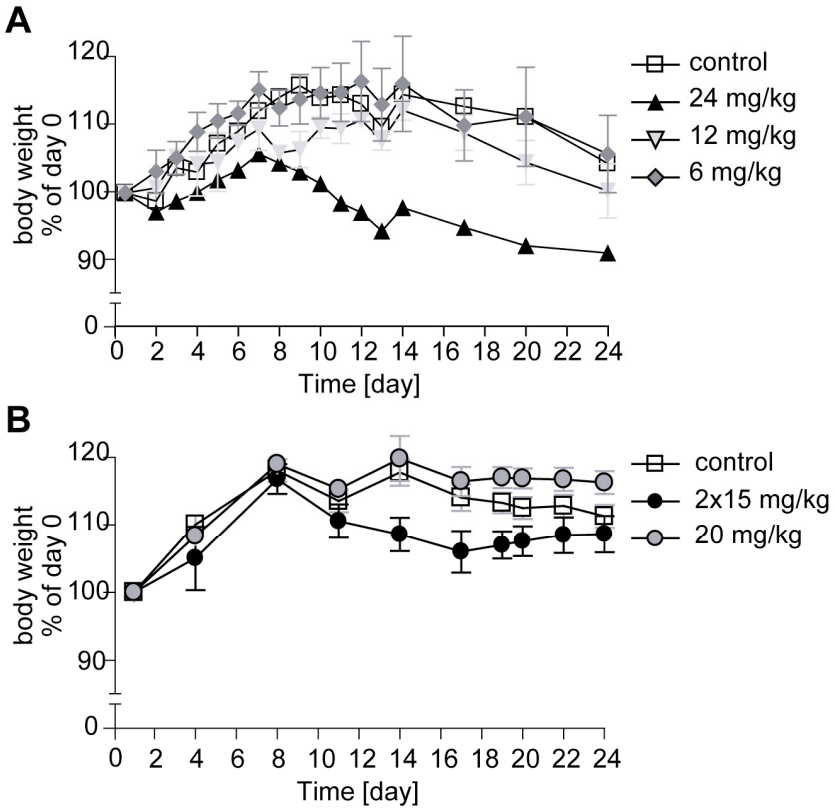

Fi**g. 4.15 Daily doses of 24 mg/kg niclosamide caused toxic side effects in xenograft mice.** Indicated concentrations of niclosamide were injected intraperitoneally and daily into NODSCID mice bearing an intrasplenal HCT116/LUC tumor. Body weight was determined as an indicator for toxic side effects. (A) Weight loss in mice treated with 24 mg/kg niclosamide was increased compared to solvent-treated control. Data represent mean ± SD (2 animals/group) (B) No difference in weight loss was observed in solvent or niclosamide-treated mice. Data represent mean ± SD (9 animals/group)

4.6.2. *In vivo* metastasis can be visualized by bioluminescence imaging

Bioluminescence imaging (BLI) presents a non-invasive tool which allows visualizing the process of metastasis formation over time (173). To allow tracking of the colon cancer cells within the organism, HCT116/LUC cells were used. These cells had an endogenously increased level of S100A4 expression as also seen in HCT116 cells, but further expressed a CMV-promoter controlled firefly luciferase. This enzyme allows the oxidation of D-Luciferin, which leads to the emission of light.

To monitor the effect of niclosamide on metastasis formation *in vivo*, HCT116/LUC cells were intrasplenically injected into SCID mice and the animals were treated daily with 20 mg/kg niclosamide or the respective amount of solvent. A lateral signal became visible on day 8 post-transplantation in solvent- and niclosamide-treated mice, which was assigned to the spleen (Fig. 4.16A). This spleen tumor signal increased in solvent-

and niclosamide-treated mice until it reached a maximum on day 22. In control mice ventral imaging revealed a very low signal in the liver region on day 8 indicating that liver metastases had formed (Fig. 4.16B). This liver signal became clearly visible until day 22. In contrast, in niclosamide-treated mice no liver signal was detected until day 22.

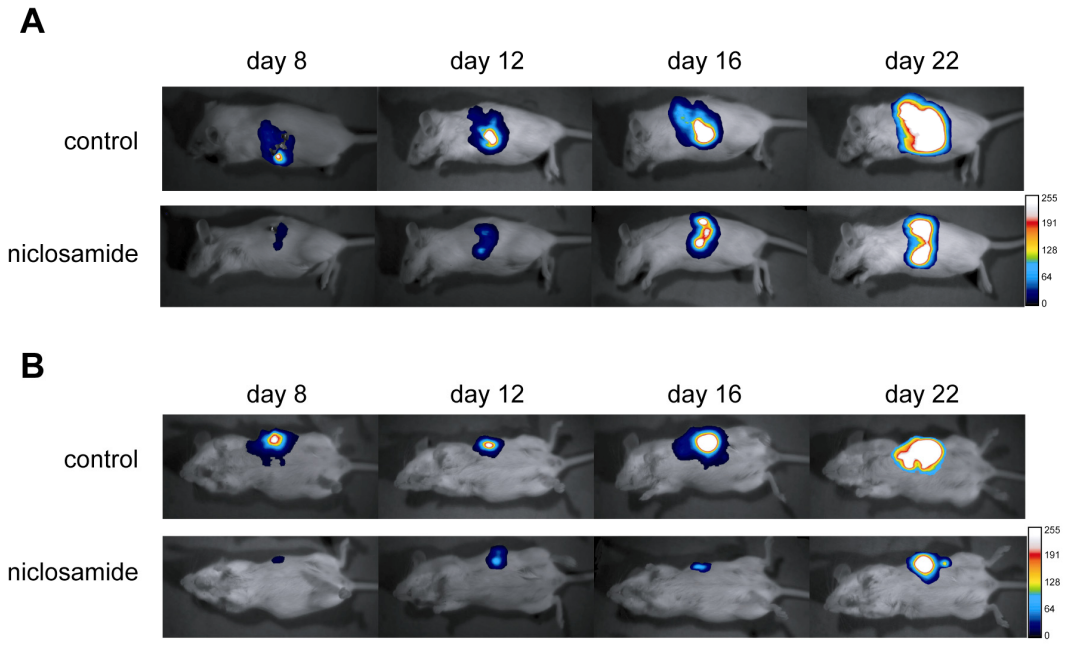

Fig. 4.16 Metastasis formation in colon cancer xenograft mice is monitored by non-invasive bioluminescence imaging. SCID mice were intrasplenically transplanted with HCT116/LUC cells. Bioluminescence was measured by intraperitoneal application of 150 mg/kg D-Luciferin and exposure for 20 sec in the NightOWL LB 981 system. (A) The lateral signal from the spleen tumor is increasing over time in solvent- and niclosamide-treated mice. (B) Control mice present a ventral liver metastases signal which is absent in niclosamide-treated mice. Data are representative of 4 animals per group.

In situ imaging was performed to confirm the origin of the lateral and ventral signals. Dissection of control mice presented liver metastases which were absent in niclosamide-treated mice (Fig. 4.17). Since only the HCT116/LUC cells expressed the firefly luciferase, bioluminescence imaging could confirm that the expected liver metastases were formed by these human colon cancer cells. Imaging of the isolated liver and spleen showed that control mice had increased liver metastases. In contrast, no or only tiny liver metastases signals could be detected in niclosamide-treated mice.

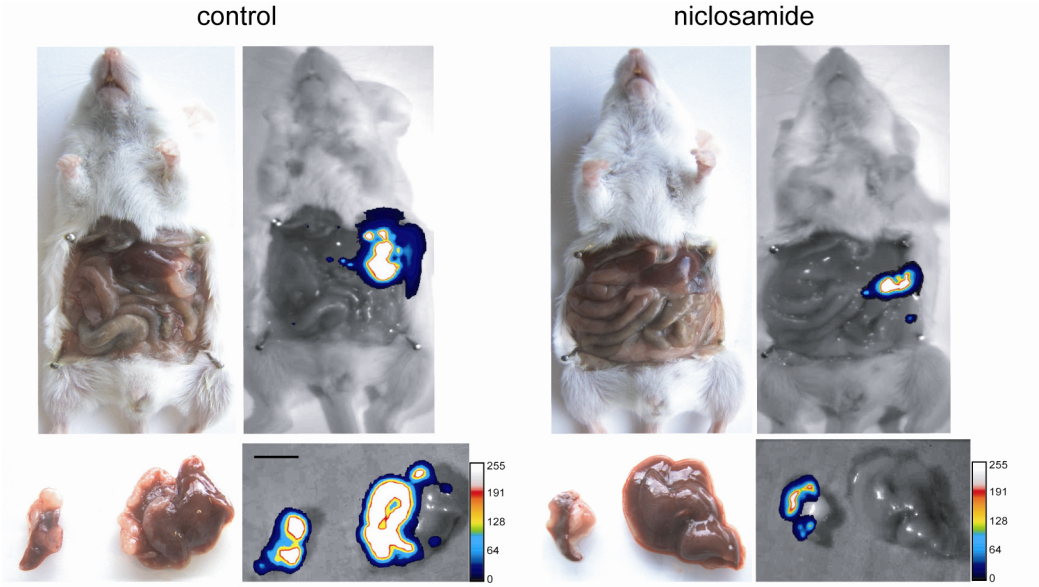

Fig. 4.17 *In situ* imaging confirmed the presence or absence of metastasis formation in colon cancer xenograft mice. Intrasplenically transplanted HCT116/LUC cells SCID xenograft mice were intraperitoneally injected of 150 mg/kg D-Luciferin, dissected and exposed for 1 sec in the NightOWL LB 981 system. *In situ* imaging and imaging of isolated organs confirmed that the signals seen in Fig. 4.16 originated from the spleen tumor and liver metastasis. The latter was absent in niclosamide treated mice. Data are representative of 4 animals per group.

4.6.3. Niclosamide restricts metastasis formation in mouse xenografts

Metastasis formation under niclosamide treatment was quantified in cooperation with PD. Dr. Induna Fichtner. NODSCID mice bearing an intrasplenical tumor of HCT116/LUC cells were treated either daily with 20 mg/kg niclosamide or twice a day with 15 mg/kg niclosamide.

All mice developed a spleen tumor until day 24, which was dissected to analyze the S100A4 mRNA levels in the tumor tissues. In niclosamide treated mice the S100A4 mRNA level in the spleen tumors was significantly reduced to 56-64 % of the S100A4 expression level found in tumors from solvent-treated mice (Fig. 4.18A). These results indicated that niclosamide does also inhibit S100A4 expression *in vivo*.

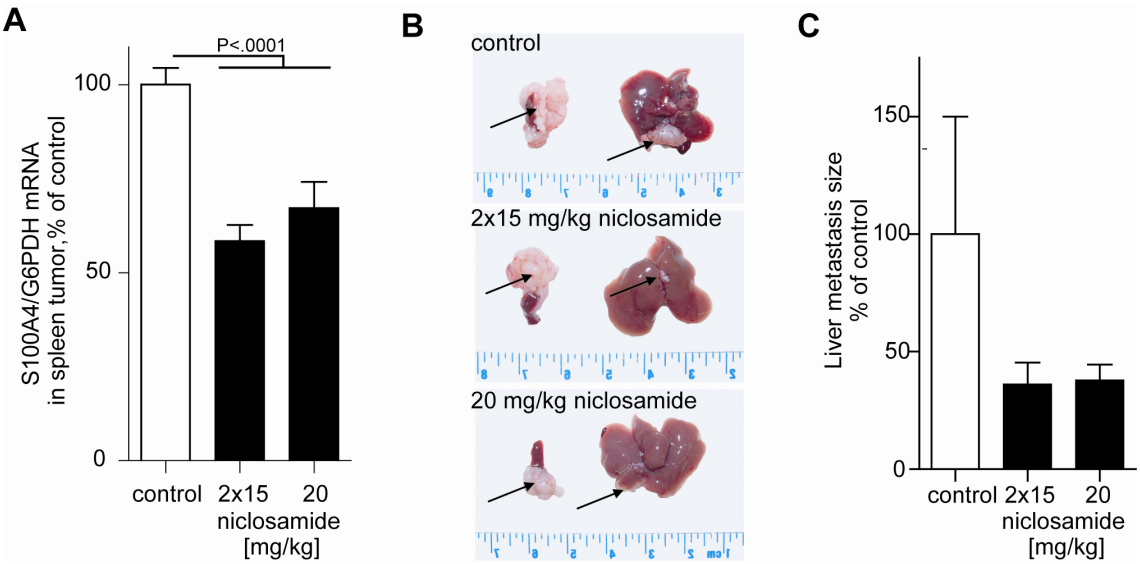

Fig. 4.18 Niclosamide inhibits metastasis formation in human colon cancer xenograft mice. HCT116/LUC cells were intrasplenically transplanted into NODSCID mice and mice were treated intraperitoneally with 20 mg/kg niclosamide every 24 h or with 15 mg/kg niclosamide every 12 h. The S100A4 mRNA level in the spleen tumor was determined on day 24 by qRT-PCR. Liver metastases were quantified by scoring. (A) Niclosamide treatment inhibited S100A4 expression *in vivo*. Data represent mean ± SE (9 animals/group). Statistical significance was analyzed by two-sided ANOVA and Bonferroni post hoc multiple comparison test. (B) Niclosamide treatment restricted liver metastasis in xenograft mice. (C) Liver metastases were reduced in number and size in niclosamide-treated mice. Data represent mean ± SE (9 animals/group).

In contrast to niclosamide treated mice, in solvent-treated animals large liver metastases were found, which were absent in animals from both niclosamide-treated groups (Fig. 4.18B). Scoring of the liver metastases including their number and size revealed that both niclosamide treatments inhibited liver metastasis formation to less than 35 % of solvent-treated mice (Fig. 4.18C). In conclusion, niclosamide inhibited the S100A4-expression and thus the metastatic potential of human colon cancer cells in xenograft mice.

4.7. Relation of the DKK-1 and S100A4 expression in colon cancer cells

The studies on niclosamide and calcimycin targeting S100A4 expression in colon cancer cells emphasized the power of S100A4 to increase cell migration and invasion and to drive metastasis formation. Many interaction partners for S100A4 are known that explain its metastasis-promoting ability. However, less is known about the transcriptional changes that occur upon S100A4 overexpression which might form the basis for metastasis formation. Based on microarray data, Stein and colleagues were the first to observe that S100A4 overexpression represses the expression of DKK-1, a prominent inhibitor of the Wnt pathway. Based on those findings the relation of S100A4 and DKK-1 expression was analyzed.

4.7.1. DKK-1 and S100A4 expression is inversely correlated in cells with mutated or non-mutated β-catenin

S100A4 and DKK-1 were both described as target genes of the canonical Wnt pathway in colon cancer cells (60, 65). Therefore, their expression was analyzed in HCT116 cells and its derivatives HAB68^{mut} and HAB92^{wt}. The mRNA levels of S100A4 and DKK-1 did not significantly differ between HCT116 and HAB68^{mut} cells (Fig. 4.19A). In contrast, the S100A4 mRNA level in HAB92^{wt} cells was reduced to about 10% of HCT116 cells. Interestingly, HAB92^{wt} cells expressed about 10-fold more DKK-1 mRNA compared to HCT116 or HAB68^{mut} cells that expressed mutated β-catenin. Similarly, S100A4 protein was high in HCT116 and HAB68^{mut} cells, but clearly lower in HAB92^{wt} cells. On the opposite, the amount of secreted DKK-1 protein in HCT116 and HAB68^{mut} cells was less than 30% of the amount of secreted DKK-1 found in HAB92^{wt} cells.
While S100A4 expression was related to the Wnt pathway activity found in HCT116, HAB68^{mut} and HAB92^{wt} cells (Fig. 4.12A/B), the expression of DKK-1 was inversely regulated.

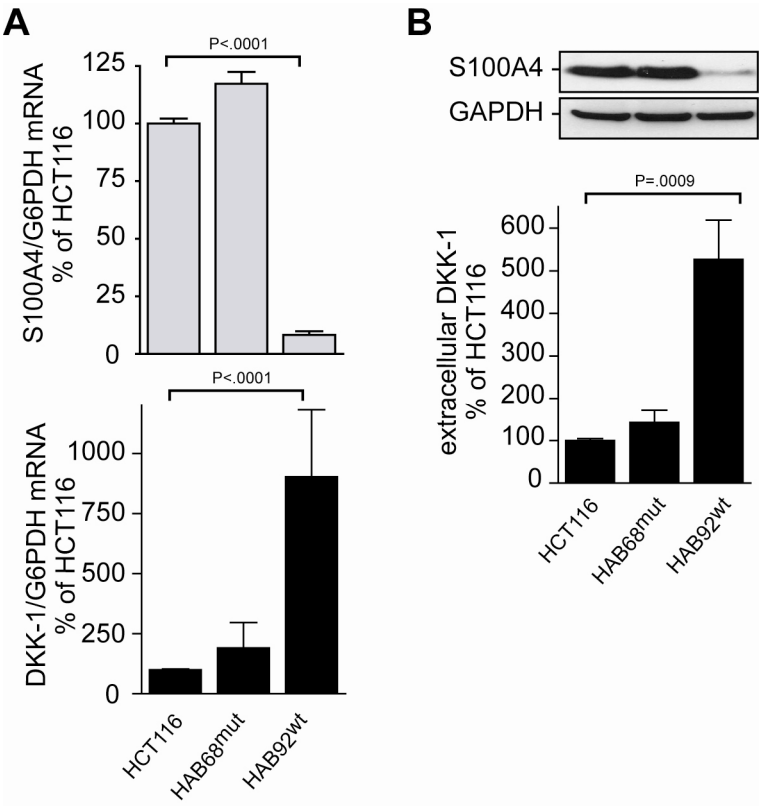

Fig. 4.19 S100A4 and DKK-1 are inversely expressed in cells with mutated or wildtype β-catenin. S100A4 and DKK-1 mRNA levels were analyzed by qRT-PCR, S100A4 and DKK-1 protein was analyzed by Western blot and ELISA, respectively. (A) S100A4 mRNA expression is high in cells with mutated β-catenin genotype while DKK-1 mRNA levels are high in cells with wildtype β-catenin. (C) The S100A4 protein is low in cells with wildtype β-catenin while DKK-1 expression is low in cells with mutated β-catenin. Data represent mean ± SE (n>3). Statistical significance was analyzed by two-sided ANOVA and Bonferroni post hoc multiple comparison test.

4.7.2. DKK-1 and S100A4 expression is negatively correlated in human colon cancer cell lines.

The inverse expression of S100A4 and DKK-1 found in HCT116 and its derivative cells was further investigated in a set of 13 colon cancer cell lines. In comparison to HCT116 cells the S100A4 mRNA levels in SW620, LS174T Colo205 and SW480 cells was at least 2.5-fold more than in HCT116 cells. Further these cells presented very low levels of DKK-1 mRNA (Fig. 4.20A). In contrast, HCT15, Lovo, HT29, HAB92^{wt} and Caco-2 cells presented at least 2.5-fold higher levels of DKK-1 and very low levels of S100A4 mRNA. The mRNA levels of both genes were low in WiDr, KM12, SW48 and DLD1 cells.

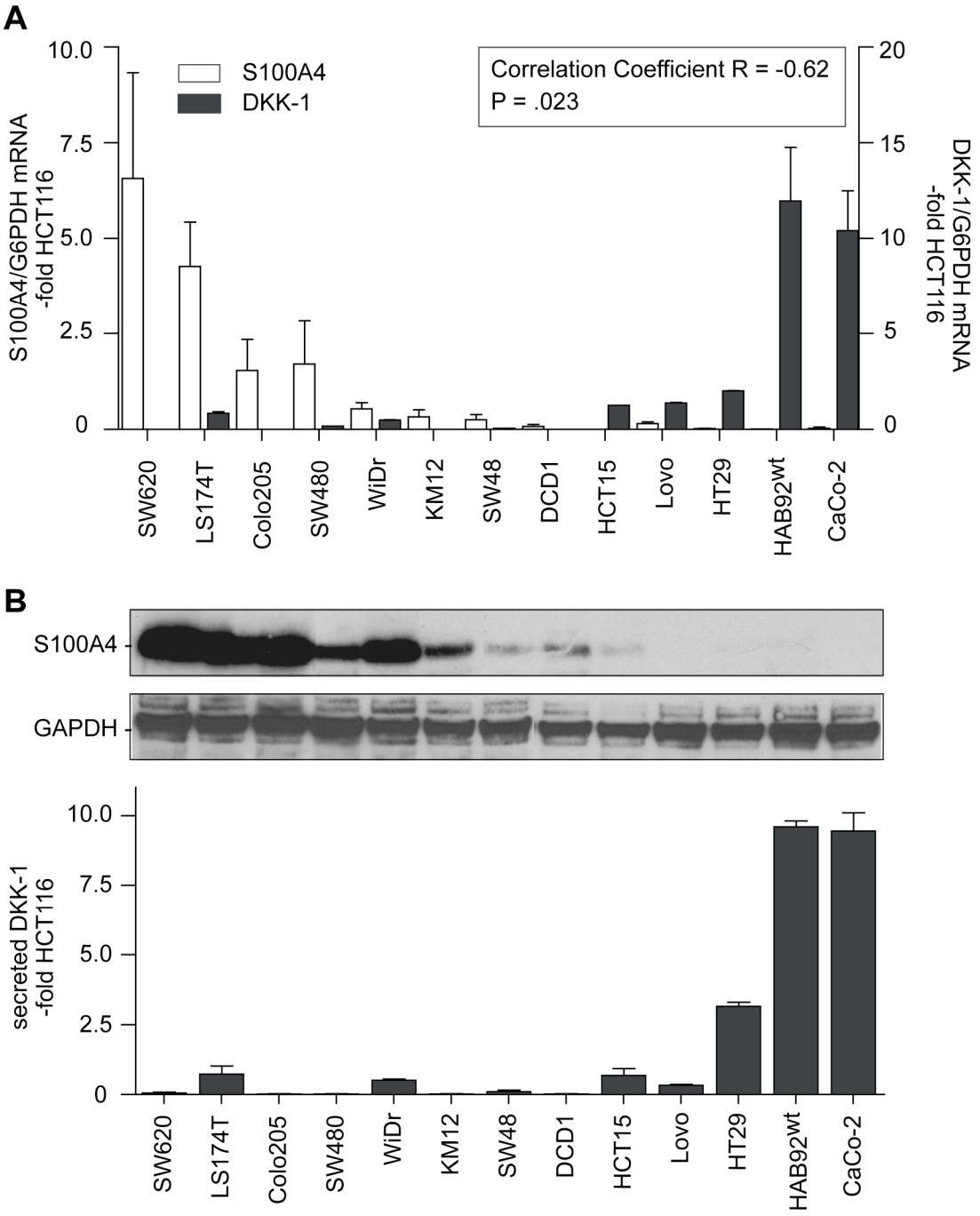

Fig. 4.20 S100A4 and DKK-1 are inversely expressed in colon cancer cell lines. In a set of 13 colon cancer cell lines the mRNA level of S100A4 and DKK-1 were analyzed by qRT-PCR. S100A4 and DKK-1 protein was analyzed by Western blot and ELISA, respectively. (A) In the 13 colon cancer cell lines that expressed increased S100A4 mRNA levels, DKK-1 mRNA was decreased and vice versa. Data represent mean ± SE (n>3). Correlation was analyzed by non-parametric Spearman correlation test. (B) On the protein level, cell lines in which S100A4 protein was high, only low levels of secreted DKK-1 protein could be detected. ELISA data represent mean ± SE (n>3).

Similar results were found on the protein level (Fig. 4.20B). In SW620, LS174T, Colo205 and WiDr cells increased levels of S100A4 protein were found and only low levels of secreted DKK-1 were detected in those cell lines. In contrast, in HT29, HAB92^{wt} and Caco-2 cells secreted DKK-1 protein levels were increased while the S100A4 protein was very low.

In summary, this set of colon cancer cell lines comprised cells that either expressed increased S100A4 or increased DKK-1 or both genes were expressed to a low level. Surprisingly, none of the cell lines had both genes upregulated. From this result it was hypothesized that the expression of either S100A4 or DKK-1 has a repressing function on the respective opponent gene.

4.8. S100A4 is a negative regulator of DKK-1 expression

4.8.1. Exogenous overexpression of S100A4 inhibits DKK-1 expression

If S100A4 had a repressing function on the DKK-1 expression, its exogenous overexpression should reduce the mRNA and protein levels of DKK-1. To assess this, HAB92^{wt} cells were used, since they had endogenously increased levels of DKK-1. The cells were stably transfected to express a CMV-promoter controlled S100A4 cDNA or the empty vector as control. HAB92^{wt} cells and its stable transfected derivatives were homozygous for the wildtype β-catenin as was shown by RFLP (Fig. 4.21A).

Analysis of the S100A4 and DKK-1 expression level showed that no significant difference between HAB92^{wt} and empty vector-transfected HAB92^{wt} cells was found neither for S100A4 nor DKK-1 (Fig. 4.21B). Hence, the vector backbone itself did not interfere. In contrast, the S100A4 mRNA level of S100A4 cDNA-transfected cells was 15-fold increased compared to the level of HAB92^{wt} cells. Moreover, the DKK-1 mRNA level in those cells was more than 2.5-fold decreased compared to non- or vector-transfected HAB92^{wt} cells.

S100A4 protein levels were clearly increased in S100A4-transfected HAB92^{wt} cells compared to the non- or vector-transfected control (Fig. 4.21C). However, the amount of secreted DKK-1 protein was significantly reduced in those cells. In summary increased levels of S100A4 mRNA and protein inhibited the expression of DKK-1 in HAB92^{wt}.

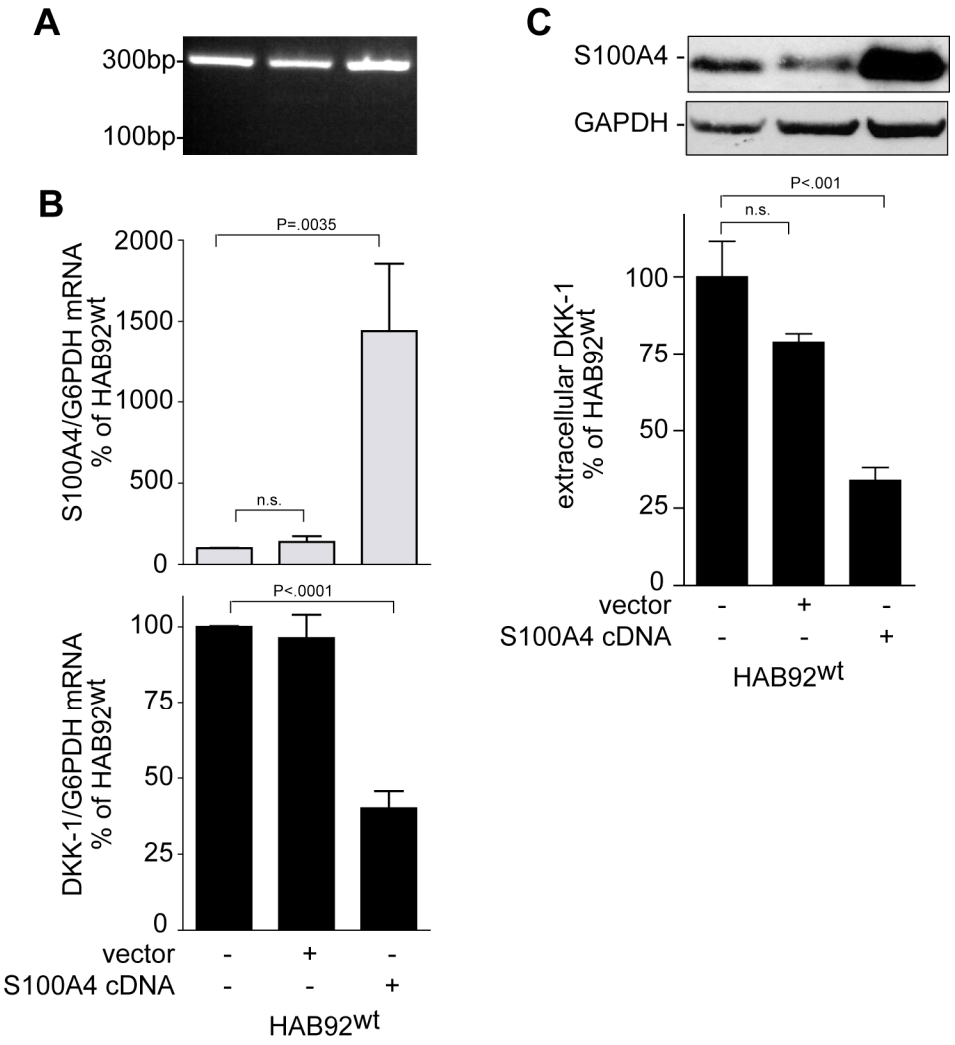

Fig. 4.21 Exogenous overexpression of S100A4 inhibits DKK-1 expression. In HAB92^{wt} cells the β-catenin genotype was analyzed by RFLP. S100A4 and DKK-1 mRNA levels were analyzed by qRT-PCR. S100A4 and DKK-1 protein was analyzed by Western blot and ELISA, respectively. (A) HAB92^{wt} cells and its stable transfected derivatives were homozygous for wildtype β-catenin. (B) Overexpression of S100A4 cDNA increased S100A4, but decreased the DKK-1 mRNA level. (C) Overexpression of S100A4 cDNA increased the S100A4 protein amount, but repressed the amount of secreted DKK-1 protein. Data represent mean ± SE (n>3). Statistical significance was analyzed by two-sided ANOVA and Bonferroni post hoc multiple comparison test.

4.8.2. Reduction of S100A4 expression recovers DKK-1 expression

Since S100A4 overexpression inhibited DKK-1 expression, it was hypothesized that reduced S100A4 expression would result in increased DKK-1 mRNA and protein levels. To address this, HCT116 cells were used since those cells presented an increased endogenous S100A4 expression level. HCT116 cells were either stably transfected to express a non-targeting control shRNA or a shRNA targeting the S100A4 mRNA. Stable transfection did not interfere with the β-catenin genotype

(Fig 4.22A). No significant differences in the expression level of S100A4 and DKK-1 were detected in HCT116 cells treated with non-targeting control shRNA compared to the non-transfected HCT116 cells (Fig. 4.22B). In contrast, transfection with shRNA targeting the S100A4 mRNA reduced the latter to less than 50 % of HCT116 cells. Furthermore, in those cells, the DKK-1 mRNA level was 2-fold increased compared to HCT116 cells.

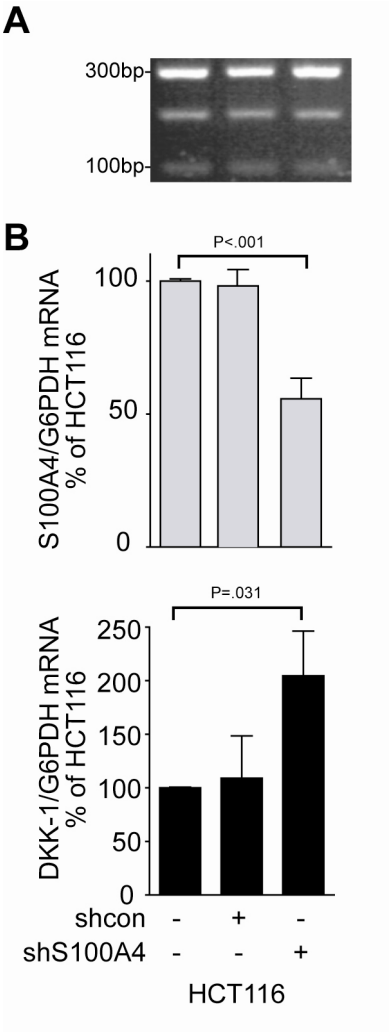

Fig. 4.22 Inhibition of endogenous S100A4 recovers DKK-1 expression. In HCT116 cells the β-catenin genotype was analyzed by RFLP. S100A4 and DKK-1 mRNA levels were analyzed by qRT-PCR. S100A4 and DKK-1 protein was analyzed by Western blot and ELISA, respectively. (A) HCT116 cells and its derivatives were heterozygous for wildtype and mutated β-catenin. (B) Transfection of HCT116 cells with non-targeting shRNA (shcon) had no effect on S100A4 and DKK-1 expression. Transfection with a shRNA targeting S100A4 expression decreased S100A4 and increased DKK-1 mRNA levels. Data represent mean ± SE (n>3). Statistical significance was analyzed by two-sided ANOVA and Bonferroni post hoc multiple comparison test.

4.9. DKK-1 inhibits S100A4 expression

Since S100A4 inhibits DKK-1 expression, the functional consequences of this gene regulation were further analyzed. Secreted DKK-1 was found to interact with the membranous co-receptor LRP-5/6 and thereby sequesters it from the Wnt-frizzled signaling complex (53, 58). Thus, DKK-1 inhibits the Wnt pathway.

Transfection of HAB92^{wt} cells with shRNA targeting DKK-1 mRNA decreased the DKK-1 mRNA level to less than 10 % of HAB92^{wt} cells which were transfected with a non-targeting control shRNA (Fig. 4.23A). Upon decreased DKK-1 expression, the S100A4 mRNA level was 4-fold increased in those cells compared to control shRNA-transfected cells.

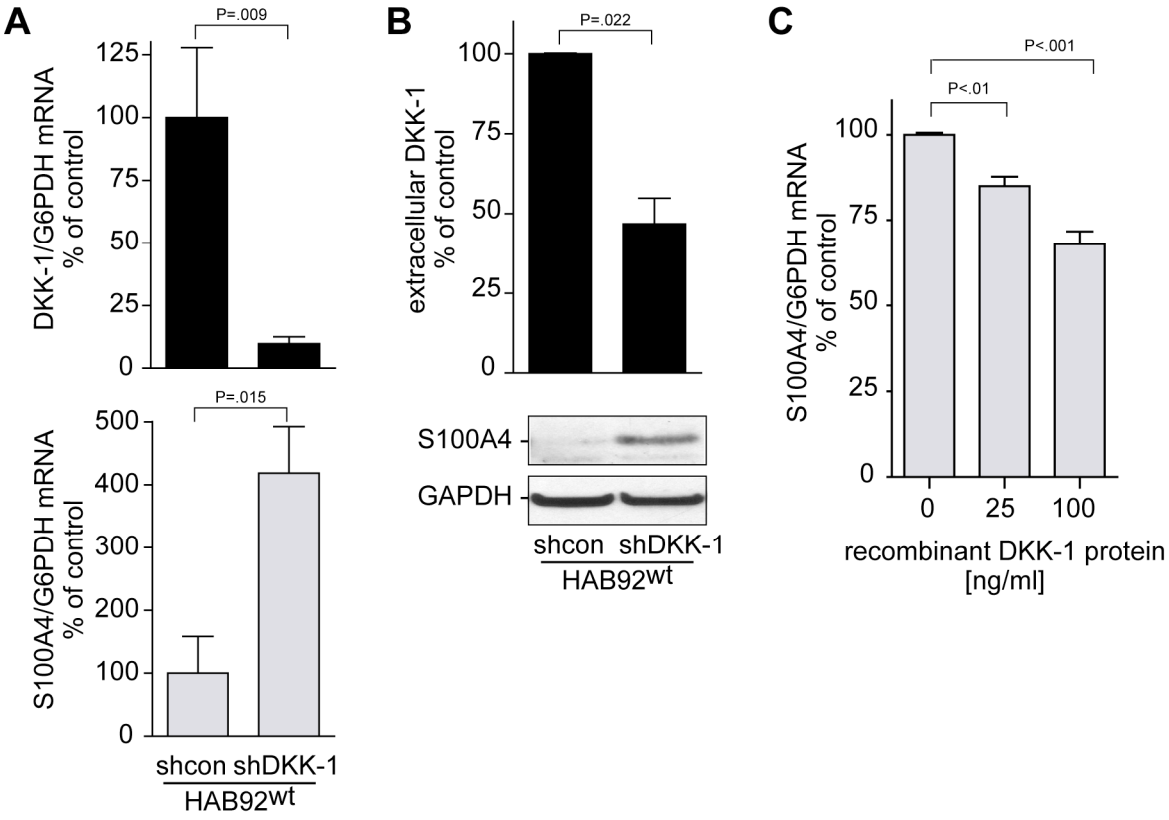

Fig. 4.23 DKK-1 is a negative regulator of S100A4 expression. S100A4 and DKK-1 mRNA levels were analyzed by qRT-PCR. S100A4 and DKK-1 protein was analyzed by Western blot and ELISA, respectively. (A) HAB92^{wt} stably transfected with non-targeting (shcon) or DKK-1 targeting shRNA. Upon reduction of DKK-1 mRNA levels with DKK-1 targeting shRNA, the S100A4 expression is increased. (B) Transfection of HAB92^{wt} cells with DKK-1 targeting shRNA reduced the amount of secreted DKK-1 protein and increased the expression of S100A4 protein. Data represent mean ± SE (n=3). Statistical significance was analyzed by Student's t-test. (C) Treatment of HCT116 cells with 25 or 100 ng/ml recombinant DKK-1 (rDKK-1) protein inhibits the S100A4 mRNA level concentration-dependently. Data represent mean ± SE (n>2). Statistical significance was analyzed by two-sided ANOVA and Bonferroni post hoc multiple comparison test.

Compared to control-shRNA transfected cells, the amount of secreted DKK-1 protein was significantly reduced in HAB92^{wt} cells which were transfected with DKK-1 targeting shRNA (Fig. 4.23B). Further, in those cells the S100A4 protein level was clearly increased.

Since DKK-1 is expected to act extracellularly, recombinant DKK-1 protein was added onto HCT116 cells and the S100A4 mRNA expression was analyzed. Treatment of HCT116 cells with 25 or 100 ng/ml recombinant DKK-1 protein for 24 h reduced the S100A4 mRNA level in a concentration-dependent manner (Fig 4.23C). These results further confirmed that also DKK-1 is an inhibitor of S100A4 expression.

5. DISCUSSION

The multidisciplinary clinical management of metastatic colon cancer has improved the five-year survival of patients in recent years (174). However, colon cancer is still the second most frequent cause of cancer related death which, in most cases, is provoked by the formation of metastases (4, 175, 176). In this respect, the understanding of the molecular mechanisms regulating the process of colon cancer metastasis is indispensable for the development of anti-metastatic treatments.

The last two decades of translational research indicated that the calcium-binding protein S100A4 is directly involved in cellular processes such as migration, invasion, adhesion and angiogenesis, all of which are fundamental to metastasis formation (69, 71). Many interaction partners of S100A4 were described to promote its function as metastasis mediator whereas the knowledge of gene regulation that follows S100A4 overexpression is very poor. Moreover, there are very few studies on the inhibition of S100A4 function. Hence, the inhibition of S100A4 provides a promising therapeutic strategy for metastatic intervention (159, 177) while more profound knowledge is needed.

Therefore this study investigated two novel inhibitors for S100A4 transcription in colon cancer cells which interfere with a constitutively active Wnt pathway, thereby inhibiting S100A4 expression. Reduced S100A4 levels further impaired S100A4-induced cell migration and invasion *in vitro* and metastasis formation *in vivo*. Moreover, the study provides evidence that S100A4 forms a positive feedback loop in the Wnt pathway via downregulation of DKK-1 which broadens our understanding for the molecular mechanism underlying S100A4-induced colon cancer metastasis.

5.1. Inhibition of S100A4 transcription inhibits S100A4-induced cell motility

5.1.1. Small molecules inhibit S100A4 expression

Based-on the high throughput screening performed by Walther, Stein and colleagues, the anti-helmintic niclosamide and the antibiotic calcimycin inhibited S100A4-promoter activity suggesting that both compounds would interfere with S100A4 transcription. Consistently, it was shown in this study that both small molecules reduced S100A4 expression in colon cancer cells dependent on the drug concentration and time of treatment. For calcimycin these findings are supported by a study performed in mouse

mammary adenocarcinoma cells as well as in human monocytes and lymphocytes in which calcimycin was shown to reduce the levels of S100A4 mRNA (178).

In contrast to the constant S100A4 inhibition observed upon a single dose of calcimycin, the inhibition of S100A4 expression by niclosamide was reversible. The effect of a single dose of niclosamide to reduce S100A4 mRNA and protein was confined to a 12 h time frame, which could be overcome by serial treatment with daily doses of niclosamide. Niclosamide is an anti-helmintic drug which can be hydrolytically cleaved by cells of the gastrointestinal tract which results in a bioavailability of 10% when applied orally (179-181). Metabolism of niclosamide leads to changes in the niclosamide structure which might hinder its target binding ability. In this study, niclosamide derivatives were analyzed showing that changes on the niclosamide structure severely reduced its efficiency on S100A4 expression inhibition. Besides the fact that structural changes of niclosamide led to decreased activity, also the loss of solubility within aqueous solution rendered some derivatives with no effect on S100A4 expression.

In contrast to the endogenous S100A4 expression in colon cancer cells which was inhibited by niclosamide or calcimycin, both small molecules did not affect exogenously overexpressed S100A4 levels. This finding is consistent with the fact that both small molecules repressed the activity of the S100A4-promoter which leads to the reduction of S100A4 mRNA and protein. Exogenously overexpressed S100A4 was controlled by a CMV-promoter, which was resistant to the inhibitory mechanism induced by either niclosamide or calcimycin. Thus, these cells expressed S100A4 mRNA and protein despite the presence of either of the small molecules.

5.1.2. Small molecules restrict S100A4-induced cell motility

Reduction of S100A4 expression in colon cancer cells mediated by niclosamide or calcimycin inhibited cell motility including cell migration, wound healing and cell invasion. S100A4 is a major regulator of cell migration (65, 69, 98). Knockdown of S100A4 mRNA in RNAi experiments was shown to reduce the ability of cells to migrate (124, 131). S100A4 protein is found at the leading edge of migrating cells were it mobilizes myosin II-A and enhances directed migration (98). Reduced levels of S100A4 protein due to treatment with niclosamide or calcimycin might thus, for instance, sequester S100A4 protein from its interaction with myosin II-A. Thereby, cell migration would be impaired. Being consistent with this expectation, this study showed that the overall migration rate as well as directed migration was inhibited by niclosamide or calcimycin treatment.

In contrast, both small molecules were unable to suppress cell migration in colon cancer cells that exogenously overexpressed S100A4. In those cells, S100A4 expression was still increased despite the treatment with either of the small molecules, which allowed S100A4 to interact with its manifold partner proteins and transcriptional targets to promote cell migration. *Vice versa*, these observations provide clear evidence that the anti-migratory effect of niclosamide and calcimycin is specific to their ability to inhibit S100A4 expression.

S100A4 protein drives metastasis by interaction with a multitude of partner-proteins. This interaction is mostly dependent on calcium ions (160). Calcimycin is an ionophorous, polyether antibiotic isolated from *Streptomyces chartreusensis*. It facilitates the transport of divalent cations across the membrane which renders calcimycin an useful tool to study calcium-signaling (182). Since calcimycin elevates intracellular calcium levels (183), one would expect that it increases the S100A4 protein activity. In contrast to this, the results presented above did not indicate an increased migratory or invasive phenotype in calcimycin-treated cells exogenously overexpressing S100A4. However, exogenous overexpression of S100A4 in untreated colon cancer cells did also hardly increase cell migration. This implies that the endogenous level of S100A4 already triggered migration to a maximum rate which could not be further stimulated by more S100A4 protein. Thus, it cannot be completely ruled out that calcimycin caused an increased S100A4 protein activity. Nonetheless, the results presented here definitely show that reducing the overall expression level of S100A4 with calcimycin significantly inhibits cell motility.

In this study, cell invasion through a layer of Matrigel simulating the extracellular matrix was inhibited upon treatment with either of the small molecules. S100A4 is a well known inducer of cell invasion (144, 184). S100A4 can access the intercellular space from where it interacts with receptors as RAGE or EGFR (114, 119). Receptor binding induces the expression of matrix metalloproteinases such as MMP-2, -9 or -13 which allows enhanced degradation of the extracellular matrix, and enables cell invasion into the neighboring tissue (119, 123, 125). Inhibition of S100A4 expression by RNA interference or overexpression of endogenous inhibitors such as PLA2G2A phospholipase or interferon-γ (IFN-γ) was shown to reduce cell invasiveness (73, 185, 186). In consistency to these earlier results, the inhibition of S100A4 transcription with niclosamide or calcimycin reduced the amount of overall S100A4 protein, which impaired its ability to induce cell invasion. Interestingly, the anti-invasive effect of niclosamide or calcimycin could be overcome by ectopic overexpression of S100A4, suggesting that the anti-invasive effect of the small molecules was caused by the downregulation of S100A4 expression. These observations again emphasize the

central role of S100A4 in cell motility which is the basis for the development of colon cancer metastasis.

5.2. The small molecules inhibit colon cancer cell proliferation

Treatment of colon cancer cells with niclosamide or calcimycin inhibited anchorage-dependent and –independent cell proliferation. Knockdown of S100A4 mRNA levels with shRNA was shown to inhibit cell proliferation *in vitro* and to reduce tumor growth and metastasis *in vivo* (187). Moreover, shRNA knockdown of S100A4 increased the occurrence of apoptosis in gastric cancer cells and resulted in a G2/M arrest of pancreatic cancer cells (131, 188). In fact, the reduction of S100A4 expression in colon cancer cells following the treatment with niclosamide or calcimycin was accompanied by a simultaneous reduction in cell proliferation and colony formation. However, these two effects seemed to be independent of the S100A4 expression level, since ectopic overexpression of S100A4 could not rescue cell proliferation.

Recently, several studies reported anti-proliferative effects of niclosamide in other cell systems describing mechanisms that might be applicable to the findings of presented by the study at hand (189-191). For instance, in acute myelogenous leukemia cells niclosamide inhibits NF-κB signaling which results in the generation of reactive oxygen species followed by apoptosis (189). In the present study with colon cancer cells, niclosamide and calcimycin were shown to inhibit, besides S100A4, the expression of other β-catenin/TCF target genes such as Cyclin D1 and c-myc. Both genes are known oncogenes and their overexpression causes increased cell proliferation (170, 171). Moreover, inhibition of Cyclin D1 and c-myc expression by shRNA-mediated knockdown of β-catenin levels was previously shown to result in reduced cell proliferation rates in colon cancer cells (192). Considering that exogenous overexpression of S100A4 was ineffective in overcoming the anti-proliferative effect of niclosamide or calcimycin, it is plausible to assume that this effect might rather be caused by the reduced Cyclin D1 and c-myc levels.

5.3. Both small molecules interfere with constitutively active Wnt pathway

In this study, niclosamide and calcimycin were shown to repress Wnt pathway activity in colon cancer cells. S100A4 is a target gene of the canonical Wnt pathway (65). Inhibition of this pathway presents, therefore, a basis for the mechanism by which the

two small molecules reduce the S100A4-promoter activity. However, the two small molecules targeted the Wnt pathway through different mechanisms.

5.3.1. Calcimycin inhibits β-catenin expression

Calcimycin treatment reduced the expression level of β-catenin which further impaired β-catenin/TCF-mediated target gene transcription. Consequently, prominent target genes such as Cyclin D1, c-myc or DKK-1 were reduced by calcimycin treatment. Calcimycin was previously described to inhibit Wnt pathway activity in HEK293 cells that stably expressed the TOPflash reporter plasmid (183). Upon exposure to calcimycin the intrinsic Ca^{2+} level was increased which activated protein kinase C (PKC)-mediated phosphorylation of β-catenin and induced β-catenin degradation. In this study, calcimycin treatment reduced the β-catenin protein expression also in colon cancer cells. Interestingly, β-catenin protein was reduced even in cells which were heterozygous or even homozygous for gain-of-function-mutated β-catenin. Analysis of the β-catenin mRNA level revealed that calcimycin also inhibited β-catenin transcription, suggesting that calcimycin inhibits the Wnt pathway activity via several mechanisms targeting the expression level of β-catenin.

5.3.2. Niclosamide inhibits β-catenin/TCF complexation

In contrast to calcimycin, niclosamide treatment did not have any effect on the β-catenin expression level, but also repressed Wnt pathway activity and consequently inhibited β-catenin/TCF target gene transcription of Cyclin D1, c-myc, DKK-1 and especially S100A4. Niclosamide was previously shown to inhibit the Wnt pathway in osteosarcoma cells (191). However, in those cells niclosamide treatment induced the internalization of Wnt receptor frizzled-1 which further resulted in proteasomal degradation of β-catenin. In this study, no reduction in β-catenin protein was detected upon niclosamide treatment suggesting that in colon cancer cells niclosamide targets the Wnt pathway via a different mechanism.

Translocation of β-catenin to the nucleus is a central step in the Wnt pathway. In the nucleus β-catenin binds to transcription factors of the TCF/LEF family to activate target gene transcription (47). The present study showed that nuclear β-catenin was unaffected by niclosamide treatment in colon cancer cells. However, despite high levels of β-catenin in the nucleus under niclosamide treatment, β-catenin/TCF target gene transcription was impaired in colon cancer cells. Analysis of the β-catenin/TCF complex revealed that with increasing concentrations of niclosamide the interaction between β-catenin and TCF in complex with the S100A4-promoter was disrupted. On the one

hand, niclosamide could cause this complex disruption by directly binding to either β-catenin or TCF, thereby destabilizing the β-catenin/TCF complex. On the other hand, niclosamide could activate other negative regulators interfering with the β-catenin/TCF complex such as groucho proteins, which are known competitors for β-catenin on their binding site to TCF (193, 194). Indeed, within the scope of this study it was demonstrated that niclosamide interferes with the β-catenin/TCF complex on the S100A4-promoter, thereby impairing S100A4-transcripion in colon cancer cells.

5.3.3. Niclosamide and calcimycin inhibit constitutively active Wnt pathway

Mutation of the Wnt pathway is a profound step for colon cancer development leading to constitutive pathway activity and target gene expression (37). Most mutations in this pathway occur either on the destruction complex regulating the cytoplasmic level of β-catenin or on β-catenin itself (38). With respect to their therapeutic value, Wnt pathway inhibitors should preferably target downstream of β-catenin to switch off the constitutively active signaling (159, 195). In this study, HCT116 derivative cells were used to analyze the capability of niclosamide or calcimycin to reduce Wnt pathway activity under mutated or wildtype conditions. Consistently with findings from Kim et al., $HAB68^{mut}$ cells presented increased Wnt pathway activity due to the expression of mutated β-catenin and $HAB92^{wt}$ cells represented low levels of Wnt pathway activity, since these cells expressed wildtype β-catenin which could be targeted for proteasomal degradation (164). Interestingly, niclosamide and calcimycin repressed the Wnt pathway activity despite the presence of a gain-of-function mutated β-catenin in $HAB68^{mut}$ cells to the level found in $HAB92^{wt}$ cells. Deregulated β-catenin action was restricted by both small molecules either by reducing the expression of β-catenin as described for calcimycin or by interfering with the β-catenin/TCF transcription complex as described for niclosamide. Therefore, both small molecules present immense potential to be useful in colon cancer treatment banning constitutively active Wnt pathway signaling.

5.4. Specificity and potential adverse effects of the small molecules

Targeting the S100A4-promoter activity with small molecules, implied to interfere within a signal transduction pathway and that this targeting will not be solely restricted to the inhibition of S100A4 expression, but will have certain side effects. However, there are several advantages of targeting the S100A4-promoter instead of the S100A4 protein and of using small molecules instead of RNA interference, for instance,.

5.4.1. Targeting the S100A4-promoter is most efficient

S100A4 as a mediator of metastasis represents an excellent target to be applied in anti-metastatic therapies (159, 196). The design of an inhibitor that would target S100A4 function is hampered by the multitude of S100A4-action which occurs intra- and extracellular, as homo-, heterodimer or as oligomer and in a calcium-dependent or -independent manner (110, 160).

One approach targeting the Ca^{2+}-binding ability of S100A4 was recently described by Bresnick and colleagues (196, 197). They developed a fluorescent S100A4 protein, which increased its fluorescence signal upon Ca^{2+}-binding. High throughput screening of FDA-approved drugs revealed phenothiazines to inhibit Ca^{2+}-binding on S100A4 and consistently the interaction of S100A4 with myosin II-A . However, inhibition of the calcium-binding ability of S100A4 does not target all S100A4 functions. For instance, S100A4 was described to interact with liprin β1, annexin II or other S100A4 molecules in a calcium-independent manner (89, 115, 121). Indeed, phenothiazines were shown to provoke the oligomerisation of S100A4 which would promote the S100A4 oligomer-induced activation of thrombospondin I and MMP expression leading to angiogenesis and invasion, respectively (126, 137, 196).

Targeting extracellular S100A4 protein function with an S100A4-specific antibody was shown to inhibit invasive growth of mouse endothelial cells *in vitro* and cell proliferation and vascularisation of the skin *in vivo.* However, extracellular application of S100A4-antibody did not target the intracellular functions of S100A4 (122, 198).

In this study, niclosamide and calcimycin were used to inhibit the Wnt pathway thereby repressing the S100A4-promoter activity. Inhibition of S100A4 transcription reduced the overall amount of available S100A4 protein in the cell, which targeted its manifold interactions with all partner proteins simultaneously. Consequently, the small molecules efficiently inhibited S100A4-induced cell migration as well as cell invasion *in vitro*, and further metastasis formation *in vivo*.

5.4.2. Advantage of using small molecules to inhibit S100A4 expression

Small molecules are by definition monomeric or short oligomeric organic compounds which due to their low molecular weight of less than 800 Dalton can easily transfer the plasma membrane to enter the cytoplasm. Using small molecules for targeting the expression of S100A4 had several advantages instead of using other expression inhibitors such as RNA interference. For instance, the finding of the optimal dose, in terms of a maximal degree of S100A4 expression inhibition with the lowest concentration possible, was simplified due to the fast inhibitory effect of both small

molecules of less than 24 h. In contrast, using RNA interference the depletion of the target gene occurs gradually and in most cases takes more than 24 h which hampers the finding of the optimal dose (199). Moreover, the therapeutic use and the systemic application to organisms is less well explored for RNA interference and challenged by the efficient delivery into the cell (200). In contrast, both small molecules were able to induce their inhibitory effect, suggesting that they entered the cell without further additives. Systemic niclosamide application further inhibited the S100A4 expression in vivo providing the basic evidence for its applicability to treat colon cancer metastasis.

One major concern in the use of inhibitors, independent of what kind, is the potential lack of specificity. In this study, the small molecules targeted the S100A4-promoter activity, which, of course, implied targeting within a certain pathway and thereby affecting the expression of other genes. Therefore, any effect caused by either of the small molecules needed to be analyzed for the specificity of their ability to repress S100A4 expression. To address this challenge, a cell system was installed which expressed S100A4 also despite the treatment with either of the small molecules. All effects observed upon niclosamide or calcimycin treatment which were rescued upon S100A4 expression were specific to the inhibitor-mediated reduction of S100A4 expression. For instance, niclosamide and calcimycin were identified as Wnt pathway inhibitors. Beside S100A4 also the tyrosine kinase Met is a prominent mediator of metastasis and a target gene of Wnt signaling in colon cancer cells (201). Inhibition of cell motility by the small molecules could also have been caused by downregulation of Met. However, inhibition of cell motility by calcimycin or niclosamide was completely rescued by S100A4 overexpression. Thus, the anti-migratory and anti-invasive effects of the small molecules were specific to their ability to reduce S100A4 expression. In contrast, niclosamide and calcimycin inhibited cell proliferation, which was independent on their ability to inhibit S100A4 expression. However, within the scope of an efficient colon cancer treatment, anti-proliferative effects might even be favorable for the therapeutic outcome.

5.5. Niclosamide as novel anti-metastatic treatment

5.5.1. Niclosamide is a favorable inhibitor to be applied *in vivo*

The Wnt pathway is the most central pathway in the development of colon cancer. However, under non-pathologic conditions it is needed for the homeostasis of the colon epithelium (11, 12, 55). Systemic interference with this pathway bears the risk of adverse effects for instance on the healthy colon epithelium (195).

In this study, both small molecules were active on S100A4 expression inhibition at concentrations that did not affect cell viability in general. Moreover, both small molecules did not completely switch off the Wnt pathway, but rather reduced its activity to a basal level found in HAB-92^{wt} cells. These cells bore no Wnt pathway mutation and therefore represented a wildtype level of Wnt pathway activity.

In contrast to niclosamide, which did not interfere with the β-catenin expression level, calcimycin inhibited β-catenin transcription. Beside its function as transcription regulator, β-catenin together with E-cadherin plays a role in the formation of cell adhesion contacts (49). Deregulation of cell adhesion by calcimycin treatment could inhibit the metastatic cell to enter the secondary tumor site. However, also the focal contacts in healthy tissue could be destroyed which might also favor metastasis formation. Thus, the systemic application of calcimycin might cause adverse effects on the colon tissue.

Niclosamide as a FDA-approved drug is already used in the clinic to treat helmintosis in human and veterinary medicine. When taken orally niclosamide proved to have only slight adverse effects in humans and mice such as diarrhea or skin rash (202-204). Therefore, niclosamide rather than calcimycin was chosen to be further applied in xenograft mice to defeat S100A4-induced metastasis. Consistently, daily systemic treatment of xenograft mice with niclosamide caused no visible toxic side effects during the period of investigation of 24 days.

5.5.2. Non-invasive bioluminescence imaging visualized S100A4-induced metastasis

Experimental metastasis in immune-deficient mice has proven to be suitable to evaluate the metastatic potential of a certain population of cells (35, 65, 205). However, the problem of this *in vivo* application is the determination of the optimal endpoint. The optimal endpoint should be neither too early, otherwise metastases might not be visible, nor too late to reduce the suffering of the animal and avoid tumor burden-caused death.

In this study the endpoint decisions were optimized by using non-invasive bioluminescence imaging to follow the process of S100A4-induced metastasis of human colon cancer cells *in vivo*. Bioluminescence imaging is based on the detection of photons, which are excised as a side product in an enzymatic reaction. In this study, firefly luciferase was applied, which stems from the North American firefly *Photinus pyralis* and catalyzes the oxidation of luciferin under ATP consumption and emission of light. Monitoring of intrasplenically implanted human colon cancer xenograft mice

revealed an increased bioluminescence signal in the spleen region and, until day 24, a liver signal in the solvent-treated control mice.

Many non-invasive imaging modalities besides bioluminescence have been described for their use in small animals, such as magnetic resonance imaging, computed tomography, positron emission tomography and fluorescence imaging (206). However, bioluminescence bears several advantages compared to other modalities such as its ease of application and its high-sensitivity. It is free from exposure to radiation and provides a relative measure of signal to amount of viable cells. Moreover, mammalian tissue has only a very low intrinsic bioluminescence, which therefore generates an optimized signal-to-noise ratio (207). The main limitation of bioluminescence is its anatomic resolution which is restricted to the organ level. However, bioluminescence imaging is useful to detect lung or liver metastases from a multitude of cancer cells, such as breast and sarcoma, or prostate, respectively (173, 208-211). In this study, the bioluminescence signal from liver metastases formed by colon cancer cells appeared already on day 6 as a weak signal in the liver region of solvent-treated control mice. Due to its high sensitivity bioluminescence imaging detected even micrometastases which may be not visible at that stage. The liver metastasis signal increased over time until day 24 and autopsy further confirmed the presence of liver metastases in solvent-treated xenografts. In conclusion, the non-invasive bioluminescence imaging is a helpful tool to monitor the process of S100A4-induced metastasis, and to test potential anti-metastatic drugs such as niclosamide.

5.5.3. Intrasplenic xenograft model revealed anti-metastatic function of niclosamide

Niclosamide inhibited the formation of liver metastases in colon cancer xenografts. The experimental metastasis model was based on intrasplenic injection of colon cancer cells into immune-deficient mice. The spleen is intensively blooded which allows intrasplenically injected cells to easily enter the blood circulation (212). Consequently, the intrasplenic model does not represent the whole process of metastasis formation since it excludes the processes of dissemination from the tumor tissue and invasion of the blood circulation (213).

Metastasis formation starts with the local tumor from which cells invade the vascular and lymphatic system, circulate and finally extravasate into the foreign tissue of the target organ (28). The entire metastatic cascade is simulated in orthotopic transplanted xenograft mice. However, the orthotopic model has several disadvantages, beginning with the time-consuming and not always successful surgical set up including a

subcutaneous grown tumor which will be sliced and transplanted into the cecum (214). Only in 50 % of successful transplanted mice the tumor metastasizes to the lymph nodes and very rarely to the liver (213, 214). Further, in most cases the tumor burden causes death before liver metastases might become visible (215).

The appropriate model to study human cancer metastasis needs to fulfill two requirements which are based on the 'seed and soil' theory (28, 205). Firstly, it must include metastatic cells which performed EMT, are able to survive under non-adherent conditions and to invade the foreign tissue. Secondly, it must provide tumor growth in the targeting organ tissue, which can then be inhibited by potential anti-metastatic drugs. In this study, the intrasplenic model used fulfilled both requirements including S100A4-overexpressing cells, which presented increased cell motility, and their formation of liver metastases. Thus, intrasplenic injection was efficient to analyze the anti-metastatic potential of niclosamide, although it only simulated the final processes of metastasis formation.

In xenograft mice, niclosamide treatment reduced the S100A4 expression level in colon tumor cells. Furthermore, it restricted the number and size of metastases. However, in some niclosamide-treated mice, micrometastases were still found. Reasons for that may lie in the concentration of niclosamide or its metabolism. However, a third restriction was the time of treatment. The treatment with niclosamide started 24h after cells were transplanted, meaning that the cells had at least 24h to circulate in the blood and further 24h until niclosamide inhibited S100A4 protein expression. These rationales indicate that the micrometastases found could have been an artifact of the xenograft model. Nevertheless, the study definitely provides evidence that by inhibiting S100A4-expression, niclosamide impaired the metastatic steps of cell extravasation and invasion into the foreign tissue as well as restricted the proliferation of metastases *in vivo*.

5.5.4. Niclosamide as anti-metastatic drug for colon cancer patients

This study provides evidence that niclosamide inhibits S100A4-induced cell motility *in vitro* and metastasis formation and outgrowth in xenograft mice. Based on these results, the application of niclosamide is suggested in the management and treatment of colon cancer patients. S100A4 expression in tumors from colon cancer patients was shown to be prognostic for the development of metastases (34, 65). Moreover, studies performed by Stein and colleagues show that the level of free circulating S100A4 mRNA in the blood of colon cancer patients is specific and sensitive to predict the

occurrence of metastases (158). The prognostic value of S100A4 therefore allows identifying colon cancer patients which are at high risk to form metastases.

The majority of colon cancer patients are diagnosed with a colon tumor before detectable metastases have formed, and about 20% of those patients will develop metachronous metastasis within five years (216, 217). In a treatment scenario, suitable patients could be identified for high S100A4 expression either post-tumor-resection via immunohistology or RT-PCR or even pre-tumor-resection via blood analysis. In patients with increased S100A4 levels, niclosamide treatment could be of immense value to restrict colon cancer metastasis.

To discuss the potential efficiency of niclosamide to successfully treat colon cancer patients, the time point of metastatic seed is of particular interest. As discussed in the introduction, there are two models for the origin of metastasis: the concurrent model and the sequential model. In the sequential model, the metastatic cells stem from the late carcinoma, which is based on the observation that mutations of the late carcinoma are also found in the respective metastasis (23). In this scenario, patients who might develop metachronous metastases could be treated with niclosamide as described above.

In contrast, the concurrent model describes metastatic dissemination to occur early in tumor development, planting metastatic seeds which can persist in a dormant state. Activation of the latter will give rise to metastasis even after the resection of the primary tumor (218, 219). In this scenario, one might think that niclosamide treatment after tumor resection might be too late, since metastases could have already formed at the time of diagnosis. The model was based on the observation that even years after tumor resection metastases can form (32, 218). However, those metastases might not arise from dormant cells, but rather from tumor cells that were shedded during surgical resection (220). This is in line with the observation that the amount of circulating tumor cells increased intraoparatively dependent on the method of surgery (221). Nevertheless, 15-25% of colon cancer patients are diagnosed with synchronous metastasis (216). These patients might also be eligible for niclosamide treatment, given their tumor expressed increased levels of S100A4. In the intrasplenic model niclosamide did not only inhibit the extravasation and invasion of cancer metastasis, but also the metastatic growth of cells which entered the liver within the first 48 h until the niclosamide effect took place. Thus, niclosamide treatment of colon cancer patients with synchronous metastasis could reduce their metastatic load and promote their eligibility for liver metastasis resection (222).

Current treatment conditions of colon cancer patients with synchronous or metachronous liver metastases are colonic tumor resection along with

hepatoectomie (174, 222). In most cases surgical resection is accompanied by chemotherapy, such as 5-fluoruracil/leucovorin, irinotecan or oxaliplatin, mostly targeting at the increased proliferation rate of cancer cells (223). In the management of colon cancer metastasis, however, novel drugs are needed that target at the metastatic potential of cells, since metastatic dissemination is the major cause for cancer death. In this respect, niclosamide presents substantial potential to be applied as adjuvant chemotherapy to tumor and liver metastasis resection.

5.6. The inhibitor of the inhibitor – S100A4 and DKK-1

Negative correlation of gene expression is a first indicator to identify antagonists. In this study S100A4 and DKK-1 expression was negatively correlated. In a set of 13 colon cancer cell lines both genes were inversely expressed on the mRNA as well as on the protein level. Thus, the study presents a novel mechanism of a positive feedback loop in the Wnt pathway formed by S100A4 and DKK-1.

5.6.1. S100A4 inhibits DKK-1 expression

In this study, colon cancer cells with non-mutated β-catenin expressed significantly higher levels of DKK-1 mRNA and protein than cells with mutated β-catenin. DKK-1-promoter reporter assays revealed that promoter activity was inducible by β-catenin and TCF-4 leading to the conclusion that in colon cancer cells DKK-1 is a β-catenin/TCF target gene (60). In this case one would expect DKK-1 to be upregulated in cells with mutated β-catenin, which was not the case in this study. However, the DKK-1 expression in colon tumor tissue is regulated downwards, but increased in normal colon epithelium. This is consistent with the observations obtained from the cell system where cells with mutated β-catenin, simulating the tumor tissue, expressed reduced levels of DKK-1 and cells with wildtype β-catenin as it is found in normal colon epithelium expressed high levels of DKK-1 mRNA and protein (14, 60). These observations suggest that DKK-1 expression in colon cells is regulated via a second mechanism apart from the β-catenin/TCF complex.

In colon cancer cells with mutated β-catenin the S100A4 expression was increased accompanied by high Wnt pathway activity. In contrast, in colon cancer cells with non-mutated β-catenin the S100A4 expression was hardly detectable and Wnt pathway activity was low. These cell line based observations are consistent with findings in tumor tissue of colon cancer patients, in which S100A4 expression and Wnt pathway

activity are increased (48, 65). On the opposite, in normal colon epithelium S100A4 expression is very low accompanied by low Wnt pathway activity (65, 224).

Exogenous overexpression of S100A4 in cells with increased DKK-1 levels inhibited the expression of DKK-1 mRNA and decreased the amount of secreted and thus functional DKK-1 protein. These results indicate that S100A4 is an inhibitor for DKK-1 expression. Consistently, removal of the inhibitor S100A4 rescued the mRNA expression of DKK-1 in cells with mutated β-catenin. A similar gene regulation was described for S100A4 and E-cadherin. Several independent studies described their negative correlation (85, 87, 88, 225). Moreover S100A4 inhibited BNI3 expression thereby inducing chemo-resistance in pancreatic cancer (226). However the mechanism of expression inhibition was not yet identified in either case.

S100A4 protein can translocate to the nucleus and nuclear localization of S100A4 was found to be of better prognostic value for the formation of metastasis than cytoplasmic S100A4 expression (152, 157). These results indicate a considerable role for S100A4 in gene regulation. A recent study on chrondrocytes described promoter-binding activity of S100A4. Upon sumoylation S100A4 translocated to the nucleus were it bound to the promoter-region of MMP-13 and induced target gene transcription (227). Similarly, S100A4 could function as a repressor on the DKK-1 promoter. In lung and colon cancer, downregulation of DKK-1 and other Wnt antagonists is a frequent event which is often accompanied by promoter hypermethylation (14, 228, 229). In a set of 54 colon tumors expressing low level of DKK-1, 17% presented DKK-1 promoter hypermethylation. Therefore, besides direct transcriptional regulation, S100A4 could also induce epigenetic inhibition of DKK-1 expression, a hypothesis that will be addressed by further investigations.

5.6.2. DKK-1 is an endogenous inhibitor for S100A4 expression

Colon cancer cells with non-mutated β-catenin presented high levels of DKK-1 expression and very low levels of S100A4. Inhibition of DKK-1 expression using RNA interference rescued the expression of S100A4 indicating that DKK-1 functioned as inhibitor for S100A4 expression. DKK-1 belongs to the group of secreted Wnt antagonists. It blocks the canonical Wnt pathway by binding to LRP-5/6, the co-receptors of the Wnt/frizzled signaling complex (51). Binding of DKK-1 to LRP-6 sequesters the latter from the Wnt/frizzled signaling complex and induces endocytosis of the co-receptor together with the transmembrane protein kremen (57, 59). Consequently, the Wnt pathway and its target gene transcription are disabled.

In cells with non-mutated β-catenin, DKK-1 overexpression caused the inhibition of β-catenin/TCF target gene transcription such as S100A4. Consistently, in cells with endogenously high levels of S100A4, expression of the latter was inhibited when cells were treated with recombinant DKK-1 (rDKK-1) protein. The inhibition was concentration-dependent. However, the concentrations used were fairly high. Only the lower concentration was physiologically found in chronically inflamed colon epithelium of Crohn's cholitis patients (54). The colon cancer cells used in this study were heterozygous for mutated β-catenin, which is resistant to upstream signaling processes (195). However, these cells also expressed wildtype β-catenin, which responds to active Wnt signaling and its inhibition by rDKK-1. Very high concentrations of rDKK-1 were thus able to stimulate wildtype β-catenin degradation to a level that could not be compensated by mutated β-catenin, leading to a reduction of S100A4 expression. A recent study on colon cancer cells reported that 100 ng/ml rDKK-1 inhibited cell migration and wound healing. Moreover, rDKK-1 inhibited the polarization of migrating cells at the leading edge (54). All these functions can be induced by S100A4 expression. These observations are consistent with the findings of the present study showing that rDKK-1 inhibits S100A4 expression.

5.7. The new roles for small molecules, S100A4 and DKK-1 in the Wnt pathway

In colon cancer the Wnt pathway is the most frequently deregulated pathway leading to uncontrolled β-catenin levels in the cells and, thus, to constitutively active β-catenin/TCF target gene transcription (38, 42, 230). The identification of molecular mechanisms influencing this pathway is of great interest in the understanding of colon cancer and forms the lead for the development of potential therapies (159, 195).This study presents several novel interactions that occur in the Wnt pathway which systematically enrich our knowledge on its regulation and the possilities of controlling it (Fig. 5.1).

This study provides evidence that S100A4 inhibits DKK-1 expression, which by itself is a negative regulator of S100A4 expression (Fig. 5.1A). The ubiquitous protein S100A4 is a target gene of the Wnt pathway and is a central mediator of metastasis, thereby promoting one of the leading causes for colon cancer death. During tumorigenesis mutations within the Wnt pathway are initial events leading to S100A4 overexpression (37, 65, 231). This study entered a new step to the colon cancer cascade, namely that S100A4 overexpression leads to inhibition of the Wnt antagonist DKK-1 function by

repressing its expression. By inhibition of its endogenous inhibitor, S100A4 induces a positive feedback loop which supports the constitutively active Wnt pathway and thus ensures its own expression. This novel regulation within the Wnt pathway further underscores the pivotal role of S100A4 in the process of tumor development and metastases.

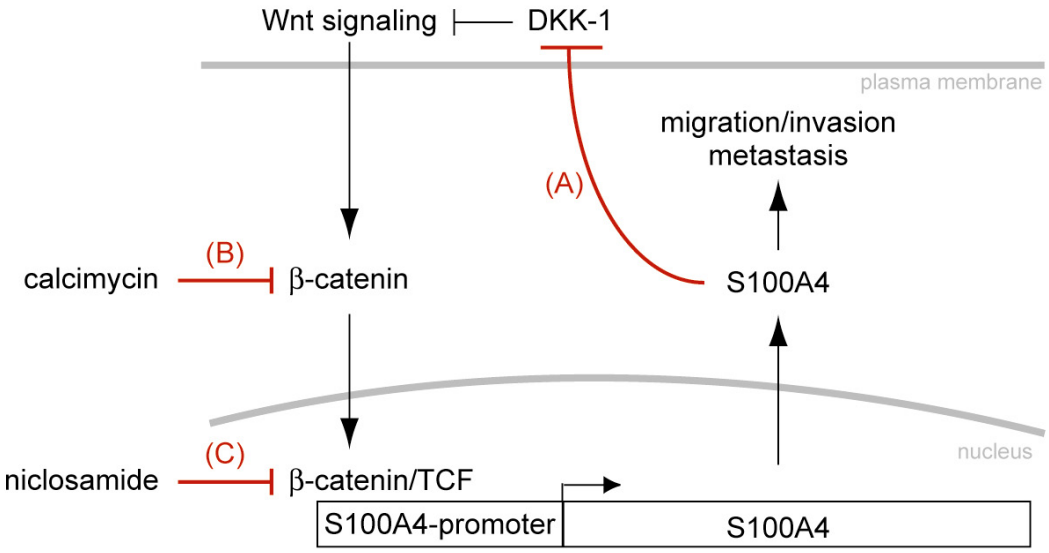

Fig. 5.1 Novel regulations in the Wnt pathway. Schematic representation of the novel regulations of S100A4 and DKK-1 as well as of the small molecules niclosamide and calcimycin in the Wnt pathway. (A) S100A4 inhibits the Wnt antagonist DKK-1, thereby forming a positive feedback loop. Loss of endogenous inhibitor can be compensated by niclosamide and calcimycin. (B) Calcimycin inhibits β-catenin expression, thereby reducing intracellular β-catenin levels. (C) Niclosamide inhibits the complexation of β-catenin and TCF. Thus, both small molecules inhibit S100A4 transcription, thereby restricting cell migration and invasion as well as metastasis of colon cancer cells.

Loss of the endogenous inhibitor for S100A4 was compensated, in this study, by niclosamide and calcimycin, two small molecules which inhibit S100A4 expression despite a mutated, and thus constitutively active, Wnt pathway. Wnt pathway inhibition by niclosamide and calcimycin occurred with different mechanisms. The antibiotic calcimycin disabled constitutive β-catenin/TCF target gene expression by inhibition of β-catenin transcription (Fig. 5.1B). By decreasing β-catenin overall levels in the cell, calcimycin sequestered the most essential regulator for Wnt signaling induced β-catenin/TCF target gene transcription. In contrast, the anti-helmintic compound niclosamide switched off constitutively active β-catenin/TCF target gene transcription by disrupting the transcription-inducing complex of β-catenin and TCF. Inhibiting the

Wnt pathway, both small molecules restricted S100A4 transcription in colon cancer cells and thus inhibited S100A4-induced cell migration, wound healing and cell invasion, all fundamental processes in the course of metastasis formation. Moreover, niclosamide significantly inhibited the S100A4 expression *in vivo* resulting in clearly reduced liver metastasis.

Since metastasis is still the major cause for colon cancer death there is an urgent need for anti-metastatic treatment and S100A4, as a mediator of this disease progression, provides a potential therapeutic target. This study contributes with fundamental evidence for the anti-metastatic potential of small molecules targeting S100A4 expression which could be beneficial for colon cancer patients at high risk for S100A4-induced metastasis. These inhibitors might provide another strong weapon in the combat of colon cancer metastasis.

6. OUTLOOK

The findings of the present study revealed the anti-metastastic potential of niclosamide. In a future treatment scenario of colon cancer patients, this drug might be administered as adjuvant chemotherapy on a daily basis. In this respect, the long-term effects of daily niclosamide administration to xenograft mice are currently investigated. The focus lies on the analysis of the long-term drug tolerability and repression of S100A4 expression. Moreover, it will be analyzed whether growth of metastases reoccurs if the niclosamide treatment is discontinued. Further investigation will evaluate the delivery mechanism of niclosamide to patients, since its oral bioavailability is limited. Therefore, other forms of drug administration, such as intramuscular injection, need to be addressed. These investigations will further help to clarify the potential benefits of the clinical application of niclosamide to colon cancer patients with high risk of S100A4-induced metastasis.

The present study revealed a novel mechanism for S100A4 function forming a positive feedback loop within the Wnt pathway. The findings are based on expression data, leaving the mechanism behind this gene regulation yet unexplored.

Current investigations concentrate on understanding if S100A4 inhibits DKK-1 expression by targeting DKK-1 mRNA through the activation of miRNA mechanisms, or by targeting the DKK-1 transcription through inhibiting DKK-1-promoter activity. DKK-1-promoter reporter assays followed by EMSA and ChIP analysis will evaluate if S100A4 directly interferes with the DKK-1-promoter. In parallel, research in bioinformatics on the DKK-1 mRNA revealed two potential miRNAs which were already shown to act on DKK-1 expression. Their impact in this gene regulation will be analyzed.

Wnt pathway activity and S100A4-induced cell motility in rDKK-1-treated colon cancer cells will be analyzed to investigate the power of antibodies mimicking DKK-1 function on LRP-5/-6 receptors as potential anti-metastatic drugs.

The prognostic value of high levels of S100A4 along with low levels of DKK-1 is currently investigated in well-characterized colon cancer tissues with 5-year follow-up data to predict metastasis formation of colon cancer patients and to allow the early diagnosis for those patients that are eligible for anti-metastatic treatment.

REFERENCES

1. Garcia M, Jema lA, Ward E, et al. Global Cancer Facts & Figures. American Cancer Society. Atlanta, GA: American Cancer Society; 2007.
2. Ferlay J, Parkin DM, Steliarova-Foucher E. Estimates of cancer incidence and mortality in Europe in 2008. Eur J Cancer 2010 Mar;46(4):765-81.
3. Husmann G, Kaatsch P, Katalinic A, et al. Krebs in Deutschland 2005/2006 Häufigkeiten und Trends. Robert Koch-Institut, Gesellschaft der epidemiologischen Krebsregister in Deutschland eV 2010;7:1-120.
4. Stein U, Schlag PM. Clinical, biological, and molecular aspects of metastasis in colorectal cancer. Recent Results Cancer Res 2007;176:61-80.
5. Weitz J, Koch M, Debus J, Hohler T, Galle PR, Buchler MW. Colorectal cancer. Lancet 2005 Jan 8-14;365(9454):153-65.
6. Jasperson KW, Tuohy TM, Neklason DW, Burt RW. Hereditary and familial colon cancer. Gastroenterology 2010 Jun;138(6):2044-58.
7. Half E, Bercovich D, Rozen P. Familial adenomatous polyposis. Orphanet J Rare Dis 2009;4:22.
8. Boland CR, Goel A. Microsatellite instability in colorectal cancer. Gastroenterology 2010 Jun;138(6):2073-87 e3.
9. Hamer HM, Jonkers D, Venema K, Vanhoutvin S, Troost FJ, Brummer RJ. Review article: the role of butyrate on colonic function. Aliment Pharmacol Ther 2008 Jan 15;27(2):104-19.
10. de Santa Barbara P, van den Brink GR, Roberts DJ. Development and differentiation of the intestinal epithelium. Cell Mol Life Sci 2003 Jul;60(7):1322-32.
11. de Lau W, Barker N, Clevers H. WNT signaling in the normal intestine and colorectal cancer. Front Biosci 2007;12:471-91.
12. Radtke F, Clevers H. Self-renewal and cancer of the gut: two sides of a coin. Science 2005 Mar 25;307(5717):1904-9.
13. Humphries A, Wright NA. Colonic crypt organization and tumorigenesis. Nat Rev Cancer 2008 Jun;8(6):415-24.
14. Aguilera O, Fraga MF, Ballestar E, et al. Epigenetic inactivation of the Wnt antagonist DICKKOPF-1 (DKK-1) gene in human colorectal cancer. Oncogene 2006 Jul 6;25(29):4116-21.
15. Shih IM, Wang TL, Traverso G, et al. Top-down morphogenesis of colorectal tumors. Proc Natl Acad Sci U S A 2001 Feb 27;98(5):2640-5.
16. Wright NA, Poulsom R. Top down or bottom up? Competing management structures in the morphogenesis of colorectal neoplasms. Gut 2002 Sep;51(3):306-8.
17. Preston SL, Wong WM, Chan AO, et al. Bottom-up histogenesis of colorectal adenomas: origin in the monocryptal adenoma and initial expansion by crypt fission. Cancer Res 2003 Jul 1;63(13):3819-25.
18. Smith AJ, Stern HS, Penner M, et al. Somatic APC and K-ras codon 12 mutations in aberrant crypt foci from human colons. Cancer Res 1994 Nov 1;54(21):5527-30.

19. Wasan HS, Park HS, Liu KC, et al. APC in the regulation of intestinal crypt fission. J Pathol 1998 Jul;185(3):246-55.

20. Siu IM, Robinson DR, Schwartz S, et al. The identification of monoclonality in human aberrant crypt foci. Cancer Res 1999 Jan 1;59(1):63-6.

21. Raica M, Cimpean AM, Ribatti D. Angiogenesis in pre-malignant conditions. Eur J Cancer 2009 Jul;45(11):1924-34.

22. Markowitz SD, Bertagnolli MM. Molecular origins of cancer: Molecular basis of colorectal cancer. N Engl J Med 2009 Dec 17;361(25):2449-60.

23. Jones S, Chen WD, Parmigiani G, et al. Comparative lesion sequencing provides insights into tumor evolution. Proc Natl Acad Sci U S A 2008 Mar 18;105(11):4283-8.

24. Shinagawa K, Kitadai Y, Tanaka M, et al. Mesenchymal stem cells enhance growth and metastasis of colon cancer. Int J Cancer 2010 May 6.

25. Weinberg RA. Mechanisms of malignant progression. Carcinogenesis 2008 Jun;29(6):1092-5.

26. Yang J, Weinberg RA. Epithelial-mesenchymal transition: at the crossroads of development and tumor metastasis. Dev Cell 2008 Jun;14(6):818-29.

27. Zeidman I, Mc CM, Coman DR. Factors affecting the number of tumor metastases; experiments with a transplantable mouse tumor. Cancer Res 1950 Jun;10(6):357-9.

28. Fidler IJ. The pathogenesis of cancer metastasis: the 'seed and soil' hypothesis revisited. Nat Rev Cancer 2003 Jun;3(6):453-8.

29. Pantel K, Brakenhoff RH. Dissecting the metastatic cascade. Nat Rev Cancer 2004 Jun;4(6):448-56.

30. Riethdorf S, Pantel K. Clinical relevance and current challenges of research on disseminating tumor cells in cancer patients. Breast Cancer Res 2009;11 Suppl 3:S10.

31. Vincan E, Barker N. The upstream components of the Wnt signalling pathway in the dynamic EMT and MET associated with colorectal cancer progression. Clin Exp Metastasis 2008;25(6):657-63.

32. Barkan D, Kleinman H, Simmons JL, et al. Inhibition of metastatic outgrowth from single dormant tumor cells by targeting the cytoskeleton. Cancer Res 2008 Aug 1;68(15):6241-50.

33. Pantel K, Brakenhoff RH, Brandt B. Detection, clinical relevance and specific biological properties of disseminating tumour cells. Nat Rev Cancer 2008 May;8(5):329-40.

34. Gongoll S, Peters G, Mengel M, et al. Prognostic significance of calcium-binding protein S100A4 in colorectal cancer. Gastroenterology 2002 Nov;123(5):1478-84.

35. Stein U, Walther W, Arlt F, et al. MACC1, a newly identified key regulator of HGF-MET signaling, predicts colon cancer metastasis. Nat Med 2009 Jan;15(1):59-67.

36. Hanahan D, Weinberg RA. The hallmarks of cancer. Cell 2000 Jan 7;100(1):57-70.

37. Fearon ER, Vogelstein B. A genetic model for colorectal tumorigenesis. Cell 1990 Jun 1;61(5):759-67.

38. Giles RH, van Es JH, Clevers H. Caught up in a Wnt storm: Wnt signaling in cancer. Biochim Biophys Acta 2003 Jun 5;1653(1):1-24.

39. Kemp Z, Rowan A, Chambers W, et al. CDC4 mutations occur in a subset of colorectal cancers but are not predicted to cause loss of function and are not associated with chromosomal instability. Cancer Res 2005 Dec 15;65(24):11361-6.

40. Barber TD, McManus K, Yuen KW, et al. Chromatid cohesion defects may underlie chromosome instability in human colorectal cancers. Proc Natl Acad Sci U S A 2008 Mar 4;105(9):3443-8.

41. Parsons DW, Wang TL, Samuels Y, et al. Colorectal cancer: mutations in a signalling pathway. Nature 2005 Aug 11;436(7052):792.

42. Reya T, Clevers H. Wnt signalling in stem cells and cancer. Nature 2005 Apr 14;434(7035):843-50.

43. Klaus A, Birchmeier W. Wnt signalling and its impact on development and cancer. Nat Rev Cancer 2008 May;8(5):387-98.

44. Komiya Y, Habas R. Wnt signal transduction pathways. Organogenesis 2008 Apr;4(2):68-75.

45. Amit S, Hatzubai A, Birman Y, et al. Axin-mediated CKI phosphorylation of beta-catenin at Ser 45: a molecular switch for the Wnt pathway. Genes Dev 2002 May 1;16(9):1066-76.

46. Wang Z, Vogelstein B, Kinzler KW. Phosphorylation of beta-catenin at S33, S37, or T41 can occur in the absence of phosphorylation at T45 in colon cancer cells. Cancer Res 2003 Sep 1;63(17):5234-5.

47. Barker N. The canonical Wnt/beta-catenin signalling pathway. Methods Mol Biol 2008;468:5-15.

48. Brabletz T, Jung A, Hermann K, Gunther K, Hohenberger W, Kirchner T. Nuclear overexpression of the oncoprotein beta-catenin in colorectal cancer is localized predominantly at the invasion front. Pathol Res Pract 1998;194(10):701-4.

49. Jeanes A, Gottardi CJ, Yap AS. Cadherins and cancer: how does cadherin dysfunction promote tumor progression? Oncogene 2008 Nov 24;27(55):6920-9.

50. Alves-Guerra MC, Ronchini C, Capobianco AJ. Mastermind-like 1 Is a specific coactivator of beta-catenin transcription activation and is essential for colon carcinoma cell survival. Cancer Res 2007 Sep 15;67(18):8690-8.

51. Kawano Y, Kypta R. Secreted antagonists of the Wnt signalling pathway. J Cell Sci 2003 Jul 1;116(Pt 13):2627-34.

52. Niehrs C. Function and biological roles of the Dickkopf family of Wnt modulators. Oncogene 2006 Dec 4;25(57):7469-81.

53. Glinka A, Wu W, Delius H, Monaghan AP, Blumenstock C, Niehrs C. Dickkopf-1 is a member of a new family of secreted proteins and functions in head induction. Nature 1998 Jan 22;391(6665):357-62.

54. Koch S, Capaldo CT, Samarin S, et al. Dkk-1 inhibits intestinal epithelial cell migration by attenuating directional polarization of leading edge cells. Mol Biol Cell 2009 Nov;20(22):4816-25.

55. Pinto D, Gregorieff A, Begthel H, Clevers H. Canonical Wnt signals are essential for homeostasis of the intestinal epithelium. Genes Dev 2003 Jul 15;17(14):1709-13.

56. Bafico A, Liu G, Yaniv A, Gazit A, Aaronson SA. Novel mechanism of Wnt signalling inhibition mediated by Dickkopf-1 interaction with LRP6/Arrow. Nat Cell Biol 2001 Jul;3(7):683-6.

57. Mao B, Wu W, Li Y, et al. LDL-receptor-related protein 6 is a receptor for Dickkopf proteins. Nature 2001 May 17;411(6835):321-5.

58. Semenov MV, Tamai K, Brott BK, Kuhl M, Sokol S, He X. Head inducer Dickkopf-1 is a ligand for Wnt coreceptor LRP6. Curr Biol 2001 Jun 26;11(12):951-61.

59. Mao B, Wu W, Davidson G, et al. Kremen proteins are Dickkopf receptors that regulate Wnt/beta-catenin signalling. Nature 2002 Jun 6;417(6889):664-7.

60. Gonzalez-Sancho JM, Aguilera O, Garcia JM, et al. The Wnt antagonist DICKKOPF-1 gene is a downstream target of beta-catenin/TCF and is downregulated in human colon cancer. Oncogene 2005 Feb 3;24(6):1098-103.

61. Aguilera O, Pena C, Garcia JM, et al. The Wnt antagonist DICKKOPF-1 gene is induced by 1alpha,25-dihydroxyvitamin D3 associated to the differentiation of human colon cancer cells. Carcinogenesis 2007 Sep;28(9):1877-84.

62. Kinzler KW, Vogelstein B. Lessons from hereditary colorectal cancer. Cell 1996 Oct 18;87(2):159-70.

63. Liu W, Dong X, Mai M, et al. Mutations in AXIN2 cause colorectal cancer with defective mismatch repair by activating beta-catenin/TCF signalling. Nat Genet 2000 Oct;26(2):146-7.

64. Morin PJ, Sparks AB, Korinek V, et al. Activation of beta-catenin-Tcf signaling in colon cancer by mutations in beta-catenin or APC. Science 1997 Mar 21;275(5307):1787-90.

65. Stein U, Arlt F, Walther W, et al. The metastasis-associated gene S100A4 is a novel target of beta-catenin/T-cell factor signaling in colon cancer. Gastroenterology 2006 Nov;131(5):1486-500.

66. Garrett SC, Varney KM, Weber DJ, Bresnick AR. S100A4, a mediator of metastasis. J Biol Chem 2006 Jan 13;281(2):677-80.

67. Marenholz I, Lovering RC, Heizmann CW. An update of the S100 nomenclature. Biochim Biophys Acta 2006 Nov;1763(11):1282-3.

68. Schneider M, Hansen JL, Sheikh SP. S100A4: a common mediator of epithelial-mesenchymal transition, fibrosis and regeneration in diseases? J Mol Med 2008 May;86(5):507-22.

69. Boye K, Maelandsmo GM. S100A4 and metastasis: a small actor playing many roles. Am J Pathol 2010 Feb;176(2):528-35.

70. Fernandez-Fernandez MR, Veprintsev DB, Fersht AR. Proteins of the S100 family regulate the oligomerization of p53 tumor suppressor. Proc Natl Acad Sci U S A 2005 Mar 29;102(13):4735-40.

71. Helfman DM, Kim EJ, Lukanidin E, Grigorian M. The metastasis associated protein S100A4: role in tumour progression and metastasis. Br J Cancer 2005 Jun 6;92(11):1955-8.

72. Hernan R, Fasheh R, Calabrese C, et al. ERBB2 up-regulates S100A4 and several other prometastatic genes in medulloblastoma. Cancer Res 2003 Jan 1;63(1):140-8.

73. Kim TH, Kim HI, Soung YH, Shaw LA, Chung J. Integrin (alpha6beta4) signals through Src to increase expression of S100A4, a metastasis-promoting factor: implications for cancer cell invasion. Mol Cancer Res 2009 Oct;7(10):1605-12.

74. Cohn MA, Hjelmso I, Wu LC, Guldberg P, Lukanidin EM, Tulchinsky EM. Characterization of Sp1, AP-1, CBF and KRC binding sites and minisatellite DNA

as functional elements of the metastasis-associated mts1/S100A4 gene intronic enhancer. Nucleic Acids Res 2001 Aug 15;29(16):3335-46.

75. Hjelmsoe I, Allen CE, Cohn MA, Tulchinsky EM, Wu LC. The kappaB and V(D)J recombination signal sequence binding protein KRC regulates transcription of the mouse metastasis-associated gene S100A4/mts1. J Biol Chem 2000 Jan 14;275(2):913-20.

76. Tulchinsky E, Kramerov D, Ford HL, Reshetnyak E, Lukanidin E, Zain S. Characterization of a positive regulatory element in the mts1 gene. Oncogene 1993 Jan;8(1):79-86.

77. Zhang R, Fu H, Chen D, et al. Subcellular distribution of S100A4 and its transcriptional regulation under hypoxic conditions in gastric cancer cell line BGC823. Cancer Sci 2010 Feb 15.

78. Tulchinsky E, Ford HL, Kramerov D, et al. Transcriptional analysis of the mts1 gene with specific reference to 5' flanking sequences. Proc Natl Acad Sci U S A 1992 Oct 1;89(19):9146-50.

79. Ambartsumian N, Tarabykina S, Grigorian M, et al. Characterization of two splice variants of metastasis-associated human mts1 gene. Gene 1995 Jun 14;159(1):125-30.

80. Gingras AR, Basran J, Prescott A, Kriajevska M, Bagshaw CR, Barsukov IL. Crystal structure of the Ca(2+)-form and Ca(2+)-binding kinetics of metastasis-associated protein, S100A4. FEBS Lett 2008 May 28;582(12):1651-6.

81. Dutta K, Cox CJ, Huang H, Basavappa R, Pascal SM. Calcium coordination studies of the metastatic Mts1 protein. Biochemistry 2002 Apr 2;41(13):4239-45.

82. Pathuri P, Vogeley L, Luecke H. Crystal structure of metastasis-associated protein S100A4 in the active calcium-bound form. J Mol Biol 2008 Oct 31;383(1):62-77.

83. Vallely KM, Rustandi RR, Ellis KC, Varlamova O, Bresnick AR, Weber DJ. Solution structure of human Mts1 (S100A4) as determined by NMR spectroscopy. Biochemistry 2002 Oct 22;41(42):12670-80.

84. Kohya N, Kitajima Y, Jiao W, Miyazaki K. Effects of E-cadherin transfection on gene expression of a gallbladder carcinoma cell line: repression of MTS1/S100A4 gene expression. Int J Cancer 2003 Mar 10;104(1):44-53.

85. Moriyama-Kita M, Endo Y, Yonemura Y, et al. S100A4 regulates E-cadherin expression in oral squamous cell carcinoma. Cancer Lett 2005 Dec 18;230(2):211-8.

86. Andersen K, Nesland JM, Holm R, Florenes VA, Fodstad O, Maelandsmo GM. Expression of S100A4 combined with reduced E-cadherin expression predicts patient outcome in malignant melanoma. Mod Pathol 2004 Aug;17(8):990-7.

87. Kimura K, Endo Y, Yonemura Y, et al. Clinical significance of S100A4 and E-cadherin-related adhesion molecules in non-small cell lung cancer. Int J Oncol 2000 Jun;16(6):1125-31.

88. Yonemura Y, Endou Y, Kimura K, et al. Inverse expression of S100A4 and E-cadherin is associated with metastatic potential in gastric cancer. Clin Cancer Res 2000 Nov;6(11):4234-42.

89. Kriajevska M, Fischer-Larsen M, Moertz E, et al. Liprin beta 1, a member of the family of LAR transmembrane tyrosine phosphatase-interacting proteins, is a new target for the metastasis-associated protein S100A4 (Mts1). J Biol Chem 2002 Feb 15;277(7):5229-35.

90. Serra-Pages C, Streuli M, Medley QG. Liprin phosphorylation regulates binding to LAR: evidence for liprin autophosphorylation. Biochemistry 2005 Dec 6;44(48):15715-24.

91. Watanabe Y, Usada N, Minami H, et al. Calvasculin, as a factor affecting the microfilament assemblies in rat fibroblasts transfected by src gene. FEBS Lett 1993 Jun 7;324(1):51-5.

92. Takenaga K, Nakamura Y, Sakiyama S, Hasegawa Y, Sato K, Endo H. Binding of pEL98 protein, an S100-related calcium-binding protein, to nonmuscle tropomyosin. J Cell Biol 1994 Mar;124(5):757-68.

93. Kriajevska MV, Cardenas MN, Grigorian MS, Ambartsumian NS, Georgiev GP, Lukanidin EM. Non-muscle myosin heavy chain as a possible target for protein encoded by metastasis-related mts-1 gene. J Biol Chem 1994 Aug 5;269(31):19679-82.

94. Ford HL, Zain SB. Interaction of metastasis associated Mts1 protein with nonmuscle myosin. Oncogene 1995 Apr 20;10(8):1597-605.

95. Li ZH, Spektor A, Varlamova O, Bresnick AR. Mts1 regulates the assembly of nonmuscle myosin-IIA. Biochemistry 2003 Dec 9;42(48):14258-66.

96. Ford HL, Silver DL, Kachar B, Sellers JR, Zain SB. Effect of Mts1 on the structure and activity of nonmuscle myosin II. Biochemistry 1997 Dec 23;36(51):16321-7.

97. Kim EJ, Helfman DM. Characterization of the metastasis-associated protein, S100A4. Roles of calcium binding and dimerization in cellular localization and interaction with myosin. J Biol Chem 2003 Aug 8;278(32):30063-73.

98. Li ZH, Bresnick AR. The S100A4 metastasis factor regulates cellular motility via a direct interaction with myosin-IIA. Cancer Res 2006 May 15;66(10):5173-80.

99. Wang G, Rudland PS, White MR, Barraclough R. Interaction in vivo and in vitro of the metastasis-inducing S100 protein, S100A4 (p9Ka) with S100A1. J Biol Chem 2000 Apr 14;275(15):11141-6.

100. Tarabykina S, Kriajevska M, Scott DJ, et al. Heterocomplex formation between metastasis-related protein S100A4 (Mts1) and S100A1 as revealed by the yeast two-hybrid system. FEBS Lett 2000 Jun 23;475(3):187-91.

101. Wang G, Zhang S, Fernig DG, Martin-Fernandez M, Rudland PS, Barraclough R. Mutually antagonistic actions of S100A4 and S100A1 on normal and metastatic phenotypes. Oncogene 2005 Feb 17;24(8):1445-54.

102. Bronckart Y, Decaestecker C, Nagy N, et al. Development and progression of malignancy in human colon tissues are correlated with expression of specific Ca(2+)-binding S100 proteins. Histol Histopathol 2001 Jul;16(3):707-12.

103. Koshelev YA, Kiselev SL, Georgiev GP. Interaction of the S100A4 (Mts1) protein with septins Sept2, Sept6, and Sept7 in vitro. Dokl Biochem Biophys 2003 Jul-Aug;391:195-7.

104. Hall PA, Russell SE. The pathobiology of the septin gene family. J Pathol 2004 Nov;204(4):489-505.

105. Li CL, Martinez V, He B, Lombet A, Perbal B. A role for CCN3 (NOV) in calcium signalling. Mol Pathol 2002 Aug;55(4):250-61.

106. Endo H, Takenaga K, Kanno T, Satoh H, Mori S. Methionine aminopeptidase 2 is a new target for the metastasis-associated protein, S100A4. J Biol Chem 2002 Jul 19;277(29):26396-402.

107. Dulyaninova NG, Malashkevich VN, Almo SC, Bresnick AR. Regulation of myosin-IIA assembly and Mts1 binding by heavy chain phosphorylation. Biochemistry 2005 May 10;44(18):6867-76.

108. Dukhanina EA, Dukhanin AS, Lomonosov MY, Lukanidin EM, Georgiev GP. Spectral studies on the calcium-binding properties of Mts1 protein and its interaction with target protein. FEBS Lett 1997 Jun 30;410(2-3):403-6.

109. Grigorian M, Andresen S, Tulchinsky E, et al. Tumor suppressor p53 protein is a new target for the metastasis-associated Mts1/S100A4 protein: functional consequences of their interaction. J Biol Chem 2001 Jun 22;276(25):22699-708.

110. Ismail TM, Zhang S, Fernig DG, et al. Self-association of calcium-binding protein S100A4 and metastasis. J Biol Chem 2010 Jan 8;285(2):914-22.

111. van Dieck J, Brandt T, Teufel DP, Veprintsev DB, Joerger AC, Fersht AR. Molecular basis of S100 proteins interacting with the p53 homologs p63 and p73. Oncogene 2010 Apr 8;29(14):2024-35.

112. van Dieck J, Fernandez-Fernandez MR, Veprintsev DB, Fersht AR. Modulation of the oligomerization state of p53 by differential binding of proteins of the S100 family to p53 monomers and tetramers. J Biol Chem 2009 May 15;284(20):13804-11.

113. van Dieck J, Teufel DP, Jaulent AM, et al. Posttranslational modifications affect the interaction of S100 proteins with tumor suppressor p53. J Mol Biol 2009 Dec 18;394(5):922-30.

114. Klingelhofer J, Moller HD, Sumer EU, et al. Epidermal growth factor receptor ligands as new extracellular targets for the metastasis-promoting S100A4 protein. FEBS J 2009 Oct;276(20):5936-48.

115. Semov A, Moreno MJ, Onichtchenko A, et al. Metastasis-associated protein S100A4 induces angiogenesis through interaction with Annexin II and accelerated plasmin formation. J Biol Chem 2005 May 27;280(21):20833-41.

116. Watanabe Y, Usuda N, Tsugane S, Kobayashi R, Hidaka H. Calvasculin, an encoded protein from mRNA termed pEL-98, 18A2, 42A, or p9Ka, is secreted by smooth muscle cells in culture and exhibits Ca(2+)-dependent binding to 36-kDa microfibril-associated glycoprotein. J Biol Chem 1992 Aug 25;267(24):17136-40.

117. Kiryushko D, Novitskaya V, Soroka V, et al. Molecular mechanisms of Ca(2+) signaling in neurons induced by the S100A4 protein. Mol Cell Biol 2006 May;26(9):3625-38.

118. Leclerc E, Fritz G, Vetter SW, Heizmann CW. Binding of S100 proteins to RAGE: an update. Biochim Biophys Acta 2009 Jun;1793(6):993-1007.

119. Yammani RR, Carlson CS, Bresnick AR, Loeser RF. Increase in production of matrix metalloproteinase 13 by human articular chondrocytes due to stimulation with S100A4: Role of the receptor for advanced glycation end products. Arthritis Rheum 2006 Sep;54(9):2901-11.

120. Ambartsumian N, Klingelhofer J, Grigorian M, et al. The metastasis-associated Mts1(S100A4) protein could act as an angiogenic factor. Oncogene 2001 Aug 2;20(34):4685-95.

121. Burkitt WI, Derrick PJ, Lafitte D, Bronstein I. Protein-ligand and protein-protein interactions studied by electrospray ionization and mass spectrometry. Biochem Soc Trans 2003 Oct;31(Pt 5):985-9.

122. Schmidt-Hansen B, Ornas D, Grigorian M, et al. Extracellular S100A4(mts1) stimulates invasive growth of mouse endothelial cells and modulates MMP-13 matrix metalloproteinase activity. Oncogene 2004 Jul 15;23(32):5487-95.

123. Mathisen B, Lindstad RI, Hansen J, et al. S100A4 regulates membrane induced activation of matrix metalloproteinase-2 in osteosarcoma cells. Clin Exp Metastasis 2003;20(8):701-11.

124. Gao XN, Tang SQ, Zhang XF. S100A4 antisense oligodeoxynucleotide suppresses invasive potential of neuroblastoma cells. J Pediatr Surg 2005 Apr;40(4):648-52.

125. Saleem M, Kweon MH, Johnson JJ, et al. S100A4 accelerates tumorigenesis and invasion of human prostate cancer through the transcriptional regulation of matrix metalloproteinase 9. Proc Natl Acad Sci U S A 2006 Oct 3;103(40):14825-30.

126. Senolt L, Grigorian M, Lukanidin E, et al. S100A4 is expressed at site of invasion in rheumatoid arthritis synovium and modulates production of matrix metalloproteinases. Ann Rheum Dis 2006 Dec;65(12):1645-8.

127. Hsieh HL, Schafer BW, Weigle B, Heizmann CW. S100 protein translocation in response to extracellular S100 is mediated by receptor for advanced glycation endproducts in human endothelial cells. Biochem Biophys Res Commun 2004 Apr 9;316(3):949-59.

128. Chuong C, Katz J, Pauley KM, Bulosan M, Cha S. RAGE expression and NF-kappaB activation attenuated by extracellular domain of RAGE in human salivary gland cell line. J Cell Physiol 2009 Nov;221(2):430-4.

129. Belot N, Pochet R, Heizmann CW, Kiss R, Decaestecker C. Extracellular S100A4 stimulates the migration rate of astrocytic tumor cells by modifying the organization of their actin cytoskeleton. Biochim Biophys Acta 2002 Nov 4;1600(1-2):74-83.

130. Rakic JM, Maillard C, Jost M, et al. Role of plasminogen activator-plasmin system in tumor angiogenesis. Cell Mol Life Sci 2003 Mar;60(3):463-73.

131. Tabata T, Tsukamoto N, Fooladi AA, et al. RNA interference targeting against S100A4 suppresses cell growth and motility and induces apoptosis in human pancreatic cancer cells. Biochem Biophys Res Commun 2009 Dec 18;390(3):475-80.

132. Berge G, Maelandsmo GM. Evaluation of potential interactions between the metastasis-associated protein S100A4 and the tumor suppressor protein p53. Amino Acids 2010 Feb 24.

133. Berge G, Costea DE, Berg M, et al. Coexpression and nuclear colocalization of metastasis-promoting protein S100A4 and p53 without mutual regulation in colorectal carcinoma. Amino Acids 2010 Feb 27.

134. Liang SH, Clarke MF. Regulation of p53 localization. Eur J Biochem 2001 May;268(10):2779-83.

135. Ebralidze A, Tulchinsky E, Grigorian M, et al. Isolation and characterization of a gene specifically expressed in different metastatic cells and whose deduced gene product has a high degree of homology to a Ca2+-binding protein family. Genes Dev 1989 Jul;3(7):1086-93.

136. Grigorian M, Ambartsumian N, Lykkesfeldt AE, et al. Effect of mts1 (S100A4) expression on the progression of human breast cancer cells. Int J Cancer 1996 Sep 17;67(6):831-41.

137. Schmidt-Hansen B, Klingelhofer J, Grum-Schwensen B, et al. Functional significance of metastasis-inducing S100A4(Mts1) in tumor-stroma interplay. J Biol Chem 2004 Jun 4;279(23):24498-504.

138. Suemizu H, Monnai M, Ohnishi Y, Ito M, Tamaoki N, Nakamura M. Identification of a key molecular regulator of liver metastasis in human pancreatic carcinoma using a novel quantitative model of metastasis in NOD/SCID/gammacnull (NOG) mice. Int J Oncol 2007 Oct;31(4):741-51.

139. Ambartsumian NS, Grigorian MS, Larsen IF, et al. Metastasis of mammary carcinomas in GRS/A hybrid mice transgenic for the mts1 gene. Oncogene 1996 Oct 17;13(8):1621-30.

140. Davies MP, Rudland PS, Robertson L, Parry EW, Jolicoeur P, Barraclough R. Expression of the calcium-binding protein S100A4 (p9Ka) in MMTV-neu transgenic mice induces metastasis of mammary tumours. Oncogene 1996 Oct 17;13(8):1631-7.

141. Grum-Schwensen B, Klingelhofer J, Grigorian M, et al. Lung metastasis fails in MMTV-PyMT oncomice lacking S100A4 due to a T-cell deficiency in primary tumors. Cancer Res 2010 Feb 1;70(3):936-47.

142. Li ZH, Dulyaninova NG, House RP, Almo SC, Bresnick AR. S100A4 regulates macrophage chemotaxis. Mol Biol Cell 2010 Aug 1;21(15):2598-610.

143. Grum-Schwensen B, Klingelhofer J, Berg CH, et al. Suppression of tumor development and metastasis formation in mice lacking the S100A4(mts1) gene. Cancer Res 2005 May 1;65(9):3772-80.

144. Olsen CJ, Moreira J, Lukanidin EM, Ambartsumian NS. Human mammary fibroblasts stimulate invasion of breast cancer cells in a three-dimensional culture and increase stroma development in mouse xenografts. BMC Cancer 2010;10:444.

145. Platt-Higgins AM, Renshaw CA, West CR, et al. Comparison of the metastasis-inducing protein S100A4 (p9ka) with other prognostic markers in human breast cancer. Int J Cancer 2000 Mar 20;89(2):198-208.

146. Ninomiya I, Ohta T, Fushida S, et al. Increased expression of S100A4 and its prognostic significance in esophageal squamous cell carcinoma. Int J Oncol 2001 Apr;18(4):715-20.

147. Nakamura T, Ajiki T, Murao S, et al. Prognostic significance of S100A4 expression in gallbladder cancer. Int J Oncol 2002 May;20(5):937-41.

148. Saleem M, Adhami VM, Ahmad N, Gupta S, Mukhtar H. Prognostic significance of metastasis-associated protein S100A4 (Mts1) in prostate cancer progression and chemoprevention regimens in an autochthonous mouse model. Clin Cancer Res 2005 Jan 1;11(1):147-53.

149. Ai KX, Lu LY, Huang XY, Chen W, Zhang HZ. Prognostic significance of S100A4 and vascular endothelial growth factor expression in pancreatic cancer. World J Gastroenterol 2008 Mar 28;14(12):1931-5.

150. Tsuna M, Kageyama S, Fukuoka J, et al. Significance of S100A4 as a prognostic marker of lung squamous cell carcinoma. Anticancer Res 2009 Jul;29(7):2547-54.

151. Bandiera A, Melloni G, Freschi M, et al. Prognostic factors and analysis of S100a4 protein in resected pulmonary metastases from renal cell carcinoma. World J Surg 2009 Jul;33(7):1414-20.

152. Cho YG, Kim CJ, Nam SW, et al. Overexpression of S100A4 is closely associated with progression of colorectal cancer. World J Gastroenterol 2005 Aug 21;11(31):4852-6.

153. Takenaga K, Nakanishi H, Wada K, et al. Increased expression of S100A4, a metastasis-associated gene, in human colorectal adenocarcinomas. Clin Cancer Res 1997 Dec;3(12 Pt 1):2309-16.

154. Taylor S, Herrington S, Prime W, Rudland PS, Barraclough R. S100A4 (p9Ka) protein in colon carcinoma and liver metastases: association with carcinoma cells and T-lymphocytes. Br J Cancer 2002 Feb 1;86(3):409-16.

155. Hemandas AK, Salto-Tellez M, Maricar SH, Leong AF, Leow CK. Metastasis-associated protein S100A4--a potential prognostic marker for colorectal cancer. J Surg Oncol 2006 May 1;93(6):498-503.

156. Flatmark K, Pedersen KB, Nesland JM, et al. Nuclear localization of the metastasis-related protein S100A4 correlates with tumour stage in colorectal cancer. J Pathol 2003 Aug;200(5):589-95.

157. Boye K, Nesland JM, Sandstad B, Maelandsmo GM, Flatmark K. Nuclear S100A4 is a novel prognostic marker in colorectal cancer. Eur J Cancer 2010 Aug 16.

158. Stein U, Burock S, Herrmann P, et al. Diagnostic and prognostic value of metastasis inducer S100A4 transcripts in plasma of colon, rectal, and gastric cancer patients. J Mol Diagn 2010.

159. Sack U, Stein U. Wnt up your mind - intervention strategies for S100A4-induced metastasis in colon cancer. Gen Physiol Biophys 2009;28(Focus Issue):F55-F64.

160. Santamaria-Kisiel L, Rintala-Dempsey AC, Shaw GS. Calcium-dependent and -independent interactions of the S100 protein family. Biochem J 2006 Jun 1;396(2):201-14.

161. Tusher VG, Tibshirani R, Chu G. Significance analysis of microarrays applied to the ionizing radiation response. Proc Natl Acad Sci U S A 2001 Apr 24;98(9):5116-21.

162. Tibshirani R, Hastie T, Narasimhan B, Chu G. Diagnosis of multiple cancer types by shrunken centroids of gene expression. Proc Natl Acad Sci U S A 2002 May 14;99(10):6567-72.

163. Hosack DA, Dennis G, Jr., Sherman BT, Lane HC, Lempicki RA. Identifying biological themes within lists of genes with EASE. Genome Biol 2003;4(10):R70.

164. Kim JS, Crooks H, Dracheva T, et al. Oncogenic beta-catenin is required for bone morphogenetic protein 4 expression in human cancer cells. Cancer Res 2002 May 15;62(10):2744-8.

165. Chomczynski P, Sacchi N. Single-step method of RNA isolation by acid guanidinium thiocyanate-phenol-chloroform extraction. Anal Biochem 1987 Apr;162(1):156-9.

166. Smith PK, Krohn RI, Hermanson GT, et al. Measurement of protein using bicinchoninic acid. Anal Biochem 1985 Oct;150(1):76-85.

167. Boyden S. The chemotactic effect of mixtures of antibody and antigen on polymorphonuclear leucocytes. J Exp Med 1962 Mar 1;115:453-66.

168. Spencer VA, Sun JM, Li L, Davie JR. Chromatin immunoprecipitation: a tool for studying histone acetylation and transcription factor binding. Methods 2003 Sep;31(1):67-75.

169. Rodriguez LG, Wu X, Guan JL. Wound-healing assay. Methods Mol Biol 2005;294:23-9.

170. Shtutman M, Zhurinsky J, Simcha I, et al. The cyclin D1 gene is a target of the beta-catenin/LEF-1 pathway. Proc Natl Acad Sci U S A 1999 May 11;96(10):5522-7.

171. He TC, Sparks AB, Rago C, et al. Identification of c-MYC as a target of the APC pathway. Science 1998 Sep 4;281(5382):1509-12.

172. Workman P, Balmain A, Hickman JA, et al. United Kingdom Co-ordinating Committee on Cancer Research (UKCCCR) Guidelines for the Welfare of Animals in Experimental Neoplasia (Second Edition). Br J Cancer 1998;77(1):1-10.

173. O'Neill K, Lyons SK, Gallagher WM, Curran KM, Byrne AT. Bioluminescent imaging: a critical tool in pre-clinical oncology research. J Pathol 2010 Feb;220(3):317-27.

174. Gallagher DJ, Kemeny N. Metastatic colorectal cancer: from improved survival to potential cure. Oncology 2010;78(3-4):237-48.

175. Jemal A, Siegel R, Ward E, et al. Cancer statistics, 2008. CA Cancer J Clin 2008 Mar-Apr;58(2):71-96.

176. Segal NH, Saltz LB. Evolving treatment of advanced colon cancer. Annu Rev Med 2009;60:207-19.

177. Sherbet GV. Metastasis promoter S100A4 is a potentially valuable molecular target for cancer therapy. Cancer Lett 2009 Jul 18;280(1):15-30.

178. Grigorian M, Tulchinsky E, Burrone O, Tarabykina S, Georgiev G, Lukanidin E. Modulation of mts1 expression in mouse and human normal and tumor cells. Electrophoresis 1994 Mar-Apr;15(3-4):463-8.

179. Campbell WC. The chemotherapy of parasitic infections. J Parasitol 1986 Feb;72(1):45-61.

180. Chang Y, Yeh T, Lin K, et al. Pharmacokineticts of Anti-SARS-CoV Agent Niclosamdie and Its Analogs in Rats. Journal of Food and Drug Analysis 2006;14(4):329-33.

181. Espinosa-Aguirre JJ, Reyes RE, Cortinas de Nava C. Mutagenic activity of 2-chloro-4-nitroaniline and 5-chlorosalicylic acid in Salmonella typhimurium: two possible metabolites of niclosamide. Mutat Res 1991 Nov;264(3):139-45.

182. Pressman BC. Biological applications of ionophores. Annu Rev Biochem 1976;45:501-30.

183. Gwak J, Cho M, Gong SJ, et al. Protein-kinase-C-mediated beta-catenin phosphorylation negatively regulates the Wnt/beta-catenin pathway. J Cell Sci 2006 Nov 15;119(Pt 22):4702-9.

184. Moriyama-Kita M, Endo Y, Yonemura Y, et al. Correlation of S100A4 expression with invasion and metastasis in oral squamous cell carcinoma. Oral Oncol 2004 May;40(5):496-500.

185. Ganesan K, Ivanova T, Wu Y, et al. Inhibition of gastric cancer invasion and metastasis by PLA2G2A, a novel beta-catenin/TCF target gene. Cancer Res 2008 Jun 1;68(11):4277-86.

186. Andersen K, Smith-Sorensen B, Pedersen KB, et al. Interferon-gamma suppresses S100A4 transcription independently of apoptosis or cell cycle arrest. Br J Cancer 2003 Jun 16;88(12):1995-2001.

187. Shi Y, Zou M, Collison K, et al. Ribonucleic acid interference targeting S100A4 (Mts1) suppresses tumor growth and metastasis of anaplastic thyroid carcinoma in a mouse model. J Clin Endocrinol Metab 2006 Jun;91(6):2373-9.

188. Hua J, Chen D, Fu H, et al. Short hairpin RNA-mediated inhibition of S100A4 promotes apoptosis and suppresses proliferation of BGC823 gastric cancer cells in vitro and in vivo. Cancer Lett 2009 Nov 27.

189. Jin Y, Lu Z, Ding K, et al. Antineoplastic Mechanisms of Niclosamide in Acute Myelogenous Leukemia Stem Cells: Inactivation of the NF-{kappa}B Pathway and Generation of Reactive Oxygen Species. Cancer Res 2010 Mar 15;70(6):2516-27.

190. Balgi AD, Fonseca BD, Donohue E, et al. Screen for chemical modulators of autophagy reveals novel therapeutic inhibitors of mTORC1 signaling. PLoS One 2009;4(9):e7124.

191. Chen M, Wang J, Lu J, et al. The anti-helminthic niclosamide inhibits Wnt/Frizzled1 signaling. Biochemistry 2009 Nov 3;48(43):10267-74.

192. Huang WS, Wang JP, Wang T, Fang JY, Lan P, Ma JP. ShRNA-mediated gene silencing of beta-catenin inhibits growth of human colon cancer cells. World J Gastroenterol 2007 Dec 28;13(48):6581-7.

193. Brantjes H, Roose J, van De Wetering M, Clevers H. All Tcf HMG box transcription factors interact with Groucho-related co-repressors. Nucleic Acids Res 2001 Apr 1;29(7):1410-9.

194. Daniels DL, Weis WI. Beta-catenin directly displaces Groucho/TLE repressors from Tcf/Lef in Wnt-mediated transcription activation. Nat Struct Mol Biol 2005 Apr;12(4):364-71.

195. Barker N, Clevers H. Mining the Wnt pathway for cancer therapeutics. Nat Rev Drug Discov 2006 Dec;5(12):997-1014.

196. Malashkevich VN, Dulyaninova NG, Ramagopal UA, et al. Phenothiazines inhibit S100A4 function by inducing protein oligomerization. Proc Natl Acad Sci U S A 2010 May 11;107(19):8605-10.

197. Garrett SC, Hodgson L, Rybin A, et al. A biosensor of S100A4 metastasis factor activation: inhibitor screening and cellular activation dynamics. Biochemistry 2008 Jan 22;47(3):986-96.

198. Zibert JR, Skov L, Thyssen JP, Jacobsen GK, Grigorian M. Significance of the S100A4 protein in psoriasis. J Invest Dermatol 2010 Jan;130(1):150-60.

199. Eggert US, Field CM, Mitchison TJ. Small molecules in an RNAi world. Mol Biosyst 2006 Feb;2(2):93-6.

200. Higuchi Y, Kawakami S, Hashida M. Strategies for in vivo delivery of siRNAs: recent progress. BioDrugs 2010 Jun;24(3):195-205.

201. Boon EM, van der Neut R, van de Wetering M, Clevers H, Pals ST. Wnt signaling regulates expression of the receptor tyrosine kinase met in colorectal cancer. Cancer Res 2002 Sep 15;62(18):5126-8.

202. Jones WE. Niclosamide as a treatment for Hymenolepis diminuta and Dipylidium caninum infection in man. Am J Trop Med Hyg 1979 Mar;28(2):300-2.

203. Merschjohann K, Steverding D. In vitro trypanocidal activity of the anti-helminthic drug niclosamide. Exp Parasitol 2008 Apr;118(4):637-40.

204. Pearson RD, Hewlett EL. Niclosamide therapy for tapeworm infections. Ann Intern Med 1985 Apr;102(4):550-1.

205. Fidler IJ. Critical factors in the biology of human cancer metastasis: twenty-eighth G.H.A. Clowes memorial award lecture. Cancer Res 1990 Oct 1;50(19):6130-8.

206. Koo V, Hamilton PW, Williamson K. Non-invasive in vivo imaging in small animal research. Cell Oncol 2006;28(4):127-39.

207. Sadikot RT, Blackwell TS. Bioluminescence imaging. Proc Am Thorac Soc 2005;2(6):537-40, 11-2.

208. Sloan EK, Priceman SJ, Cox BF, et al. The sympathetic nervous system induces a metastatic switch in primary breast cancer. Cancer Res 2010 Sep 15;70(18):7042-52.

209. Vikis HG, Jackson EN, Krupnick AS, et al. Strain-specific susceptibility for pulmonary metastasis of sarcoma 180 cells in inbred mice. Cancer Res 2010 Jun 15;70(12):4859-67.

210. Drake JM, Gabriel CL, Henry MD. Assessing tumor growth and distribution in a model of prostate cancer metastasis using bioluminescence imaging. Clin Exp Metastasis 2005;22(8):674-84.

211. Jenkins DE, Oei Y, Hornig YS, et al. Bioluminescent imaging (BLI) to improve and refine traditional murine models of tumor growth and metastasis. Clin Exp Metastasis 2003;20(8):733-44.

212. Giavazzi R, Jessup JM, Campbell DE, Walker SM, Fidler IJ. Experimental nude mouse model of human colorectal cancer liver metastases. J Natl Cancer Inst 1986 Dec;77(6):1303-8.

213. Kubota T. Metastatic models of human cancer xenografted in the nude mouse: the importance of orthotopic transplantation. J Cell Biochem 1994 Sep;56(1):4-8.

214. Tan MH, Holyoke ED, Goldrosen MH. Murine colon adenocarcinoma: syngeneic orthotopic transplantation and subsequent hepatic metastases. J Natl Cancer Inst 1977 Nov;59(5):1537-44.

215. Bibby MC. Orthotopic models of cancer for preclinical drug evaluation: advantages and disadvantages. Eur J Cancer 2004 Apr;40(6):852-7.

216. Adam R. Colorectal cancer with synchronous liver metastases. Br J Surg 2007 Feb;94(2):129-31.

217. Manfredi S, Lepage C, Hatem C, Coatmeur O, Faivre J, Bouvier AM. Epidemiology and management of liver metastases from colorectal cancer. Ann Surg 2006 Aug;244(2):254-9.

218. Hedley BD, Chambers AF. Tumor dormancy and metastasis. Adv Cancer Res 2009;102:67-101.

219. Ossowski L, Aguirre-Ghiso JA. Dormancy of metastatic melanoma. Pigment Cell Melanoma Res 2010 Feb;23(1):41-56.

220. Taniguchi T, Makino M, Suzuki K, Kaibara N. Prognostic significance of reverse transcriptase-polymerase chain reaction measurement of carcinoembryonic antigen mRNA levels in tumor drainage blood and peripheral blood of patients with colorectal carcinoma. Cancer 2000 Sep 1;89(5):970-6.

221. Papavasiliou P, Fisher T, Kuhn J, Nemunaitis J, Lamont J. Circulating tumor cells in patients undergoing surgery for hepatic metastases from colorectal cancer. Proc (Bayl Univ Med Cent) 2010 Jan;23(1):11-4.

222. Kemeny N. The management of resectable and unresectable liver metastases from colorectal cancer. Curr Opin Oncol 2010 Jul;22(4):364-73.

223. Kim R, Yamaguchi Y, Toge T. Adjuvant therapy for colorectal carcinoma. Anticancer Res 2002 Jul-Aug;22(4):2413-8.

224. Iwamoto M, Hoffenberg EJ, Carethers JM, et al. Nuclear accumulation of beta-catenin occurs commonly in the epithelial cells of juvenile polyps. Pediatr Res 2005 Jan;57(1):4-9; discussion 1-3.

225. Keirsebilck A, Bonne S, Bruyneel E, et al. E-cadherin and metastasin (mts-1/S100A4) expression levels are inversely regulated in two tumor cell families. Cancer Res 1998 Oct 15;58(20):4587-91.

226. Mahon PC, Baril P, Bhakta V, et al. S100A4 contributes to the suppression of BNIP3 expression, chemoresistance, and inhibition of apoptosis in pancreatic cancer. Cancer Res 2007 Jul 15;67(14):6786-95.

227. Miranda KJ, Loeser RF, Yammani RR. Sumoylation and nuclear translocation of S100A4 regulates IL-1 {beta} mediated production of matrix metalloprotinase-13. J Biol Chem 2010 Aug 4.

228. Licchesi JD, Westra WH, Hooker CM, Machida EO, Baylin SB, Herman JG. Epigenetic alteration of Wnt pathway antagonists in progressive glandular neoplasia of the lung. Carcinogenesis 2008 May;29(5):895-904.

229. Hussain M, Rao M, Humphries AE, et al. Tobacco smoke induces polycomb-mediated repression of Dickkopf-1 in lung cancer cells. Cancer Res 2009 Apr 15;69(8):3570-8.

230. Kalluri R, Weinberg RA. The basics of epithelial-mesenchymal transition. J Clin Invest 2009 Jun;119(6):1420-8.

231. Vogelstein B, Kinzler KW. The multistep nature of cancer. Trends Genet 1993 Apr;9(4):138-41.

ERKLÄRUNG

Ich versichere hiermit, dass die von mir vorgelegte Dissertation eigenständig und ohne Benutzung anderer als der angegebenen Hilfsmittel angefertigt wurde. Ich versichere, dass alle aus anderen Quellen übernommenen Daten und Konzepte, sowie Ergebnisse aus Kooperationsprojekten unter Angabe der Referenz gekennzeichnet sind.
Außerdem versichere ich, dass mir die aktuelle Promotionsordnung bekannt ist und ich mich nicht anderwärts um einen Doktorgrad bewerbe, bzw. noch keinen entsprechenden Doktorgrad besitze. Diese Arbeit wurde in gleicher oder ähnlicher Form nicht einer anderen Prüfungsbehörde vorgelegt.

Berlin, 19.10.2010

_____

Ulrike Sack

PUBLICATIONS

JOURNAL ARTICLES

Sack U, Walther W, Scudiero D, Selby M, Kobelt D, Lemm M, Fichtner I, Schlag PM, Shoemaker RH, Stein U. Novel effect of anti-helmintic niclosamide on S100A4-induced metastasis in colon cancer. *In revision at JNCI, Sep 2010.*

Sack U, Walther W, Scudiero D, Selby M, Schlag PM, Shoemaker RH, Stein U. Calcimycin inhibits the canonical Wnt/β-catenin pathway and blocks S100A4-induced cell invasion in colon cancer cells. *In revision at MBoC, Sep 2010.*

Stein U, Arlt F, Smith J, Sack U, Herrmann P, Walther W, Lemm M, Fichtner I, Shoemaker RH, Schlag PM. Intervening in β-catenin signaling by sulindac inhibits S100A4-dependent colon cancer metastasis. *In revision at Neoplasia, Sep 2010.*

Weiller M, Weiland T, Dunstl G, Sack U, Kunstle G, Wendel A. Differential immunotoxicity of histone deacetylase inhibitors on malignant and naive hepatocytes. Exp Toxicol Pathol 2010 May 25.

Sack U, Stein U. Wnt up your mind - intervention strategies for S100A4-induced metastasis in colon cancer. Gen Physiol Biophys 2009;28(Focus Issue):F55-F64.

CONFERENCES

“Niclosamide, a newly identified inhibitor that restricts S100A4-induced metastasis formation in colon cancer” (Poster), Sack U, Walther W, Shoemaker RH, Fichtner I, Schlag PM, Stein U; Deutscher Krebskongress 2010; Berlin, Germany; Feb 24-27, 2010, *honored with poster award*

“Identification of a small molecule inhibitor to restrict S100A4-induced metastasis formation in colon cancer” (Talk), Sack U and Stein U; MDC/FMP PhD Retreat 2009; Kremmen, Germany; Sep 3-5, 2009

“Knockdown of S100A4 expression by small molecules restricts metastasis formation in colon cancer” (Poster), Sack U, Walther W, Shoemaker RH, Fichtner I, Schlag PM, Stein U; ECS Workshop on Annexins, Targets and Calcium-binding Proteins in Pathology; Smolenice, Slovakia; Jun 3-6, 2009

"Small Molecules restrict S100A4 induced metastasis formation in Colon Carcinoma" (Poster), Sack U, Walther W, Scudiero D, Selby M, Shoemaker RH, Schlag PM, Stein U; International AEK Cancer Congress; Berlin, Germany; Mar 18-20, 2009

"S100A4-Suppression: A prospective intervention against metastasis formation in colon carcinoma" (Poster), Sack U, Walther W, Herrmann P, Scudiero D, Selby M, Shoemaker RH, Schlag PM, Stein U; MDC/FMP PhD Retreat 2008, Berlin Döllnsee, Germany, Sep 10-13, 2008

"A novel assay for improving the identification of internal ribosome entry sequences" (Poster), Sack U, Willet M, Morley SJ, Coldwell MJ; 2nd EMBO Conference on Protein synthesis and translational control, Heidelberg, Germany, Sep 12-16 2007

"A novel assay for improving the identification of internal ribosome entry sequences" (Poster), Sack U, Sivakumaran K, Morley SJ, Coldwell MJ; Conference Translation UK, Nottingham, England, Jul 10-12, 2007

Berlin, 19.10.2010

Ulrike Sack

ACKNOWLEDGMENT

I would like to thank Prof. Dr. Peter M. Schlag and Prof. Dr. Ulrike Stein for giving me the opportunity to research in their lab, providing me with all I needed to contribute to their impressive research in the field of metastasis formation in colon cancer. I am thankful to Prof. Dr. Thomas Börner for taking over my supervision for the Humboldt-University Berlin enabling me to fulfill my degree. I would like to thank the PhD Programme for Molecule Cell Biology of the MDC for their financial and scientific support, for giving me the opportunity to organize a scientific meeting and for supplying me with lectures and courses.

I am deeply grateful to Prof. Dr. Ulrike Stein for taking over my supervision, for sharing her time with me, for financially support all my ideas on that project and giving me the chance to work and publish self-determined. Without her patience, her endurance and her unlimited help this work would not have been possible.

I would like to thank PD Dr. Wolfgang Walther, Dr. Robert H Shoemaker, Dr. Dominic Scudiero and Mike Selby for their great cooperation on the small molecule project. I further like to thank Dr. Robert H Shoemaker for supporting this work with niclosamide derivatives and PD Dr. Wolfgang Walther for his scientific support and his helpful comments on the small molecule project.

I am thankful to PD Dr. Iduna Fichtner and Margit Lemm for their fruitful cooperation on all the animal work. Without their help and scientific advice concerning *in vivo* experiments, this work would have not been possible.

I am very thankful to Dennis Kobelt and Dr. Franziska Siegel who got me started in the lab and with their patients for my questions made this time most enjoyable. My very warm gratitude goes to Pia Hermann, Janice Smith and Jutta Aumann for their great and unlimited technical assistance and their work to keep the labs going. I am very thankful to Dr. Clara Lemos who, despite her short time in the Stein lab, essentially helped me by sharing her experience on publishing papers and by proof-reading my thesis. I am deeply thankful to all the members of the Stein and Walther Lab. Our team spirit and our exceptionally nice and relaxed atmosphere full of helping hands and ideas was the best motivation to go through the ups and downs of research.

Last but not least, I want to thank my family and friends. Their unlimited support, understanding, tolerance and love were the best motivation to keep me going.